FUNCTIONAL ANALYSIS OF THE RABBITPOX VIRUS SERPIN SPI-1: CHARACTERIZATION *IN VITRO* AND *IN VIVO*

By

KRISTIN LAURIE MOON

A DISSERTATION PRESENTED TO THE GRADUATE SCHOOL
OF THE UNIVERSITY OF FLORIDA IN PARTIAL FULFILLMENT
OF THE REQUIREMENTS FOR THE DEGREE OF
DOCTOR OF PHILOSOPHY

UNIVERSITY OF FLORIDA

2000

Dedicated to my husband Joel for his love, support and his constant faith in me.

ACKNOWLEDGEMENTS

I would like to take this opportunity to thank the many people that have contributed to this study. First, I would like to thank my mentor Dr. Richard Moyer for his supervision, support, and guidance through the years. He has provided a unique environment in which to learn and work that has made the daily process of doctoral research easier to bear. I wish to thank him for allowing me the chance to think on my own and the opportunity to try things in the lab that may not have seemed logical at the time. I am completely satisfied with my experience in his lab and consider him an excellent teacher. In addition, I wish to thank the members of my supervisory committee. Along with Dr. Moyer, Dr. Bill Dunn, Dr. John Aris, Dr. Tom Rowe, and Dr. Al Lewin have each contributed valuable insight to my research project. I came away from every committee meeting with optimism and great ideas for future experiments. Each member of my committee took the time to individually meet with me to give me advice and help me to interpret my results and I thank them for their support.

The members of the departmental administrative, editorial and fiscal staff have been essential to my success as a graduate student. Their hard work and attention to detail allows every student in the program more time to focus on classwork and research and no one would be able to make it through the program without them. In particular, I wish to acknowledge Joyce Conners for her special contribution. My occasional visits to her office have provided only a glimpse into her stressful daily routine and I am very glad

that I don't have her job! I wish to thank her for putting up with me for six years and for being such a delightful person.

The members of the Moyer lab have been a constant source of enjoyment for me in my years as a doctoral student. Though some of the faces have changed over time, the lighthearted atmosphere present in the lab has remained the same. In particular, I wish to acknowledge the following people for their special contributions, although my words won't do justice to my feelings for each of them. Dr. Pete Turner provided excellent guidance and tutelage over the years, and I thank him for his assistance. Mike Duke did an excellent job running the lab, making us smile, exposing us to alternative forms of music and food, and keeping us informed with (useless) trivia. In addition, he has been a truly wonderful friend whose daily companionship I miss. I wish to thank Mike Duke, Lauren Morges, Traci Ness, Dr. Allison Bawden and Dr. Amy MacNeill for their excellent rabbit-wrangling techniques and I hope they each realize that I would still be stuck down in Animal Resources without their help. Finally, I want to thank Traci Ness for many things. She has been my partner in misery and in crime, my second set of hands in the lab, and a constant source of encouragement and support to me. She remains a very special friend and adopted family member.

Saving the best for last, I wish to acknowledge my family. They have supported me through six agonizing years of stress, anxiety, disappointment, excitement, and all of the ups and downs of scientific research at the graduate level. They have been patient and understanding, not really knowing what I was doing but all the while having faith that one day I would finish. Without their love and encouragement I could not have made it through the rough times, and the good times would not have been nearly as good. Most

of all, I want to thank my husband Joel for everything that he has endured and for the many sacrifices that he has made so that I could finish my degree. I thank him for his patience, encouragement, and his prayers. I thank him for the many times that he challenged me to stick it out and follow through with the goals that I had set. I thank him for having more faith in me than I ever had in myself and for his unconditional love.

TABLE OF CONTENTS

LIST OF TABLES

LIST OF FIGURES

KEY TO ABBREVIATIONS

a	adenosine
aa	amino acid
A	alanine
Å	Angstrom
ACT	α1-antichymotrypsin
AIDS	acquired immunodeficiency syndrome
AIF	apoptosis inducing factor
APS	ammonium persulfate
AT	α1-antitrypsin
ATIII	antithrombin III
bp	base pair
BSA	bovine serum albumin
c	cytosine
C	cysteine
CAM	chorioallantoic membrane
CARD	caspase recruitment domain
CBP	chemokine binding protein
cDNA	complementary DNA
cm	centimeter
CPE	cytopathic effect
CPV	cowpox virus
CTL	cytotoxic T-lymphocyte
DAPI	4'6-diamidino-2-phenylindole
DMSO	dimethyl sulfoxide
DNA	deoxyribonucleic acid
dsRNA	double stranded RNA
DTT	dithiothreitol
EDTA	ethylenediaminetetraacetic acid
EEV	extracellular enveloped virus
EGF	epidermal growth factor
EM	electron microscopy
ER	endoplasmic reticulum
EV	ectromelia virus
F	phenylalanine
FADD	Fas-associating protein with death domain
FBS	fetal bovine serum
FPV	fowlpox virus

g	gravity
g	guanosine
HA	hemagglutinin
HBSS	Hank's buffered standard saline
His	histadine
HIV	human immunodeficiency virus
HNE	human neutrophil elastase
hpi	hours post infection
hr	hour
ICE	interleukin-1β converting enzyme
IFN	interferon
IL	interleukin
IMV	intracellular mature virus
ITR	inverted terminal repetition
kbp	kilobase pair
kDa	kilodalton
LB	Luria broth
LD_{50}	lethal dose 50
M	molar
MCS	multiple cloning site
MCV	molluscum contagiosum virus
MEM	minimal essential media
mg	milligram
MHC	major histocompatability complex
µg	microgram
µl	microliter
µm	micron
µM	micromolar
min	minute
ml	milliliter
mm	millimeter
mM	millimolar
MOI	multiplicity of infection
MPV	monkeypox virus
mRNA	messenger RNA
MV	myxoma virus
N	asparagine
ng	nanogram
NK	natural killer
nM	nanomolar
nm	nanometer
NOS	nitric oxide synthase
nt	nucleotide
ORF	open reading frame
PAGE	polyacrylamide gel electrophoresis
PAI	plasminogen activator inhibitor

PARP	poly(ADP-ribose) polymerase
PBS	phosphate-buffered saline
PCR	polymerase chain reaction
pfu	plaque forming units
PMN	polymorphonucleocyte
PMSF	phenylmethylsulfonyl fluoride
PT	permeability transition
R	arginine
RCA	regulators of complement activation
RNA	ribonucleic acid
RNI	reactive nitrogen intermediate
RPV	rabbitpox virus
RSL	reactive site loop
RT	room temperature
S	serine
SCCA	squamous cell carcinoma antigen
SDS	sodium dodecyl sulfate
SPI	serine proteinase inhibitor
SPV	swinepox virus
t	thymidine
T	threonine
TBS	Tris-buffered saline
TIR	terminal inverted repeat
TK	thymidine kinase
TNF	tumor necrosis factor
tPA	tissue plasminogen activator
U	unit
UV	ultraviolet
V	volt
VCP	vaccinia virus complement control protein
VGF	vaccinia growth factor
VV	vaccinia virus
wt	wild type

Abstract of Dissertation Presented to the Graduate School
of the University of Florida in Partial Fulfillment of the
Requirements for the Degree of Doctor of Philosophy

FUNCTIONAL ANALYSIS OF THE RABBITPOX VIRUS SERPIN SPI-1:
CHARACTERIZATION *IN VITRO* AND *IN VIVO*

By

Kristin Laurie Moon

December, 2000

Chairman: Richard W. Moyer
Major Department: Molecular Genetics and Microbiology

Poxviruses are the only virus family known to encode functional members of the serpin family of serine proteinase inhibitors, and the vast majority have been demonstrated to serve as important virulence factors during infection of animal hosts. The natural or engineered mutation of several poxvirus serpins has been shown to result in virus attenuation associated with an impairment in the ability to cause disease. Many orthopoxvirus members, including vaccinia virus, rabbitpox virus (RPV) and variola virus, the causative agent of smallpox, have been shown to encode the serine proteinase inhibitor (SPI)-1 gene, implying that SPI-1 expression endows the viruses with a selective advantage during natural infection. Previous studies have shown that SPI-1 expression is necessary for the complete host range of RPV in tissue culture, which has been proposed to stem from the ability of SPI-1 to inhibit apoptosis. Still, other studies have questioned the importance of SPI-1 as a virulence factor during animal infections.

Because SPI-1 shares a high degree of homology with members of the serpin superfamily, it has been widely assumed that any role that SPI-1 serves during infection is related to its ability to function as a proteinase inhibitor. However this model has remained untested until now. This study is the first to demonstrate that SPI-1 protein expressed *in vitro* has the properties of a functional serpin and appears to preferentially inhibit target proteinases of the chymotrypsin family, including cathepsin G. Furthermore, experiments using RPV recombinants expressing SPI-1 proteins with engineered mutations at amino acids critical for serpin activity are the first to suggest that it is the ability of SPI-1 to function as an inhibitory serpin which is essential for the unrestricted host range of RPV. While infection of restrictive cell lines with RPV mutants lacking SPI-1 serpin activity triggered several morphological features of apoptosis, caspase activation did not occur, implying that SPI-1 may be involved in preventing a caspase-independent form of cell death during infection. Preliminary experiments in rabbits suggests that SPI-1 is an important virulence factor *in vivo* which appears to inhibit inflammation at the primary site of infection.

CHAPTER 1
INTRODUCTION AND BACKGROUND

Poxviruses are large, double-stranded DNA viruses that replicate exclusively in the cytoplasm of infected cells. The virus family is divided into two subfamilies: the Chordopoxviruses and the Entomopoxviruses, which infect vertebrates and insects, respectively. The Chordopoxvirinae consist of eight genera: Orthopoxvirus, Parapoxvirus, Avipoxvirus, Capripoxvirus, Leporipoxvirus, Suipoxvirus, Molluscipoxvirus, and Yatapoxvirus (Table 1). Members of a Chordopoxvirinae genus are both genetically and antigenically related and have a similar morphology and host range. In contrast, the Entomopoxvirinae have been divided into three genera, Entomopoxvirus A, B and C, based on the insect host of isolation (Table 1)(12). Until recently, little was known regarding the insect poxviruses. However, the recent sequencing of the genomes of two Entomopoxvirus B viruses has provided insight into the evolutionary relationship between the two poxvirus subfamilies. Divergence between the insect and vertebrate poxviruses is indicated by the presence of only 49 identifiable Chordopoxvirus counterparts in *Melanoplus sanquinipes* with only 20-48% amino acid identity among the shared gene products, in addition to the presence of 43 novel ORFs in five gene families (2). Similarly, only 30% of the *Amsacta moorei* (AmEPV) genome was shown to encode genes with vertebrate poxvirus homologues (22).

Table 1. Taxonomy of the Poxviruses

Subfamily	Genus	Representative Species
Chordopoxvirinae	Orthopoxvirus	Vaccinia, Variola, Cowpox, Rabbitpox, Ectromelia, Monkeypox, Skunkpox, Racoonpox
	Suipoxvirus	Swinepox
	Leporipoxvirus	Myxoma, Shope Fibroma Virus
	Capripoxvirus	Sheep-pox, Goatpox, Lumpy Skin Disease Virus
	Molluscipoxvirus	Molluscum contagiosum virus
	Parapoxvirus	Orf, Psuedocowpox, Bovine papular stomatitis virus
	Avipoxvirus	Canarypox, Fowlpox, Quailpox, Turkeypox
	Yatapoxvirus	Tanapox, Yabapox
	Unclassified	Macropad poxvirus, Crocodilian poxvirus
Entomopoxvirinae	Entomopoxvirus A	*Melolontha melolontha*
	Entomopoxvirus B	*Amsacta moorei, Melanoplus sanguinipes*
	Entomopoxvirus C	*Chironimus luridus*

Remarkably, 35.1% of the AmEPV genome was shown to encode open reading frames (ORFs) with no known function and no Entomopoxvirus or Chordopoxvirus homologues (22). Still, a common *Poxviridae* core of genes was elucidated following the identification of genes common to both poxvirus subfamilies, including those encoding enzymes involved in RNA transcription and modification, DNA replication, protein processing, virion assembly, and virion structural proteins (2,22).

Poxvirus Genomic Structure

Poxviruses have linear double stranded DNA genomes that range in size from 130 kbp (parapoxviruses) (165,221) to 300 kbp (avipoxviruses) (110). Vaccinia virus, the prototypic orthopoxvirus, has a genome of nearly 190 kbp and encodes approximately 185 unique, nonoverlapping open reading frames (ORFs) of more than 65 amino acids which are expressed from both strands of DNA (89). The two strands of all poxvirus genomic DNAs are joined by hairpin loops, forming a covalently continuous nucleotide chain (17,83). Inverted terminal repetitions (inverted terminal repeats, ITRs) which are identical but oppositely oriented are present at both ends of the genome (80,316). Some poxvirus ITRs include coding regions, often resulting in the presence of diploid copies of individual genes at both ends of the genome.

Conservation of the central portion of the poxvirus genome exists among viruses across poxvirus genera but not across subfamilies. Genes located within this central core region of the genome generally encode components essential for virus growth and include the DNA polymerase, enzymes responsible for nucleotide metabolism, transcription factors, and structural proteins. Because these genes are absolutely required for

productive infection under all conditions, genes located within the conserved, central region of the genome are often referred to as "housekeeping genes." In contrast, much genetic variability exists within the ITRs at the termini of the various poxviruses. Genes located within these regions of the poxvirus genome are typically not essential for virus growth in tissue culture, but the vast majority have been shown to play a role in promoting virus spread during infection of animals. These include many proteins which interfere with the host innate response to infection such as inflammation mediated by complement, interferon, cytokines and chemokines (8,259).

Molecular Biology of Poxviruses

Poxvirus morphology. Poxviruses are the largest animal viruses and are visible using light microscopy (38). Vaccinia virus virions appear by cryoelectron microscopy as smooth, brick shaped structures of approximately 350 nm by 270 nm (66). Fixed and stained thin sections of virions reveal a membrane-bound, dumbbell-shaped nucleoprotein core which contains the viral supercoiled DNA and associated proteins together with trypsin-sensitive structures termed lateral bodies, the function of which is not known (56). The core and lateral bodies are surrounded by glycoprotein-studded lipid bilayers.

Virus attachment and entry. Study of the method of entry of poxviruses into a host cell is complicated by the fact that the viruses exist in two major forms, both of which are infectious. Intracellular mature virus (IMV) represents the majority of infectious virus and is thought to be contained within a single lipid bilayer (105). IMV remains within the cytoplasm throughout infection and is mechanically released upon cell

lysis. Extracellular enveloped virus (EEV) consists of an IMV particle with an additional outer membrane containing at least 10 proteins which are absent from IMV, including the viral hemagglutinin (HA) (202). The percentage of IMV versus EEV produced during infection depends on both the virus strain and the type of cell infected. While both IMV and EEV are infectious, it is thought that EEV is more important for spread of infection in animals and tissue culture cells (203). Primarily, the outer membrane of EEV is thought to protect the virus from immune attack, as EEV, but not IMV, is resistant to neutralization by antibodies (111,295).

A round of poxvirus replication begins with binding of the virus to the host cell by a poorly understood mechanism that likely involves association with one or more cellular chemokine receptors (130) (Figure 1). The existence of a unique viral attachment protein has not been established, but a recent study indicates that IMV and EEV attach to different cellular receptors (298). Entry of IMV into the host cell is thought to occur in a pH-independent fusion process which takes place at the plasma membrane (45,64,296). Entry of IMV into the cell releases the DNase-resistant, membrane-bound nucleoprotein core into the cytoplasm. In contrast, EEV enters the cell by an endocytosis event that requires low pH to disrupt the EEV outer membrane, allowing IMV to fuse with the endosome membrane and release the nucleoprotein core into the cytoplasm (296).

Virus gene expression. Viral early mRNA expression occurs immediately upon release of the virus core into the cytoplasm and is directed by a DNA-dependent RNA polymerase complex present within the infecting virion (176). This 500 kDa RNA core polymerase complex is comprised of two large and six small virally encoded subunits and contains all of the activities necessary to initiate nonspecific RNA transcription from any

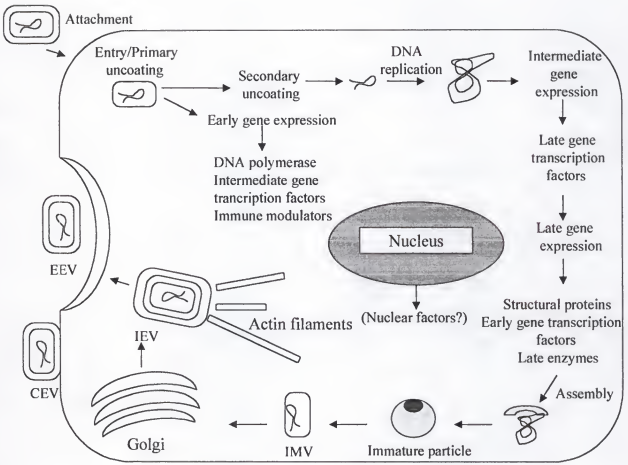

Figure 1. **Poxvirus replication cycle**. The major events that take place during a single round of poxvirus replication are depicted. Abbreviations: IMV, intracellular mature virus; IEV, intracellular enveloped virus; CEV, cell-associated enveloped virus; EEV, extracellular enveloped virus.

single stranded DNA template (176). Specificity for targeted transcription from poxvirus early gene promoters requires the early transcription factors RAP94 (94 kDa RNA polymerase associated protein) and VETF (vaccinia early transcription factor) in addition to the core RNA polymerase (5) (140). Early gene transcription is initiated at a purine nucleotide generally 12-17 nucleotides downstream of a conserved core early promoter sequence (59). Termination of early gene transcripts occurs 50-70 bases downstream of the termination sequence UUUUUNU and is dependent on the viral polymerase, VETF, and the viral capping enzyme (222,254). Following termination, the 3' ends of early mRNA are polyadenylated and the 5' ends are capped, activities which are again performed by viral enzymes (82,153,176,255). These capped and polyadenylated transcripts, which are ultimately modified in a fashion to be indistinguishable from eukaryotic transcripts, are released from the viral core into the infected cell cytoplasm. Splicing does not take place in any class of poxvirus mRNA. However, the presence of cryptic splice sites in several poxvirus genes has been detected (R. Moyer, unpublished results). Transcripts made at early times post infection are translated into a variety of proteins, including proteins necessary for further uncoating of the virus core, growth factors and immune modulators, and the enzymes and factors necessary for viral DNA replication and intermediate gene transcription.

Following early gene expression, a more complete second phase of uncoating releases a DNase-sensitive nucleoprotein core into the cytoplasm. Intermediate gene transcription, as well as viral DNA replication (discussed below), ensues after release of the core into the cytoplasm. Synthesis of the intermediate class of genes depends on the presence of *trans*-acting factors produced at early times post-infection and on DNA

replication, but is independent of *de novo* protein synthesis following DNA replication. Currently, five intermediate genes (A1L, A2L, GK1, I8 and I3) have been identified, three of which (A1L, A2L, GK1) are known to encode late gene transcription factors (122,304). No consensus intermediate gene promoter sequence has been demonstrated to date, however the factors necessary for intermediate transcription are known (302,303). These include the viral RNA polymerase, the virus capping enzyme mentioned above, and virus intermediate transcription factors (VITF)-1 and 2 (223). Of these factors necessary for intermediate gene transcription, one, VITF-2, is known to be a cellular protein as it can be purified from uninfected cells (224). To date, little is known regarding the mechanism of intermediate mRNA transcript termination. The capped intermediate transcripts are heterogeneous with typical 3' poly A ends as well as 5' poly (A) heads of up to 30 bases in length (16). The 5' poly (A) heads are thought to result from an RNA polymerase slippage mechanism (175), but their function, if any, is unknown.

Transcription from late viral promoters occurs following DNA replication and the accumulation of intermediate gene products, and has been detected for up to 48 hours following the synchronous infection of tissue culture cells (190). Many late proteins, including the major virion components, accumulate in large amounts during this long period of late gene expression. Other late proteins include factors necessary for early gene transcription which become packaged in the maturing progeny virions. Transcription of late genes requires a complex of the viral RNA polymerase and several late transcription factors produced from intermediate genes. Late gene promoters are comprised of a core sequence of approximately 20 bp containing a series of consecutive

A or T residues, separated by a region of about 6 bp from a highly conserved TAAAT element within which transcription initiates (27,60,225). Similar to intermediate viral mRNA, late mRNAs have capped, heterogeneous 5' ends containing 35-50 nontemplated polyadenylate residues that are thought to result from RNA polymerase slippage occurring at the AAA sequence within the late gene promoter (6,28,200,238). In addition, late mRNAs have heterogeneous 3' ends indicating that late gene transcription does not terminate uniformly. Since both strands of DNA are transcribed late during infection, significant levels of double stranded RNA (ds RNA) accumulate during this time.

Virus DNA replication. In cells synchronously infected with vaccinia virus, DNA replication begins 1-2 hours after infection and proceeds for at least 10 hours (282). Replication results in the production of nearly 10,000 genome copies per cell (118). Viral DNA replication occurs within electron-dense regions of the cell cytoplasm termed viral factories or virosomes. The cytoplasmic site of replication and the ability of the viral DNA to replicate within enucleated cells indicates that the virus provides most if not all of the machinery necessary for replication (205). The viral DNA polymerase is found as a monomer of 110 kDa and possesses both polymerase and 3'-5' exonuclease activity (76,283). Replication is thought to initiate by the introduction of single stranded nicks near the telomeres within the ITRs. Therefore, nicking can occur at either or both ends of the genome. Nicking results in the formation of an exposed 3' end which is used as a primer for strand extension by the viral polymerase. Elongation of this strand displaces the complementary strand which is used as a template for nascent strand synthesis. The replicated DNA strand then folds back on itself and copies the remainder of the genome.

Replication results in the production of large concatemeric intermediates with multiple genomes organized in tail-to-tail and head-to-head arrangements (181). Concatameric molecules are resolved into unit length genomes after the onset of late gene transcription through a process known as telomere resolution which is mediated by the viral resolvase (269).

Formation of virions and release from the cell. The initial stages of virion morphogenesis occur in the electron dense poxviral factories. Staining of thin sections of infected cells with DNA specific indicators reveals large quantities of DNA present in what has been termed the "viroplasm" within these factories. The first evidence of virus assembly is the presence of crescent-shaped membranous structures which will eventually form the envelope of the IMV particle (55). The origin of these crescent membranes is still under debate. Historically, it had been thought that these viral membranes are formed *de novo*. However, later studies using labeled antibodies specific for several subcellular compartments indicated that these membranes are derived from cisternae of the intermediate compartment between the endoplasmic reticulum and the Golgi stacks (261). More recent work demonstrates that crescents within poxvirus factories contain a single membrane that can form in the absence of host organelle membranes (105). Regardless of their origin, the crescent membranes assemble around viroplasm to form spherical, immature particles containing a granular center. Following production of the immature particles, the viroplasm within the particle condenses to form a dense nucleoprotein core embedded in a granular matrix. Some studies suggest that the nucleoprotein enters the immature envelopes just before they are completely sealed (173).

At this stage of virion morphogenesis, the progeny IMV particles are fully infectious. These virions move out of the assembly areas to the cell periphery where a fraction will become wrapped by additional membranes derived from the trans-Golgi or early endosomal network that contain viral proteins destined to be in EEV. These wrapped particles, known as intracellular enveloped virus (IEV), are transported along actin-containing microfilaments to the plasma membrane (53). Fusion of IEV with the plasma membrane results in the externalization of the particle, with loss of the outermost Golgi-derived membrane. Only a small percentage of the virus which is secreted from the cell is released as EEV. The majority of the virus adheres to the external cell surface and is called cell-associated enveloped virions (CEV).

Poxvirus Infections of Social and Economic Importance to Man

Variola. The orthopoxvirus variola is the causative agent of smallpox, which at its zenith, was endemic throughout the inhabited world with the exception of Australia and certain islands (38). Two strains of smallpox virus have been distinguished based on the severity of the disease and the mortality rate: variola major and variola minor. The case fatality rate of variola major was usually 20% to 30% while variola minor was rarely associated with a case fatality rate of more than 1%. People of all ages were susceptible to infection with variola, and one attack of smallpox gave almost complete immunity to re-infection. Because there is no efficient animal reservoir for variola, a successful campaign by the World Health Organization was able to eradicate smallpox and the last reported case occurred in Somalia in 1977.

There are many excellent reviews describing smallpox infection in man (72-74). The following is a brief description of the typical course of smallpox infection. The incubation period following infection with either strain of variola was between 10 and 14 days. The onset of sickness was acute, with fever, malaise, headache and backache. On the third or fourth day following the onset of symptoms, the characteristic smallpox rash appeared, first on the buccal and pharyngeal mucosa, the face, the forearms and hands which later spread to the trunk and lower limbs. The lesions of the rash began as macules, which soon became firm papules and then vesicles that quickly became opaque and pustular following the influx of inflammatory cells. At about 8 or 9 days after the onset of the rash, the pustules became umbilicated and dried up and eventually formed scabs. In addition to the ordinary type smallpox described above, two other forms of smallpox were recognized. The rare hemorrhagic-type smallpox, most common in pregnant women, was associated with bleeding from the conjunctiva and mucous membranes, severe toxemia, and early death, often before development of the rash had occurred. Flat-type smallpox was also characterized by severe toxemia, but was associated with a delay in the appearance of the rash and the slow development of the skin lesions, which were usually flat and soft. This form of smallpox was often seen in individuals with defects in cell-mediated immunity and was associated with a high mortality rate.

Monkeypox virus. Monkeypox virus, also a member of the orthopoxvirus genus, was first discovered in 1958 when it was isolated from smallpox-like lesions among captive cynomolgus monkeys at the State Serum Institute, Copenhagen (301). Between 1958 and 1968, a similar disease was described in several other captive monkey colonies

in Europe and the United States, but the disease has not been reported in captive monkeys since that time. In 1970, scientists learned that a smallpox-like disease affecting humans living in tropical rain forest areas of the Democratic Republic of the Congo was caused by monkeypox virus. Several outbreaks of monkeypox virus have occurred since 1970, with all of the cases being localized to small villages within the rain forest regions of western and central Africa. Clinically, monkeypox infections in humans resembles smallpox, with affected individuals displaying a pustular rash, fever, respiratory symptoms and marked lymphadenopathy. In contrast, monkeypox in humans who were vaccinated against smallpox typically results in a milder form of the disease. Investigation of monkeypox outbreaks in humans revealed that thirty percent of the cases occurred in June, July or August coinciding with the period of greatest outdoor activity such as farming and hunting (184). Monkeypox is known to naturally infect at least eight species of primates and four species of squirrel, and it is thought that these animals serve as a reservoir for the virus in the wild (73).

Molluscum contagiosum virus. Molluscum contagiosum virus (MCV) is the only member of the molluscipoxvirus genus. Although worldwide in its distribution, molluscum contagiosum (MC) has been frequently encountered as an easily treatable disease and has rarely been a cause of serious morbidity. The disorder mainly affects children, sexually active adults and immunocomprimised individuals. Epidemiologic studies suggest that transmission may be related to factors such as warmth and humidity of the climate as well as poor hygiene (68). Transmission of MCV in children is thought to occur by intimate skin-to-skin contact whereas in adults, MCV is most often transmitted by sexual contact. MCV causes a benign tumor on the skin which averages

between 3.0-5.0 mm in diameter, although giant lesions of up to 1.5 cm have been reported (91). The number of lesions in a given individual is usually less than 30, but up to 100 lesions may coalesce to form a plaque (91). Untreated lesions in immunocompetent individuals usually resolve within several months, although they may persist as long as five years. Since 1980, MC has been recognized as a common disorder among the HIV infected population. The prevalence of MC in HIV infected individuals is estimated to be as high as 5-18% (157). The severity of MC in HIV-infected patients has been shown to be inversely related to the CD4+ lymphocyte count (127). MCV has proven to be difficult to study in the laboratory, as no cell culture or animal model investigated to date can support MCV replication (248). In fact, MCV has the narrowest tissue tropism of any poxvirus, as it is only able to replicate in the human epidermis (38). Recently, the complete genome sequence of the type 1 subtype of MCV was reported (245). Analysis of the predicted MCV ORFs revealed that the virus encodes homologues of all orthopoxvirus genes known to be essential for virus replication (246). However, the virus was found to lack many of the genes that allow orthopoxvirus replication in resting cells, perhaps explaining the restriction of MCV productive infection to the metabolically active keritinocytes of the human epidermis (246). In addition, the MCV genome was shown to lack genes encoding homologues of many of the orthopox- and leporipoxvirus proteins necessary for modulating the host immune response to infection. However, the virus appears to encode several unique proteins unique which are predicted to allow the persistent infection of MCV in the absence of inflammation (246).

Myxoma virus. Myxoma virus is the most well known member of the genus leporipoxvirus. Two strains of myxoma virus are endemic in certain rabbit populations.

One strain is maintained in *Sylvilagus brasiliensis* (tapeti) in South America, while the second strain is maintained in the bush rabbit *Sylvilagus bachmani* in the western regions of North America. In its native host, myxoma virus is transmitted mechanically by arthropod vectors and causes a localized infection characterized by benign fibromas of the skin. In contrast, myxoma virus causes a rapid and fatal disease known as myxomatosis in the European rabbit (*Oryctolagus cuniculus*) which has been the topic of many excellent reviews (73,74,77). The disease in the European rabbit is characterized by extensive fulminating internal and external lesions and severe immunodysfunction accompanied by secondary Gram negative bacterial infections of the respiratory tract (77). Because of the high mortality associated with myxoma virus infection of European rabbits, the Australian government released the South American strain of myxoma virus into the wild in 1950 in an attempt to control the feral rabbit population in that country. The virus was able to suppress the numbers of European rabbits in Australia for nearly thirty years. However, over time, the rabbit population once again began to increase as rabbits became resistant to the disease and attenuated virus strains arose from within wild populations of *O. cuniculus*. Today, myxoma-resistant rabbit populations in Australia approach the levels found before the original virus release. Recently, a study was published which explored the basis of myxoma virus attenuation and rabbit resistance to infection and provides insight into the co-evolution of the virus and its host (30).

Vaccinia. The prototypical member of the orthopoxvirus genus, vaccinia virus is the most widely characterized member of the poxvirus family and the agent used in the vaccination effort responsible for the eradication of smallpox. Vaccination involved the introduction of approximately 10^8 pfu of virus into the deltoid. A papule appeared at the

vaccination site 4 to 5 days after vaccination, which became vesicular 2 to 3 days later. The lesion contents rapidly became turbid due to the infiltration of inflammatory cells, and the central lesion became red and enlarged, reaching its maximum diameter by the 9th or 10th day. Draining lymph nodes became swollen and patients usually developed a minor fever. The pustule dried from the center outward, and the scab which then formed sloughed away after approximately 3 weeks, leaving behind a scar which to this day is the hallmark of vaccination against smallpox. Complications to routine vaccination were rare, but included progressive vaccinia (vaccinia necrosum), eczema vaccinatum, generalized vaccinia and postvaccinal encephalitis (74). Routine vaccination of the general population was discontinued in 1971 and currently only military personnel and laboratory workers are required to be vaccinated against smallpox.

Much of what is known about poxvirus replication was discovered by studying vaccinia, which has a wide host range and can infect many cell types. In addition, because of its ability to elicit a strong humoral and cell-mediated immune response, as well as the large size of its genome which can accommodate many foreign genes, researchers are studying the ability of vaccinia virus to be used as a recombinant vaccine vector (276).

Poxvirus Replication and Spread in the Host

Poxviruses can cause either a localized, self-limiting infection associated with little dissemination from the initial site of inoculation as is the case with Molluscum contagiosum, or they may cause a generalized, systemic disease associated with a high mortality rate, as is seen following infection of humans, rabbits and mice respectively

with variola, rabbitpox virus or ectromelia virus. In some cases, the same virus can be responsible for causing both types of disease patterns but in different host species. For example, myxoma virus causes only localized benign fibromas in its native host, *S. brasiliensis* (tapeti), whereas infection of the European rabbit (*O. cuniculus*) causes the rapid and fatal systemic disease myxomatosis. Because I have restricted my work to studying rabbitpox virus (RPV) which is associated with systemic infection of the rabbit, only the pattern of poxvirus disease caused by that virus will be discussed in detail.

Collectively, poxviruses have been shown to utilize all possible routes for infecting the host (38). Infection via the skin likely occurs through microscopic abrasions which allow the virus access to the epidermal or dermal layer. Some poxviruses, including myxoma virus, depend on arthropod vectors for mechanical transmission of the virus through the skin. Virus is carried in the biting mouthparts of the insect and deposited in the epidermis or dermis of the host during a bloodmeal. Infection via the respiratory tract has been demonstrated for variola, rabbitpox, vaccinia and ectromelia viruses. In fact, epidemiological evidence suggests that smallpox was transmitted in excretions from the mouth or nose by face-to-face contact. RPV is highly infectious by the respiratory route, with 1 PFU sufficient for causing disease (26). The oral route of infection has been demonstrated for ectromelia virus infection of mice and is probably the result of cannibalism of infected mouse carcasses. However, this route is not thought to be of major importance in the natural infection of mice by the virus.

Probably the best studied animal models for systemic orthopoxvirus dissemination and disease in the host are myxoma and rabbitpox in rabbits and mousepox (ectromelia) in mice. Studies in these animals produced nearly identical results

suggesting common themes in the ability of poxviruses to cause disease. Because the pattern of spread of rabbitpox virus in the rabbit is thought to be similar to that which occurs for other poxviruses in their hosts and since I have restricted my work to the use of RPV, a brief description of the pathogenesis of rabbitpox virus will be given here. For more thorough reviews, see (38) and (26).

Rabbitpox Virus

Rabbitpox virus was first reported in 1932 when it was shown to be responsible for a spontaneous epidemic of a smallpox-like disease within a breeding colony of rabbits housed at the Rockefeller Institute for Medical Research (95). Within two weeks, one hundred percent of the colony had been infected and forty six percent had died. While the exact origin of the virus is not known, a neurovirulent strain of vaccinia was being used to infect rabbits in common areas of the breeding facility. Epidemiological studies suggest that this virus was the source of RPV, as do sequence comparisons which show 99% nucleotide homology between RPV and vaccinia virus (31).

The outbreak of rabbitpox virus within rabbit colonies resulted in excellent documentation of the progression of the disease (96-98). Clinically, rabbitpox infection of rabbits was shown to resemble smallpox infection in humans. Onset of disease was associated with malaise and fever in conjunction with enlargement of the popliteal and inguinal lymph nodes. At two to three days post infection, papules or lesions formed on all parts of the animal which eventually became umbilicated and necrotic. Infection of the upper respiratory tract often occurred which was accompanied by edema in the lungs resulting in dyspnea and obligate mouth breathing. Many of the animals developed

conjunctivitis associated with nasal mucopurulent discharges, sometimes stained with blood. Death occurred within 8-10 days in nearly fifty percent of the cases.

In laboratory studies, rabbitpox has been shown to be an acute severe generalized infection, the principle features of which are independent of the route of administration of the virus (26). Following intradermal inoculation, there is a lag or incubation period of approximately two to three days during which time the virus replicates at the local site of infection. Initially, virus is found only at the inoculation site. However, virus soon enters the lymphatics and reaches the draining lymph node as early as 36 hours post infection (26). Multiplication of virus in the lymph node and the constant generation of virus from the primary inoculation site results in necrosis of the cells of the lymph node and the passage of virus through the efferent lymphatics to the blood stream in what is termed a primary viremia. Virus within the blood is associated with the lymphocyte fraction suggesting that during viremia, virus is not free but is cell-associated (26,313). Spread of the virus through the bloodstream results in the invasion of internal organs, including the bone marrow, spleen and liver, within 2 to 3 days after infection. In the spleen, virus has been shown to infect lymphocytes, while in the liver, Kupffer and paranchymal cells become infected (171). Necrosis of these infected cells releases virus directly into the bloodstream. By day 4 or 5 post infection, this release of virus exceeds the capacity of the reticuloendothelial system to dispose of it, and virus is once again detected in the blood creating a "second viremia". Concurrent with this is the onset of fever which likely arises due to the inability of the spleen to clear the virus and the resulting systemic infection. Characteristic signs of infection, including nasal and conjunctival discharges, weakness and lack of interest in food and water usually appear

within 2-3 days of the onset of fever (26). During this period of secondary viremia, infectious virus can be detected in most tissues examined including the bone marrow, intestine, nasal mucosa, ovary, vagina, uterus and skin (71). In the skin, virus multiplies rapidly in the cells of the epidermis, hair follicles, and sweat glands, and skin lesions appear which become ulcerated within a few days (38). It is at this stage of illness when large amounts of virus are released into the environment that the animal is most infectious. Death can occur as early as day 6 post infection in rabbits showing pronounced respiratory distress. More commonly it occurs between the 8^{th} and 12^{th} days when it is frequently preceded by a sharp decrease in body temperature associated with a severe drop in blood pressure and a rise in serum potassium concentrations to levels shown to be lethal in experimental models (26). Animal survival is associated with but not dependent on the presence of circulating antibody which prevents the infection of new cells and virus content in all tissues and organs falls rapidly (71). Scabs form on the lesions which resolve between days 10 and 12 leaving behind scarring.

Poxvirus Immune Modulators that Counteract the Host Early Response to Virus Infection

Members of the Poxvirus family possess large DNA genomes which range in size from 130 to 300 kbp. Because the viruses replicate exclusively in the cytoplasm of infected cells, much of the virus genome is devoted to encoding the factors necessary for autonomous DNA synthesis and gene expression. Still, the study of natural occurring deletion mutants of vaccinia virus in addition to analysis of engineered virus mutations has revealed that at least 15% to 28% of the virus genome is not required for virus replication in tissue culture (206). The vast majority of these genes which are

"nonessential" for virus replication in tissue culture encode factors that enhance virus infection and spread within the host. While some poxviruses are capable of establishing persistent infections in susceptible hosts, members of the virus family generally cause acute primary infections that often result in lifelong immunity to re-infection. The ability of the host to mount an effective response to infection by poxviruses relies heavily on the nonspecific arm of the immune response which is present at the time of the host's primary exposure to the virus. In turn, poxviruses have evolved to encode a large number of proteins that interfere with the early host mechanisms of anti-viral immunity thus enabling efficient progeny virus replication and spread throughout the infected organism. Current models propose that the genes encoding these poxvirus immunomodulatory proteins were initially acquired from host cells, a hypothesis which is supported by the high degree of homology between many of the virus proteins and their cellular counterparts. In this section, the key components of the host innate immunity will be addressed along with the poxvirus gene products which serve to counteract each of the nonspecific elements. For a more thorough review, see reference (38).

Following infection with a virus, the host's first response involves the innate, or nonspecific components of immunity, including the induction of interferons, the alternative pathway of complement, inflammation, natural killer cells, and apoptosis. This is followed at later times by the action of the learned responses which include delayed type hypersensitivity, anti-viral cytotoxic T lymphocytes (CTLs) and virus-specific antibodies. Although no specific immune response to poxvirus infection can be detected until approximately 8 days after infection, studies have shown that the

nonspecific components of the immune system are activated almost immediately following infection.

Interferons. One of the earliest host responses to viral infection is the production of interferons. Type I interferons (IFNs), which include IFNα and IFNβ, can be induced by viral infection of virtually all cell types. In contrast, IFNγ, the only Type II IFN, is solely produced by activated T-lymphocytes and natural killer (NK) cells (for a more thorough review, see reference (117)). In tissue culture, local interferon generation has been shown to protect neighboring cells from productive virus infection resulting in the establishment of an antiviral state in surrounding cells. Studies in cell culture have shown that pre-treatment of cells with interferon prior to infection leads to an abortive infection (87). The secreted proteins act in an autocrine and paracrine fashion by binding to specific cell receptors triggering signal transduction and transcription of IFN-responsive genes. Two genes expressed in response to interferon encode enzymes which are in part responsible for the antiviral effects of the cytokine. The dsRNA-dependent protein kinase PKR, and the 2',5'-oligoisoadenylate synthetase are both produced as latent forms in response to interferon stimulation, but are activated following exposure to double stranded RNA produced during virus infection. Upon activation, PKR is responsible for phosphorylating the small subunit of eukaryotic initiation factor 2 (eIF2α), inactivating the factor and leading to inhibition of translation (231). The 2',5'-oligo A synthetase catalyzes the synthesis of a family of oligonucleotides derived from ATP which collectively activate latent RNase L. RNase L functions to cleave cellular and viral single-stranded RNA. The end result is the inhibition of mRNA translation in infected cells (32,119,168). In addition to establishing an antiviral state, interferon is able

to upregulate expression of MHC molecules on the surface of infected cells, which allows enhanced detection of viral peptides by effector cells of the immune system. While IFNγ is able to upregulate expression of both MHC class I and II molecules, IFNα and β can only exert an effect on MHC class I regulation (117).

In addition to the general effects of interferons listed above, IFNγ also serves as a potent immunoregulatory cytokine (70). IFNγ is a powerful activator of macrophages, which in turn produce the important pro-inflammatory cytokines TNFα and IL-1β, as well as reactive nitrogen intermediates (RNIs) which function to allow more effective intracellular pathogen killing (62). IFNγ has also been shown to induce nitric oxide synthase (NOS) production in activated macrophages, leading to enhanced production of nitric oxide and inhibition of viral replication (121).

Studies have shown that poxvirus infection efficiently induces interferon production both in infected animals and in tissue culture (86-88). This likely occurs following the production of double stranded RNA, a potent interferon inducer, during the late period of gene expression in poxvirus infected cells. During poxvirus infection, increased levels of all types of interferons can be detected in the serum as well as in cells taken from the site of infection, indicating that interferons are an important host response in combating the infection (270). Experiments have shown that treatment of mice with anti-interferon antisera resulted in a significant increase in the amount of virus recovered from infected animals (114). In addition, administration of alpha or beta interferon to animals prior to infection has been shown to decrease the severity of the disease as well as the mortality rate (38). Treatment of mice with monoclonal IFNγ antibodies resulted in lethal infection by vaccinia, a virus which is normally effectively cleared by the

murine immune system (230). The specific importance of IFNγ in the resolution of poxvirus infection is exemplified by the finding that athymic nude mice, which are normally incapable of clearing vaccinia virus infection, mount an effective immune response to infection of a VV recombinant expressing IFNγ (126,215).

Several poxvirus genes are responsible for specifically counteracting the effects of interferon during infection (Fig. 2). Two poxvirus proteins inhibit the interferon-induced block in mRNA translation. By binding and sequestering double stranded RNA produced during infection, the protein product of the E3L gene prevents activation of the 2',5'-A synthetase. The mechanism of E3L action and its effect on productive infection will be described in a later section. The product of the vaccinia virus K3L gene shares homology with eIF2α, the target of the dsRNA-induced PKR. The vaccinia protein acts as an alternative phosphorylation substrate for the protein kinase, thus preventing inactivation of eIF2α and relieving the block in RNA translation. Studies have shown that deletion of the vaccinia K3L gene results in the increased sensitivity of virus-induced protein synthesis and virus replication to interferon (25).

In addition to blocking the downstream effects of interferon signalling in infected cells, many poxviruses encode soluble interferon receptors which are able to bind the cytokine prior to engagement of the cell receptor. Genes encoding secreted IFNγ receptors (IFNγRs) have been discovered in the leporipoxviruses myxoma and shope fibroma viruses, as well as the orthopoxvirus members vaccinia, variola, CPV, RPV, and ectromelia (89,155,177,250,293,294). The myxoma M-T7 protein is the most studied poxvirus IFNγR, and has been shown to share 30% amino acid identity with the extracellular, ligand-binding domain of the cellular IFNγ receptor α chain (177). The

Figure 2. **Poxvirus proteins that interfere with the host early immune response.** See text for specific details. Abbreviations: CC, CC chemokine; R, receptor; NK, natural killer; IFN, interferon; TNF, tumor necrosis factor; IL, interleukin; V, viral; CCBP, CC chemokine binding protein; exp'n, expression; PKR, protein kinase R; ICE, interleukin-1β converting enzyme; RCA, regulator of complement activation; MHC, major histocompatability complex.

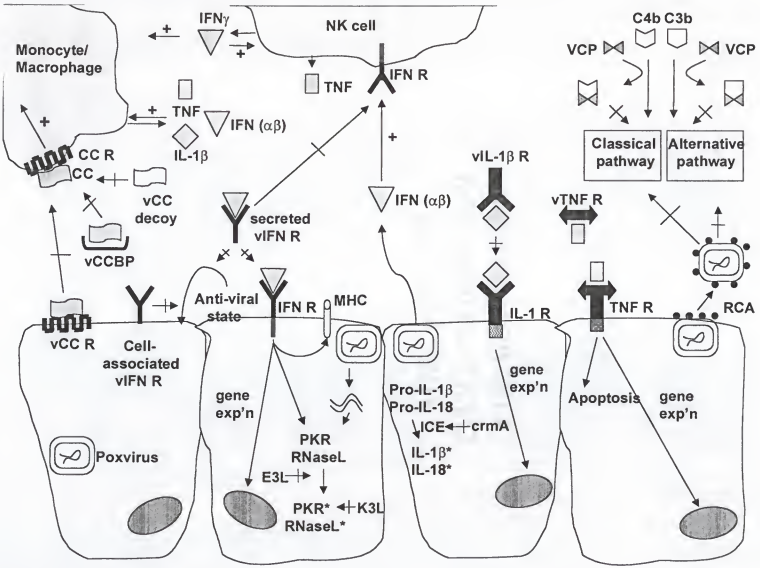
Monocyte/
Macrophage
IFNγ
NK cell
TNF
IFN R
TNF
IFN (αβ)
IL-1β
CC R
CC
vCC
decoy
vCCBP
secreted
vIFN R
IFN (αβ)
vIL-1β R
C4b C3b
VCP
VCP
Classical
pathway
Alternative
pathway
vTNF R
vCC R
Cell-
associated
vIFN R
Anti-viral
state
IFN R
MHC
IL-1 R
TNF R
RCA
gene
exp'n
PKR
RNaseL
E3L
PKR*
RNaseL*
K3L
Poxvirus
Pro-IL-1β
Pro-IL-18
ICE
crmA
IL-1β*
IL-18*
gene
exp'n
Apoptosis
gene
exp'n

protein is expressed early during infection and following secretion, accumulates as a stable, soluble glycoprotein capable of binding gamma interferon with high affinity in a species-specific manner (180). Deletion of M-T7 from myxoma resulted in severe attenuation in animals which was associated with decreased rabbit mortality and reduced virus dissemination from the primary site of inoculation (179).

Several poxviruses, including vaccinia (strain WR), CPV and ectromelia, have been demonstrated to produce a functional interferon α/β receptor during infection (52,273). Studies have shown that the vaccinia receptor, known as B18R, is able to bind and functionally inhibit IFNα (52,142,273). In contrast to the poxvirus IFNγRs, B18R is found both in secreted and cell-associated forms, suggesting that the protein may act not only to sequester IFNα thus preventing cell binding, but also may interfere with signal transduction mediated by IFNα receptor binding by functioning as a cytokine sink (289). Natural and engineered vaccinia virus B18R mutants are attenuated in mice, suggesting a role for the protein in mediating virulence *in vivo* (273).

Complement. The complement system is composed of a group of proteins that are normally present in the serum in an inactive state (1,104). When activated, these proteins participate in a coordinated series of reactions which lead to the formation of a membrane attack complex which is capable of cell membrane lysis, as well as the production of C5a, a factor which is chemotactic for neutrophils. The complement cascade can be activated by different mechanisms involving two separate pathways: the classical pathway and the alternative pathway. The classical pathway depends on the formation of antibody-antigen complexes for initiation, while the alternative pathway is initiated by the presence of complement component C3b, generated spontaneously at low

levels or as a by-product of the classical pathway. Execution of both pathways result in the formation of C3 convertase which promotes activation of C5 convertase which is responsible for catalyzing reactions leading to the assembly of the membrane attack complex.

In addition to formation of the membrane attack complex and lysis of infected cells, complement can lead to the efficient opsonization of foreign particles (1). Opsonization can take place following covalent attachment of C3 degradation products to the foreign particle. Bound C3 is then recognized by C3 receptors on leukocytes enhancing phagocytosis of the foreign particle by these cells.

Three complement proteins (C3a, C4a, and C5a) are anaphylatoxins, and are able to induce the release of mediators from mast cells which cause rapid increases in vascular permeability (1). C3a and C4a receptors are expressed on mast cells, basophils, smooth muscle cells and lymphocytes while C5a receptors are found on mast cells, basophils, neutrophils, monocytes/macrophages and endothelium. The major effects of anaphylatoxin binding to mast cells and basophils are granule exocytosis and release of vasoactive mediators, such as histamine, which increase vascular permeability and stimulation of smooth muscles. In addition, C5a is a potent chemokine and is able to stimulate neutrophil migration and at high doses is able to cause respiratory burst and the production of reactive oxygen intermediates. The combined action of these factors contributes to inflammation at the site of complement activation.

Because of the many effects of complement activation, regulation of the complement cascades are tightly regulated *in vivo*. Most of the regulation centers on the formation of C3b and C4b, components crucial for activation of the downstream effectors

of both complement pathways. Complement activation on host cells is inhibited by several membrane regulators of complement activation, or RCA. The activity of RCA molecules are restricted to complement components of the same species. In addition to these membrane bound regulatory proteins, soluble factors exist which serve to bind and sequester activated complement components.

Complement has been shown to be an important host response to poxvirus infection. *In vitro* studies have demonstrated that vaccinia virus can be neutralized by the addition of a heat labile component of serum (complement) following the binding of antibody to the virus (65,90). In a cell culture model, activation of the alternative complement cascade has been demonstrated in fowlpox virus (FPV) infection of chicken embryo cells as early as three hours post infection, which was associated with an increased killing of FPV-infected cells and a decrease in virus CPE and progeny virus yield (191). Activation of the alternative pathway has also been demonstrated following vaccinia virus infection of murine tumor cell lines (305) and a human melanoma cell line (193). In particular, the alternative complement pathway appears to play an important role in combating poxvirus infection *in vivo*. By-products of the alternative pathway have been demonstrated at 6 days following infection of chickens with FPV. Depletion of circulating factor C3 by pre-treatment of chickens with cobra venom factor prior to FPV infection resulted in an increase in the level of progeny virus recovered from lesions, a decrease in the lesion-associated inflammatory response, and a 100% mortality rate (192). These results clearly indicate that complement, especially the alternative pathway, is a host response to poxvirus infection which is important in combating disease.

Several members of the orthopoxvirus genera have been reported to encode proteins with homology to cellular complement regulatory proteins. The most widely studied of these poxvirus gene products is the vaccinia virus complement control protein (VCP). VCP is an abundant soluble protein which is secreted at late times post-infection (113). The protein shares 38% identity with the first half of mammalian C4-BP, a soluble protein that regulates the classical pathway by binding and sequestering complement component C4b (128). Unlike C4-BP, VCP is able to bind C3b as well as C4b and therefore is able to inhibit both the classical and alternative pathways (162). The protein has been demonstrated to play a role in vaccinia virus pathogenesis *in vivo* (113). VCP homologues have been identified in cowpox virus (CPV inflammation modulatory protein, IMP) and variola virus (variola smallpox inhibitor of complement enzymes, SPICE), and initial studies indicate that these proteins are also effective inhibitors of complement (169,170,226,249).

A second strategy of poxvirus complement evasion has recently been demonstrated for vaccinia virus. The virus has been shown to acquire cellular RCA molecules into the outer membrane of progeny EEV virions (297). These results help explain previous observations that EEV, but not IMV, is resistant to neutralization by antibody and complement (111,295,297).

Inflammation. Prior to the development of a specific immune response, the host reacts to a virus infection by mounting an inflammatory response consisting of vasodilation, edema and the influx of inflammatory cells (79). The first cells stimulated to the site of an infection in a naïve animal are polymorphonucleocytes (PMNs), followed approximately 24 hours later by cells of the monocyte/macrophage lineage. Each of

these cells are capable of engulfing and degrading foreign organisms. In addition, cells of the monocyte/macrophage lineage are then able to present foreign antigen on their surface for recognition by antigen-specific CTL, a step important for the generation of the late specific immune response. Leukocytes can be attracted to the site of an inflammatory response following a gradient of chemoattractants which are produced locally by resident macrophages, infected cells, or as a result of vascular reactions. Inflammatory cells, once present at the site of infection, are capable of mounting a number of responses able to limit virus spread including phagocytosis, the generation oxygen-dependent or independent antimicrobial products, and the release of cytokines. Cytokines are a family of related proteins important for the complex interplay of the elements of the immune system, including components of the inflammatory system. Cytokines are produced by many types of cells including monocytes/macrophages and lymphocytes, and can act in an autocrine or paracrine fashion by binding to specific receptors on the surface of target cells and stimulating signalling cascades. *In vivo*, cytokines play an integral role as mediators of natural immunity and function in the activation, growth and differentiation of lymphocytes, as regulators of immune-mediated inflammation, and as stimulators of leukocyte growth and differentiation.

Many studies have explored the effect of the inflammatory response on the progression of poxvirus infections. In general, the primary inflammatory response to infection was found to vary among the reported studies and was likely due to differences in the viruses used, inoculation methods, and size of the inoculum. Inflammation has been detected in the lesions following infection by vaccinia virus, shope fibroma virus (SFV), and some attenuated vaccine strains of FPV, but not virulent forms of ectromelia

virus or MCV (38). In the case of ectromelia virus, no inflammatory response was detected in the lesions of the liver until 7 days post infection, a time when the infection was well under way (11). In contrast, intradermal inoculation of guinea pigs with vaccinia virus resulted in redness and an infiltration of PMNs and mononuclear cells by 24 hours post infection (67). Similar results have been reported for vaccinia and rabbitpox virus infection of mice and rabbits (174).

Historically, the inflammatory response to poxvirus infection has been explored by studying the effects of infection of 12 day old chicken embryos, which lack mature B and T cells but possess other mediators of the inflammatory response as well as components of the complement system. Poxvirus infection of the egg at this time results in the formation of lesions (pocks) on the chorioallantoic membrane (CAM). RPV, CPV, and certain strains of vaccinia virus each produce red pocks following infection of the CAM. Examination of these pocks reveal areas of ectodermal hyperplasia, an increase in vascularization, and extensive vasodilation of the blood vessels with a complete absence of inflammation (198). During infection of the CAM, white pocks have been shown to occur spontaneously at a rate of 1% (75,81). Closer inspection of these white pocks revealed that the degree of vasodilation and congestion of the blood vessels was equivalent to that seen in the red pocks but in addition, a massive inflammatory cell influx was present comprised of activated heterophils (neutrophils), mononuclear cells and associated chemoattractants (49,198). The presence of the inflammatory response in the white pocks correlated with greatly reduced levels of virus antigen and progeny virus in the lesions compared to wild type virus pocks (198). However, despite the presence of a massive inflammatory response to infection by the white pock mutants, virus was still

able to travel to and infect the internal organs of the embryo indicating that while important, inflammation alone is not sufficient to clear a poxvirus infection (38). Genetic studies on the spontaneous white pock mutants have revealed deletions within the terminal regions of the genome (182). Researchers have since used the CAM assay as a tool to investigate the ability of specific gene products to block inflammation. Using this *in vivo* assay, researchers have discovered several poxvirus factors which are necessary for red pock formation on the CAM, including SPI-2/crmA and a TNF receptor homologue (197).

Many genes within the nonessential regions of the poxvirus genome are devoted to encoding factors important in countering the host inflammatory response. In particular, most poxviruses produce several proteins which function by binding host cytokines and chemokines, thereby inhibiting the activation and recruitment of effector cells to the site of infection. Several members of the poxvirus family encode proteins which function as secreted, soluble receptors to interferons (discussed above). Similarly, genes encoding secreted, soluble receptors of the cytokine tumor necrosis factor (TNF) have been demonstrated in several leporipoxvirus (MYX, SFV) and orthopoxvirus (CPV, VV, variola) family members (106,107,155,161,257,291). TNF is a potent cytokine produced by activated macrophages and T cells which functions during the inflammatory response by binding to specific receptors on the surface of target cells and initiating signalling cascades. The poxvirus proteins share homology with the mammalian TNF receptors, but lack the domains necessary for membrane insertion and intracellular signalling. Consequently, the poxvirus receptor homologues are able to efficiently bind and sequester the cytokine prior to its engagement of the target cell receptor. Several

lines of evidence suggest that TNF is an important host target during poxvirus infection. Deletion of the myxoma TNF receptor homologue T2 caused significant attenuation following rabbit infection (291). Furthermore, although the ITRs of variola virus are significantly smaller than the corresponding regions in other poxvirus members, the conservation of the TNF receptor homologue by the virus suggests a strong selective pressure for retention of the protein.

Interleukin-1 (IL-1) is a cytokine produced mainly by activated macrophages in response to infection and tissue injury. The pleiotropic cytokine mediates its effects by binding to distinct receptors on the surface of target cells resulting in signal transduction. The majority of the gene products which are expressed following IL-1 receptor binding have a direct role in the inflammatory and immune processes. Two forms of IL-1 exist, termed IL-1α and IL-1β, which produce similar biological effects but are mediated by interaction with distinct cellular receptors. In particular, regulation of IL-1β activity appears especially important for productive poxvirus infection given that the members of the virus family use two distinct strategies to inhibit the activity of IL-1β *in vivo*. The B15R gene of vaccinia and CPV encodes a secreted receptor that specifically binds and sequesters IL-1β (7,264). Like other poxvirus secreted cytokine receptors, the virus protein contains only the extracellular ligand binding domains and lacks the motifs necessary for intracellular signalling. *In vitro* studies have demonstrated that vaccinia B15R is an effective IL-1β inhibitor, as the protein is able to prevent IL-1β-induced lymphocyte proliferation (7,264). However, published studies have reported conflicting evidence regarding the role of the vaccinia B15R protein during infection *in vivo*. Intranasal infection of mice with a vaccinia B15R negative virus resulted in increased

morbidity but decreased mortality relative to wild type virus (7). In contrast, a second study reported that intracranial inoculation of mice with a vaccinia B15 null mutant resulted in a significant reduction in mortality relative to infection with wild type vaccinia (264). Still another study demonstrated that mice infected intranasally with a vaccinia B15R deficient virus exhibited an increased fever response compared to animals infected with the wild type virus, suggesting that IL-1β is responsible for the fever response during vaccinia virus infection (9).

Another method used to regulate IL-1β activity during poxvirus infection is the inhibition of interleukin-1β converting enzyme (ICE, caspase 1) by the orthopoxvirus serpin crmA (discussed in more detail in a later section). ICE/caspase 1 is a cysteine proteinase which is responsible for the proteolytic activation of IL-1β from its inactive pro-form. CrmA acts as a pseudosubstrate for ICE/caspase 1, forming a stable inhibitory complex with the proteinase which renders the enzyme inactive and thus unable to activate IL-1β (217). In addition, because ICE/caspase 1 is responsible for the proteolytic activation of IL-18, this cytokine is also regulated by crmA (85). IL-18, also known as IFNγ-inducing factor, is a cytokine that functions to stimulate the production of IFNγ and to augment the lytic activity of NK cells. The inhibition of ICE/caspase 1 activity by crmA and the effects of crmA mutations on infection *in vivo* will be discussed below.

Chemokines represent a subfamily of the larger cytokine family. Members of this class of proteins share the ability to stimulate leukocyte movement (chemokinesis) and directed movement (chemotaxis). Historically, chemokines have been divided into groups, termed C, CC, CXC, and CXXXC (where C=cysteine and X=any amino acid), based on the spacing of conserved cysteine residues important for function. Like other

cytokines, chemokines mediate their function by binding to specific receptors on the surface of target cells. These serpentine chemokine receptors span the cell surface seven times and are coupled to G proteins in the cytoplasm. Unlike other cytokine receptors which are specific for a single cytokine, chemokine receptors generally bind to all members of a chemokine subfamily.

Poxviruses use at least two methods to inhibit chemokine action during infection. Myxoma, RPV, CPV, variola, racoonpox, and the Lister strain of vaccinia each contain genes encoding soluble chemokine binding proteins (CBPs) (92). Initial studies indicate that while the proteins are able to bind both CC and CXC classes of chemokines, the binding affinities are much higher for the CC chemokines (92,258). The poxvirus CBPs have been shown to block the interaction of CC chemokines with their cognate cell receptors in *in vitro* assays (131,258). *In vivo*, deletion of the gene encoding the RPV 35kDa CBP was associated with a greater inflammatory influx of monocytes and lymphocytes within the primary lesion than that seen during wt RPV infection (92).

Genes encoding proteins with homology to mammalian serpentine chemokine receptors have been demonstrated in swinepox, capripox and fowlpox virus genomes (3,42,156). Though no study to date has demonstrated a role for the virus cell-associated chemokine receptors *in vivo*, the proteins are predicted to compete with cellular chemokine receptors during infection by acting as chemokine sinks and preventing the induction of chemokine-mediated signalling cascades. A similar strategy is used by several members of the herpesvirus family, including human cytomegalovirus, herpesvirus saimiri, and Kaposi's sarcoma associated herpesvirus.

A third method of poxvirus inhibition of chemokine-mediated inflammation has recently been proposed. Genomic sequencing of MCV revealed the presence of a gene encoding a protein with homology to the CC family of chemokines (MC148R) (246). The MC148R protein contains the motifs necessary for effective binding to cellular chemokine receptors, but lacks the amino-terminal domain necessary for chemokine activation of cells and was shown to serve as a broad-spectrum CC and CXC chemokine antagonist (57). Current models predict that the MCV protein likely functions by competing with host chemokines for binding to target cell receptors. Analysis of the complete genomic sequence of fowlpox virus (FPV) revealed the presence of 4 predicted proteins sharing homology with CC chemokines. Though still undetermined, a function for the FPV proteins similar to the MCV chemokine antagonist is proposed.

A number of genes encoding members of the serpin family of serine proteinase inhibitors have been demonstrated in orthopoxvirus, leporipoxviruses, suipoxviruses, and avipoxviruses. Studies have shown that many of these poxvirus serpins are important virulence factors and are able to interfere with the host inflammatory response *in vivo*. The mechanism of serpin action and the role of the poxvirus gene products in thwarting the host immune response to infection will be discussed in a later section.

NK cells. NK (natural killer) cells are a class of large granular lymphocytes which mediate lysis of infected cells and tumor cells in an MHC-independent manner (102). NK cells are activated by interferons and are capable of producing gamma interferon after exposure to interleukin-2 (99). Within the first 2 to 3 days following viral infection, an inflammatory response typically occurs at the site of inoculation with an

influx of leukocytes, followed by the production of interferon, activation of NK cells, and finally NK cell-mediated lysis of virus-infected target cells (311).

In vivo studies indicate that NK cell activity is an important host response to poxvirus infection (312). Some evidence suggests that at least 50% of the cytolytic activity against vaccinia virus infected cells in the hamster is due to NK cells rather than CTL (47). NK cell activity has been shown to be elevated in the spleen and blood following infection of mice with vaccinia (267). Depletion of NK cells prior to poxvirus infection correlates with an increased level of vaccinia virus recovered from infected mouse spleen and liver as well as an increase in the size of the virus lesions (37). Another study showed that C56BL/6 mice, a strain naturally resistant to infection by ectromelia virus, produces higher levels of NK cell-mediated lysis of infected cells compared to the susceptible DBA/2 strain of mice (114). In contrast, C57BL/6 mice carrying the *bg/bg* mutation, which is associated with NK cell deficiency, contract lethal infections when exposed to ectromelia, demonstrating a crucial role for NK cells in the defense of the host (38). Recent studies suggest that it is not the cytolytic activity of NK cells, but rather their production of gamma interferon that is important in combating poxvirus infection (120). These studies indicate that while NK cells are important in virus clearance, they are not sufficient to completely inhibit virus spread.

Although no study to date has provided experimental evidence for a poxvirus gene product specifically designed to target NK cells, many of the proteins described above function to inhibit the cytokines that activate NK cells and augment their lytic function. In addition, poxviruses encode many gene products that function to inhibit apoptosis, the form of cell death which is activated by NK cell association with target

cells. Apoptosis is a complex process, and the exact mechanisms by which it takes place have yet to be elucidated . Though a complete review of the current models of apoptosis is beyond the scope of this study, the key features of this form of cell death which are relevant to the understanding of poxvirus infection will be summarized, along with a description of the poxvirus gene products which are important in modulating the host apoptotic response during infection.

Apoptosis

Apoptosis is a form of programmed cell death by which organisms eliminate unwanted cells. It is the most common form of cell death and occurs during organismal development, tissue remodeling, cell homeostasis and immune system regulation. In addition, dysregulation of apoptosis has been demonstrated to be involved in several human pathologies including degenerative and autoimmune diseases, cancer and AIDS (280).

Biochemically and morphologically, apoptotic cell death is distinct from necrosis, a form of cell death which occurs following cell trauma (Fig. 3) (reviewed in (216)). In apoptosis, cells release contact with neighboring cells and become detached from surrounding tissue. Marked condensation occurs in both the nucleus and the cytoplasm, leading to a significant decrease in cell size. Mitochondrial integrity is compromised due to the opening of tightly-regulated pores in the organellar membrane resulting in the destabilization of the mitochondrial inner membrane potential. Cytochrome c, a component of the electron transport chain and normally confined to the mitochondrial

Figure 3. **Important features of the apoptotic cascade.** Important features of the apoptotic cascades initiated by Cytotoxic T Lymphocytes (CTL), binding to death receptors, or the introduction of external stimuli are highlighted. Abbreviations: FasL, Fas ligand; TNF, tumor necrosis factor; DD, death domain; DED, death effector domain; P.T., permeability transition; Pro, proform; C2, caspase 2; C3, caspase 3; C7, caspase 7; C8, caspase 8; C9, caspase 9; C10, caspase 10; Cyt c, cytochrome c; Ph.S., phosphatidylserine. For other abbreviations, see text.

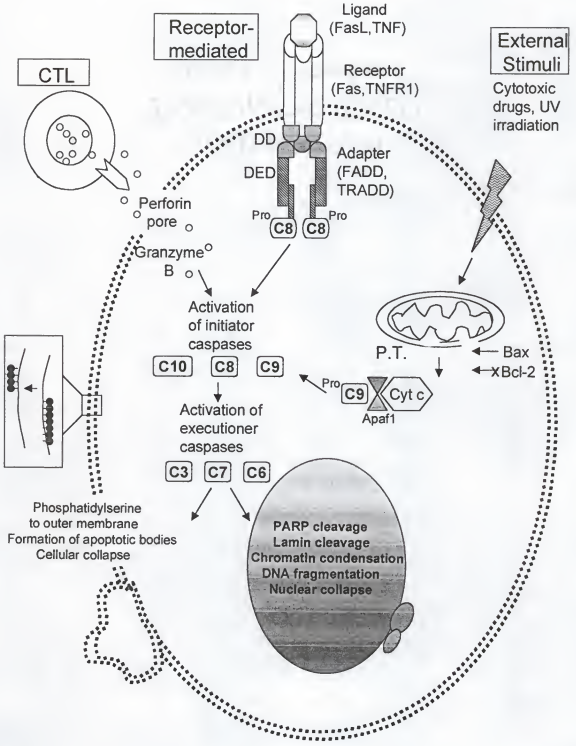
Receptor-mediated
Ligand (FasL,TNF)
Receptor (Fas,TNFR1)
External Stimuli
Cytotoxic drugs, UV irradiation
CTL
DD
DED
Adapter (FADD, TRADD)
Perforin pore
Pro
C8
C8
Pro
Granzyme B
Activation of initiator caspases
C10
C8
C9
P.T.
Bax
Bcl-2
Pro
C9
Cyt c
Apaf1
Activation of executioner caspases
C3
C7
C6
Phosphatidylserine to outer membrane
Formation of apoptotic bodies
Cellular collapse
PARP cleavage
Lamin cleavage
Chromatin condensation
DNA fragmentation
Nuclear collapse

intermembrane space, is released into the cytoplasm where it functions to amplify the apoptotic signal (discussed below). As a result of the uncoupling of the electron transport chain, reactive oxygen species accumulate in the apoptotic cell. Within the nucleus, chromatin condenses and is eventually cleaved intranucleosomally into ~180 bp fragments. The nuclei of apoptotic cells become invaginated and fragment to form membrane bound vesicles often containing condensed chromatin. The plasma membrane also begins to bleb, packaging the cellular contents into membrane bound vesicles known as apoptotic bodies. Phosphatidylserine, normally expressed on the inner layer of the plasma membrane bilayer, becomes translocated to the extracellular membrane where it acts to signal nearby cells. The end result of apoptosis is the engulfment of the dying cell by nearby cells or professional phagocytes with little or no leakage of cellular contents or generation of an inflammatory response. In contrast to apoptosis, necrosis is a disorderly form of cell death. Cells dying by necrosis swell rather than condense, causing the plasma membrane to lyse and release the cell contents into the extracellular environment. Swelling of cellular organelles leads to their lysis as well. DNA degradation occurs, but chromatin cleavage is random and does not result in the formation of discrete sized fragments. Because necrosis results in the disruption of the cell membrane and leakage of intracellular contents, this form of cell death is associated with inflammation and significant damage to surrounding cells.

Important to the process of apoptosis are caspases, a family of proteinases which to date is comprised of 14 members (144). Caspases (cysteine-dependent aspartate-specific proteases) are cysteine proteinases that share an unusual and strict requirement

for substrate cleavage following aspartic acid residues. The substrate specificities of the proteinases are further defined by the three amino acids NH_2-terminal to the caspase cleavage site (188). The larger caspase family has been further divided into three subfamilies, based on substrate specificity, phylogenetic comparisons, sequence similarity and function (125). Interleukin-1β converting enzyme (ICE, caspase 1) is the prototype of the ICE family of proteinases, which include caspases 1, 4 and 5. It is thought that members of the ICE caspase family serve mainly to regulate maturation of pro-inflammatory cytokines including IL-1β and IL-18 (discussed above) and any involvement in apoptosis is minor. Caspase 2 is the sole member of the ICH-1 subfamily, and is an important regulator of neuronal apoptosis (266). Caspases 3, 6, 7, 8, 9, and 10 belong to the CPP32 subfamily, and are the major proteinases involved in the execution of apoptosis. This third subfamily is further divided into two groups: initiator caspases and effector caspases. The initiator caspases, including caspases 8, 9, and 10, are the apical proteinases in the apoptotic cascade and are responsible for the proteolytic activation of the downstream effector caspases. Caspases 3, 6, and 7 are the major effector proteins and their proteolytic activity is responsible for many of the biochemical and morphological changes that characterize apoptotic cell death. The list of known substrates of the effector caspases, the so-called "death substrates", is constantly growing and includes structural proteins such as the nuclear lamins, enzymes involved in DNA repair including poly (ADP)-ribose polymerase (PARP), and proteins involved in cell cycle regulation such as the retinoblastoma protein (188,216). Cleavage of these and other specific caspase substrates results in the systematic and orderly disassembly of the dying cell.

Although there are many different signals that activate apoptosis, in many cases the basic pattern of events is the same. Caspases exist as inactive zymogens in healthy cells which have not been induced to undergo apoptosis and must themselves be proteolytically activated by cleavage at a conserved aspartic acid residue. Once the apoptotic signal is received by the cell, the appropriate initiator caspase proform associates with its cognate adaptor protein via shared domains (DED, death effector domain; CARD, caspase recruitment domain) present in both the caspase zymogen and the adaptor protein. Current data supports a model in which the adaptor protein serves to bring two initiator caspase proforms in close proximity in order to allow intermolecular proteolytic activation. Once activated, the initiator caspase is able to cleave and activate downstream effector caspase zymogens enabling them to attack the apoptotic death substrates.

One means of apoptotic induction important in the host response to virus infection is mediated through death receptor-ligand interactions (186,216,308). In the Fas pathway, effector cells such as NK cells and cytotoxic T lymphocytes use the Fas ligand on their surface to bind the Fas receptor of the infected target cell. Engagement of the Fas receptor induces the trimerization of the receptor and its association with the FADD (Fas-associating protein with death domain) adaptor protein. Pro-caspase 8 molecules then associate with FADD, leading to the proteolytic activation of the proteinases. Activated caspase 8 is then able to proteolytically activate other downstream caspases in a cascade-like manner. A similar mechanism of caspase activation takes place following the engagement of the cytokine TNF by its cognate receptor on target cells.

A related but different method of caspase activation takes place in response to cell damage by cytotoxic drugs, serum deprivation, UV irradiation or the action of p53 (216). In this pathway, cell damage leads to a collapse of the mitochondrial inner transmembrane potential, leading to the opening of the permeability transition (PT) pore. As a result, proteins which are normally localized to the intermitochondrial space are released into the cytoplasm. Included in this group of proteins is cytochrome c which normally functions as a component of the electron transport chain. Within the cytoplasm, cytochrome c acts with dATP to activate the adaptor protein Apaf-1 which is then able to interact with pro-caspase 9 molecules by means of a caspase recruitment domain (CARD), leading to caspase 9 activation. Caspase 9 is an initiator caspase and once activated is then able to activate downstream members of the caspase proteolytic cascade. In addition, a second mitochondrial protein termed AIF (apoptosis inducing factor) is released following the mitochondrial permeability transition. The protein shares with caspases the ability to cleave substrates after aspartic acid residues, and studies have shown that AIF is able to proteolytically activate pro-caspase 3 *in vitro* (271), providing an additional pathway for effector caspase activation.

Important in the regulation of the mitochondria-dependent form of apoptosis are members of the Bcl-2 family of proteins, which are divided into two groups. Bcl-2-like proteins, such as Bcl-2 and Bcl-x_L, promote cell survival while the Bax-like proteins, such as Bax and Bid, are pro-apoptotic molecules. Structurally, Bcl-x_L appears similar to the bacterial pore-forming toxins such as the A subunit of diphtheria toxin (183) and several Bcl-2 family members have been demonstrated to form ion channels in lipid membranes (237). Channels generated by Bcl-2 like proteins have a preference for

monovalent cations and show optimal conductance at acidic pH. In contrast, Bax-like proteins preferentially conduct anions and function over a wide range of pH. Current models propose that pro- and anti-apoptotic Bcl-2 family members function in opposite fashions to regulate polarization of the intermitochondrial space, permeability transition, and the release of cytochrome c and AIF. In this model, the endogenous ratio of Bcl-2-like to Bax-like proteins within a given cell is thought to predispose the cell to either survival or apoptosis. Interestingly, members of the Bcl-2 and Bax subfamilies are each substrates for several effector caspases. However, while caspase cleavage of Bcl-2-like proteins has been demonstrated to destroy their ability to inhibit apoptosis, cleavage of Bax subfamily members has been shown to promote their pro-apoptotic activity.

In addition to the methods of caspase activation mentioned above, caspases can be activated directly following interaction with granzyme B (58,154). The serine proteinase granzyme B is a major constituent in the cytolytic granules of CTL and NK cells. Following interaction of CTL with the appropriate target cell, the cytolytic granules are released into the extracellular space in a calcium-dependent fashion. One granule component, perforin, is a pore-forming protein which directs the formation of pores in the target cell membrane allowing the entry of granule cytolytic proteinases, including granzyme B, into the target cell. Like members of the caspase family, granzyme B cleaves substrates following aspartic acid residues and has been shown to cleave the proforms of caspases 3 and 8 *in vivo* (13,163,320), leading to their activation and the induction of the apoptotic cascade. A recent study revealed that granzyme B is also able to proteolytically activate the pro-apoptotic molecule Bid. Once activated, Bid is able to affect mitochondrial permeability transition and the release of cytochrome c and AIF,

thus providing a second method of caspase activation in cells exposed to granzyme B(19).

While there is no doubt that caspases play crucial roles in many forms of apoptosis, recent studies reporting that several features of apoptosis can occur in the absence of caspase activation and proposing that caspase-independent pathways of apoptosis exist have evoked controversy. Apoptosis has been reported to occur in the presence of z-VAD, a general inhibitor of all caspases, and the baculovirus p35 protein, an effective inhibitor of caspases 1, 3, 6, 7, 8, and 10 (39,194,318). Several other studies have shown that when apoptosis is induced in the presence of broad-range caspase inhibitors, membrane blebbing, chromatin condensation, and nuclear compaction are observed in the absence of concomitant nuclear fragmentation and DNA laddering, suggesting that caspases are responsible for some but not all of the hallmarks of apoptosis (158,194,318). Additionally, a recent study demonstrated that by proteolytically activating the pro-apoptotic molecule Bid, granzyme B introduced into target cells by CTL can promote mitochondrial collapse and cell death in the absence of caspase activation (19). In fact, several studies have indicated that mitochondrial permeability transition, cytochrome c release, and accompanying cell death can occur in the presence of caspase inhibitors (101,158,172,317). However, debate exists over whether the cell death that results in the absence of caspase activation represents a caspase-independent form of apoptosis, necrosis, or a form of cell death which can not be correctly defined using the current criteria.

Poxvirus Inhibitors of Apoptosis

Apoptosis is a common host response to viral infection. Expression of viral antigens in association with MHC I molecules on the surface of an infected cell can signal CTL or NK cell recognition. These cytolytic cells can then induce apoptosis in the target cell by the Fas- or granzyme B- dependent mechanisms mentioned above. In addition, infected cells themselves are able to induce their own suicide following virus infection. Direct cellular damage caused by infection or virus replication products such as double stranded RNA can act as triggers for a cell to undergo apoptosis. If initiated soon after infection, elimination of infected cells by apoptosis leads to a reduction in virus production and limits the spread of progeny virus in the host.

Because apoptosis is a common host response to viral infection, many viruses have evolved to encode inhibitors of apoptosis. These anti-apoptotic factors are designed to either inhibit apoptosis completely, or to delay its induction until sufficient numbers of progeny virion have been produced. In particular, the large DNA viruses including members of the Herpesvirus, Adenovirus and Poxvirus families have been demonstrated to contain many genes devoted to the control of apoptosis (21,54,299).

To date, 9 poxvirus genes have been shown to function as inhibitors of apoptosis (recently reviewed in (287)). All but one of the genes are found in the terminal regions of the genome, and each have been demonstrated to be nonessential for virus growth in infected tissue culture cells. However, deletion or mutation of 6 of the 9 genes results in a restricted host range phenotype, with the mutant virus losing the ability to productively infect certain cell types. Of the three poxvirus anti-apoptosis genes that have not been linked to virus host range, two are found in MCV which can not be studied in cell culture.

All 9 gene products are made early during infection, prior to DNA replication. In addition, a number of genes which are proposed to function in the inhibition of apoptosis have recently been discovered following the complete genomic sequencing of several poxviruses and these genes will be discussed as well.

E3L. The vaccinia virus E3L protein shares homology to eukaryotic transcription factors (Fig. 4). It is a double stranded RNA binding protein (310) and is thought to be a component of the vaccinia RNA polymerase (4). Vaccinia virus E3L deletion mutants are unable to replicate in HeLa, Vero or L929 cells (23,24). In HeLa cells, the restricted host range of VV E3L mutants is associated with the induction of apoptosis (137). In each of the restrictive cell lines, the reduced host range can be corrected by replacing the deleted E3L gene with other genes encoding double stranded RNA binding proteins, indicating that it is the ability of E3L to bind double stranded RNA which is essential for virus growth (23,132,199). The current model proposes that E3L is necessary for the sequestration of double stranded RNA produced during late gene transcription, thereby preventing the interferon-induced double stranded RNA-dependent serine/threonine kinase (PKR) from phosphorylating eIF-2 to inhibit protein synthesis (46,219,314). Furthermore, by preventing activation of PKR, E3L inhibits the kinase from activating NF-kB, a transcription factor responsible for stimulating transcription of many pro-apoptotic genes.

CP77. The CP77 gene is intact and functional only in cowpox virus, and is fragmented in other orthopoxviruses. The gene encodes a 669 amino acid cytoplasmic protein that contains ankyrin repeats, motifs important in facilitating protein-protein interactions, particularly among integral membrane and cytoskeletal proteins. Cowpox

Figure 4. **Poxvirus inhibitors of apoptosis.** Poxvirus gene products that interfere with the apoptotic cascade are depicted. Abbreviations: DD, death domain; DED, death effector domain; TNF, tumor necrosis factor; P.T., permeability transition; Pro, proform; Cyt c, cytochrome c; C2, caspase 2; C3, caspase 3; C7, caspase 7; C8, caspase 8; C9, caspase 9; C10, caspase 10. For other abbreviations, see text.

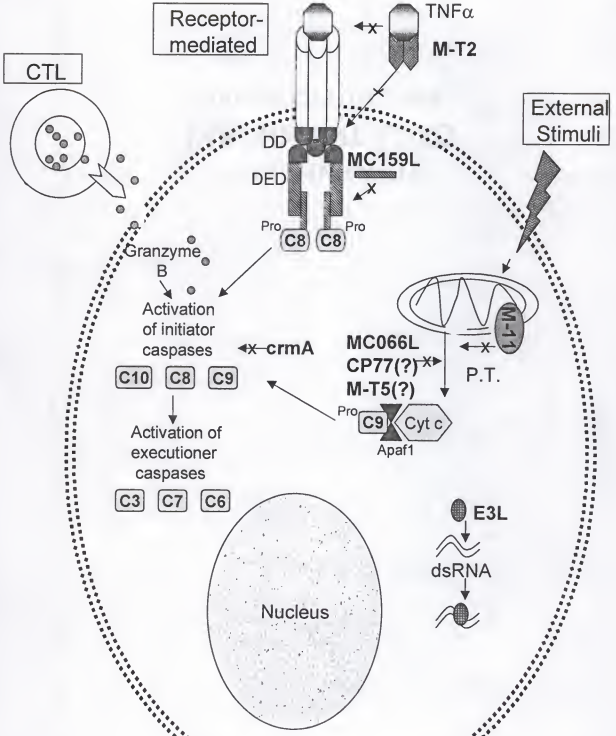
Receptor-mediated
TNFα
M-T2
CTL
External Stimuli
DD
DED
MC159L
Pro
C8
C8
Pro
Granzyme B
Activation of initiator caspases
crmA
C10
C8
C9
MC066L
CP77(?)
M-T5(?)
M-T1
P.T.
Pro
C9
Cyt c
Apaf1
Activation of executioner caspases
C3
C7
C6
E3L
dsRNA
Nucleus

virus, unlike vaccinia, is able to productively replicate in Chinese hamster ovary (CHO) cells. Vaccinia virus infection of CHO cells is characterized by a rapid shut-off of viral and host protein synthesis and apoptosis (213,214). Vaccinia virus recombinants engineered to express the CP77 gene delay apoptosis until after progeny virions are formed, leading to a productive infection (112,262). Although the exact function of CP77 during infection is not known, some studies suggest that it may function in a manner analogous to Bcl-2 family members in controlling apoptosis (112).

M-T5. The product of the myxoma M-T5 gene is a 483 amino acid protein with homology to CP77. Like CP77, M-T5 contains ankyrin repeats. Myxoma M-T5 deletion mutants display a reduced host range and are unable to productively infect RL-5 cells, an immortalized CD4+ rabbit T-cell line, as well as peripheral blood lymphocytes. Following infection of these cells, host and viral protein synthesis is rapidly inhibited and apoptosis occurs. *In vivo*, M-T5 mutants are severely attenuated and virus does not spread from the initial site of inoculation (178). Histological analysis of infected lesions showed a significant reduction in edema and an increased infiltration of heterophils (neutrophils) relative to wild type lesions. The current model proposes that M-T5 is somehow necessary for inhibiting protein synthesis shutdown during lymphocyte infection. In the absence of M-T5, apoptosis prevents productive infection of lymphocytes which are necessary for virus spread through the body.

M-T2. The M-T2 gene is found in Shope fibroma (290) and myxoma viruses (291). A similar gene has been found in variola and cowpox virus, but not in vaccinia where the homologue is fragmented. The gene encodes a secreted TNF receptor that most resembles TNFR2 and has been shown to bind with high affinity to TNFα (239,257).

Localization studies showed that the myxoma T2 protein is expressed not only as a secreted glycoprotein, but as an endoglycosidase H-sensitive cytoplasmic glycoprotein as well (240). The protein is made throughout infection, but is secreted predominately at early times post infection. Myxoma virus M-T2 deletion mutants are severely attenuated in rabbits. In addition, M-T2 deletion mutants have a reduced host range and are unable to replicate in RL-5 cells. The host range restriction is associated with the induction of apoptosis in infected cells. Several studies have implicated the intracellular form of M-T2 as important for inhibiting apoptosis in RL-5 cells by a process distinct from TNF binding (241,244). One model proposes that the intracellular form of the protein is able to form heterodimers with a member of the TNF receptor family, inhibiting the ability of the receptor to oligomerize and effectively signal downstream members of the apoptotic cascade (241).

M-11L. The myxoma M-11L gene encodes an early protein which shares no homology with any cellular protein. Like M-T2 mutants, myxoma M-11L mutants are unable to productively infect rabbit RL-5 cells. Rather, an abortive infection is observed which is associated with the induction of apoptosis (148). Deletion of the M-11L gene from myxoma greatly attenuates the virus in rabbits (195). Histological analysis of primary lesions isolated from rabbits infected with the myxoma M-11L mutant virus revealed the presence of large numbers of infiltrating lymphocytes relative to wild type lesions, suggesting that the function of M-11L is to inhibit the inflammatory response *in vivo* (195). Examination of the M-11L amino acid sequence revealed a stretch of 18 hydrophobic amino acids near the carboxy terminus of the protein which was predicted to allow insertion into infected cell plasma membranes. Indeed, indirect

immunofluorescence analysis of nonpermeablized cells infected with myxoma virus demonstrated the presence of M-11L protein on the cell surface (93). Furthermore, myxoma virus variants containing engineered mutations in the putative transmembrane region of M-11L were as attenuated as the M-11L null mutant in rabbits, leading the authors to conclude that the ability of M-11L to localize to the cell membrane is essential for function (93). However, a recent study demonstrated that while a minority of M-11L may associate with the plasma membrane of infected cells, the majority of the protein localizes to the outer mitochondrial membrane during infection(69). When transiently expressed in uninfected cells, M-11L was shown to behave in a Bcl-2-like fashion by preventing mitochondrial permeability transition following cell exposure to the apoptosis-inducing drug staurosporine, though only when M-11L was expressed at the mitochondrial membrane (69). Remarkably, while M-11L, M-T2 and M-T4 have all been demonstrated to prevent apoptosis during infection of the RL-5 rabbit lymphocyte cell line (20,93,244,253), only the M-11L gene was necessary to prevent apoptosis in infected primary rabbit monocytes (69). This suggests expression of M-11L during myxoma infection is necessary to inhibit apoptosis by preventing the mitochondrial permeability transition, particularly in cells of the monocyte/macrophage lineage.

MC159L. MC159L, along with MC160L and MC066L, are three molluscum contagiosum virus ORFs with anti-apoptosis activity that are not found in any other poxvirus. MC159L and MC160L are thought to have arisen from gene duplication, thus only MC159L will be discussed. The MC159L gene product shares sequence similarity with the death domains (DD) of the Fas/TNFR1 signaling components FADD and caspase 8 (29,108,245). Studies using the yeast two-hybrid system demonstrated that

MC159L is able to interact with FADD, blocking both the Fas and TNFR1 signalling pathways of apoptosis (29,108). Because MC159L inhibits both TNFR1 and Fas-mediated apoptosis but not other forms of apoptosis mediated by expression of active caspase 8 (108), it is likely that MC159L blocks signalling upstream of caspase 8 activation. Inhibition likely occurs by MC159L binding to the Fas and TNFR1 adaptor proteins through the shared death domain regions, preventing their subsequent association with pro-caspase molecules. Because no cell culture or animal model is able to support MCV replication, the effects of MC159L mutation on virus host range or virulence *in vivo* have not been studied.

Selenium-containing proteins. Until recently, the product of the MCV MC066L gene was assumed to be the only known example of a viral encoded selenium-containing protein (252). The protein shares 75% homology to mammalian glutathione peroxidase, an antioxidant protein responsible for reducing cytotoxic peroxides. The properties of the MC066L protein were studied by expressing the protein in cells via a transient expression system. The protein was demonstrated to be capable of protecting human keratinocytes from apoptosis induced by UV irradiation and hydrogen peroxide, consistent with a role in inactivating cytotoxic radicals (252). However, the protein was unable to protect cells from apoptosis induced through the Fas- or TNF-mediated pathways, suggesting that MC066L is only able to inhibit apoptosis triggered by cellular exposure to peroxide or UV irradiation. The recent sequencing of the fowlpox virus genome revealed the presence of a homologue of MC066L referred to as FPV064 (3). The predicted amino acid sequence of FPV064 is reported to contain the glutathione peroxidase signature sequence including the active site selenocysteine codon (3). The authors of the study

propose that FPV064 may serve to protect infected cells from cytotoxic effects caused environmental stress in a manner similar to MC066L in order to allow successful virus replication in the absence of apoptosis (3).

FPV039. Analysis of the complete FPV genome revealed a gene with homology to the Bcl-2 family of anti-apoptosis proteins (3). The predicted amino acid sequence is proposed to share homology with both MCL1, a protein induced during monocyte/macrophage differentiation in myeloid leukemia cell lines, as well as BFL1, an apoptosis inhibitor produced exclusively in the bone marrow, spleen and thymus (3). Though no studies to date have investigated the role of FPV039 during infection, the protein is presumed to prevent a cellular apoptotic response to infection by fowlpox virus.

In addition to the genes discussed above, two of the poxvirus genes important for regulating apoptosis during infection belong to the serpin family of serine proteinase inhibitors and are named Serine Proteinase Inhibitor (SPI)-1 and 2. Since the research detailed in this thesis is focused on SPI-1, a description of serpins and their mode of action precedes a discussion of SPI-1 and SPI-2 and presentation of the research.

Serpins

Serpins are a family of serine proteinase inhibitors found throughout nature. They comprise the third major protein component of blood plasma after albumin and the immunoglobulins (204). They are single chain proteins that share a conserved domain of 370-390 amino acids and a similar tertiary structure composed of three β-sheets and nine α-helices (109). A distorted α-helix extends from β-sheet A and contains the serpin reactive site loop (RSL) which interacts directly with the proteinase target. The primary

function of members of the serpin family is to govern serine proteinase activity, and serpins are involved in regulating a number of key biological processes including blood coagulation, fibrinolysis, cell migration, and extracellular matrix remodeling (228). In addition to inhibitory serpins, there is also a class of noninhibitory serpins, such as ovalbumin and angiotensinogen, which are devoid of any inhibitory activity and have evolved to fill roles other than proteinase inhibition (211).

Mechanism of Serpin Action

The inhibitory reaction of a serpin and a proteinase proceeds through a branched pathway, wherein the serpin functions as a suicide substrate (Fig. 5). The serpin RSL, located at the C-terminal region of the protein, closely mimics the natural substrate of the target proteinase. The RSL comprises amino acid residues designated P15 to P5', where proteolysis occurs between residues P1 and P1' (84). Upon recognition of the serpin RSL as a suitable substrate by the target proteinase, an initial noncovalent, reversible Michaelis complex is formed. Nucleophilic attack of the scissile bond between serpin residues P1 and P1' by the catalytic serine of the proteinase results in the formation of a covalent complex between the two proteins which is thought to exist as an acyl-enzyme intermediate (134). At this branch point, two outcomes are possible. The ratio at which the two outcomes occur is defined as the stoichiometry of inhibition and varies with reaction conditions. In the substrate reaction, hydrolysis of the acyl-enzyme releases a cleaved, inactivated form of the serpin and active proteinase. Conversely, the favored model of inhibitory serpin action proposes that concomitant with formation of the acyl-

Figure 5. **Serpin Structure and Mechanism of Action.** A) The branched pathway representing the reaction mechanism of serpins is shown. E, proteinase; S_a, active, intact form of the serpin; E·S, the noncovalent Michealis complex; E-S_a, the acyl-enzyme intermediate present prior to proteinase translocation; E-S*, the kinetically trapped covalent acyl-enzyme inhibitory complex; S_i, the inactive, cleaved form of the serpin. B) A diagram of the structural layout of a typical serpin is depicted with the region corresponding to the serpin reactive site loop (RSL) highlighted. The orientation of amino acid residues comprising the RSL from position P15 to P5' is displayed while the active site for nucleophilic attack by the target serine proteinase is boxed.

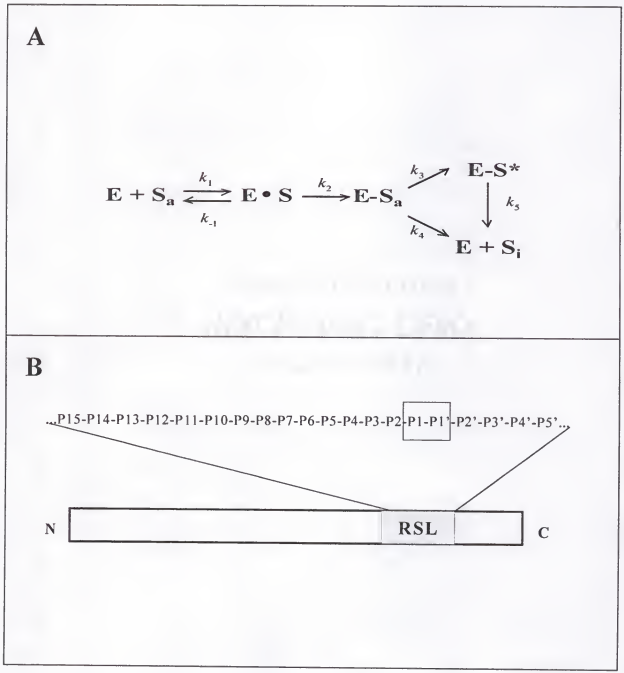
A
E + Sa
k1
k-1
E • S
k2
E-Sa
k3
E-S*
k5
k4
E + Si
B
...P15-P14-P13-P12-P11-P10-P9-P8-P7-P6-P5-P4-P3-P2-P1-P1'-P2'-P3'-P4'-P5'...
N
RSL
C

enzyme complex, the amino-terminal portion of the RSL inserts into the backbone of the serpin in a process known as strand insertion, resulting in the separation of the P1 and P1' amino acids by 70 Å (44,268). Strand insertion induces a conformational change in the serpin which produces a form of the serpin which is much more thermodynamically stable than the native form and is proposed to result from an increase in hydrogen bonding within the molecule (84). Because the proteinase within the complex is covalently bound to the serpin P1 residue through an ester linkage, strand insertion results in a substantial change in the orientation of the proteinase as well, involving translocation of the proteinase by more than 70 Å (135,268). The distortion of the proteinase active site that takes place as a result of its translocation in large part explains the inhibitory nature of the serpin-proteinase complex (164,268). The inhibitory complex is stable to boiling in SDS, and has a long half life ranging from hours to days. The extraordinary stability and slow decay of the of the acyl-enzyme intermediate accounts for the inhibitory properties of the serpin. Eventually, hydrolysis of the complex occurs which releases the cleaved, inactivated form of the serpin. Additionally, because the serpin RSL is exposed on the surface of the molecule, it is susceptible to proteolysis by nontarget proteinases but this consistently occurs in the absence of stable complex formation.

While the overall structure of serpins clearly plays a role in the inhibitory mechanism of serpin action, two regions of the serpin are especially important in determining the nature and outcome of a serpin-proteinase interaction. The first is the reactive site of the serpin which contains the target proteinase cleavage site. Within the reactive site, it is the P1 residue that largely dictates the target enzyme specificity of the serpin. At the most basic level, this specificity reflects the existence of three types of

serine proteinases: trypsin-like, chymotrypsin-like, and elastase-like, which preferentially cleave after basic, aromatic and neutral amino acids, respectively. For example, serpins that inhibit trypsin-like proteinases often have an arginine or lysine at the P1 position, while serpins that target chymotrypsin-like proteinases typically have methionine, phenylalanine or tryosine at the reactive site. Serpins are remarkably specific for the proteinases that they inhibit. The importance of the P1 residue and serpin specificity is best illustrated in several human diseases. In the serpin mutant α_1-antitrypsin Pittsburgh, the wild type P1 methionine residue is mutated to arginine, resulting in the inability of the serpin to inhibit elastase. Instead, the mutant serpin gains the ability to inhibit the trypsin-like enzymes thrombin, kallikrein, factor Xa and plasmin, resulting in a severe bleeding disorder in the affected individual (43,84,211).

Several studies have shown that residues within the region from P3 to P3', in addition to the P1 residue, contact the target proteinase and likely play a role in serpin specificity. In one study, the single P1 amino acid or residues P3 to P3' of α_1-antichymotrypsin (ACT) were replaced with the corresponding residues from the natural human neutrophil elastase (HNE) inhibitor PI, converting ACT from a substrate to an inhibitor of elastase (229). Furthermore, the ACT P3-P3' variant inhibited elastase with a greater second order inhibition constant than was seen with the ACT P1 single mutant. Inhibitory complexes between the P3-P3' variant and HNE were also more stable than complexes between elastase and the ACT P1 mutant. Still, the stability of the complexes formed between the ACT P3-P3' mutant and elastase were much less than complexes between HNE and PI, implying a role for additional regions of the serpin in inhibitory activity. The importance of serpin domains outside of the reactive site in determining

inhibitory activity has also been demonstrated in other studies (136,210) (33). Taken together with modelling experiments, these results suggest that both reactive site residues as well as the serpin scaffold are important in defining the inhibitory characteristics of a serpin.

A second region important for serpin inhibitory activity is found at the hinge of the serpin. The serpin hinge, which includes residues P14 through P10, is the part of the serpin molecule which bends allowing reactive site loop insertion following reaction with the target proteinase. In inhibitory serpins, the amino acid at the P14 position is typically serine, threonine or valine. In contrast, noninhibitory serpins such as ovalbumin or angiotensinogen, which are devoid of inhibitory activity, have arginine at the P14 location. It is thought that the presence of the large, charged arginine residue at the hinge of the noninhibitory serpins prevents strand insertion due to steric hindrance (84). Without strand insertion, the interacting proteinase does not translocate across the serpin molecule and thus stable complex formation between these serpins and potential target proteinases can not occur. Consequently, reaction of noninhibitory serpins with serine proteinases results in cleavage within the RSL followed by release of the proteinase. The importance of a small, uncharged amino acid at the P14 residue for inhibitory serpin activity has been demonstrated in several studies in which the native residue of an inhibitory serpin was altered to arginine. In each of these studies, the resulting mutant serpin lost its ability to inhibit its target proteinase and instead acted solely as a substrate (135) (242). In addition, residues at positions P12 and P10 are also highly conserved among inhibitory serpins. While alanine is typically found at both positions in inhibitory serpins, valine/glycine and proline/glutamine residues comprise these sites in the

noninhibitory serpins ovalubumin and angiotensinogen, respectively. The importance of uncharged amino acids at the P10 and P12 positions is revealed by the finding that natural point mutations at these positions in inhibitory serpins have been associated with loss of inhibitory activity and the development of disease (208,256).

Poxvirus Serpins

Although prevalent throughout nature, poxviruses are the only virus family known to encode functional serpins. A gene encoding a protein with homology to the serpin family but lacking a functional RSL has been found in gammaherpesvirus 68 (300). To date, genes encoding proteins with homology to serpins have been found in four different poxvirus genera: orthopoxvirus, leporipoxvirus, suipoxvirus, and avipoxvirus (Table 2). Each of the serpin genes is located in the nonessential regions of the genome. Poxvirus serpins were presumably originally derived and captured from host cell genes by an unknown mechanism.

CrmA/SPI-2. The first discovered and most widely studied poxvirus serpin is the orthopoxvirus crmA, known in vaccinia as ORF B13R and in RPV as SPI-2. It is a 38 kDa cytoplasmic protein which is expressed early during infection. CrmA was initially described as a protein necessary for the production of red, hemorrhagic pocks during infection of the CAM (discussed above) (209). CPV crmA mutants produce white pocks on the CAM which consist of massive numbers of inflammatory cells. It was determined that the effect of crmA on inflammation was mediated by inhibition of interleukin-1B-converting enzyme (ICE), an enzyme responsible for processing of pro-interleukin-1β into its active form (217). Later studies revealed that ICE was a member of a much larger

Table 2. Properties of the poxvirus serpins

Name	Genus	Size(kDa)	Temporal Class	Location	Function
SPI-1	Orthopoxvirus	41	Early	Cytoplasmic	Host range factor
SPI-2/ crmA	Orthopoxvirus	38	Early	Cytoplasmic	Caspase and Granzyme B inhibitor
SPI-3	Orthopoxvirus	42/50*	Early	Membrane-Associated?	Prevents cell-cell fusion Inhibits trypsin-like proteinases
SPI-7	Suipoxvirus	37	Early	Cytoplasmic	Virulence factor?
Serp1	Leporipoxvirus	42/55	Late	Secreted	Inhibits trypsin-like proteinases Prevents inflammation *in vivo*
Serp2	Leporipoxvirus	34	Early	Cytoplasmic	Prevents inflammation and Apoptosis *in vivo*
Serp3	Leporipoxvirus	30**	?	?	Truncated
FPV010	Avipoxvirus	38**	?	?	Undetermined
FPV040	Avipoxvirus	38**	?	?	Undetermined
FPV044	Avipoxvirus	41**	?	?	Undetermined
FPV204	Avipoxvirus	39**	?	?	Undetermined
FPV251	Avipoxvirus	17**	?	?	Truncated

* Size of glycosylated protein
** Predicted size of unmodified protein

family of cysteine proteinases (caspases) responsible for the regulation of apoptosis. In fact, much of what is currently known about the apoptotic cascade is due to studies involving crmA, which was the first natural caspase inhibitor ever discovered. CrmA has been shown to inhibit apoptosis induced by a variety of means (34,63,78,278,306). CrmA, which possesses an aspartic acid as its P1 residue, has been demonstrated to inhibit caspases 1 (ICE), 4,5, 8 and 10 (265,274,324). Because caspases 8 and 10 are thought to be the apical caspases in the apoptotic cascade initiated by engagement of the Fas receptor, it is thought that the ability to inhibit this pathway accounts for much of the anti-apoptotic activity of crmA. In addition, crmA is able to inhibit the CTL serine proteinase granzyme B (212) which, like members of the caspase family, has a preference for cleaving after aspartic acid residues.

Within the context of a poxvirus infection, crmA is able to inhibit CTL-mediated apoptosis mediated via the Fas receptor (147,279). In addition, researchers have demonstrated that infection of the LLC-PK1 pig kidney cell line with a CPV crmA deletion mutant results in the induction of apoptosis. However, the induction of apoptosis occurs late in infection after the formation of progeny virions and does not affect the ability of the virus to have a productive infection (218). Surprisingly, infection of LLC-PK1 cells with wtRPV results in the induction of apoptosis, even though RPV encodes a functional SPI-2 gene which is able to inhibit caspase 1 as efficiently as crmA (146). This same study demonstrated that apoptosis was inhibited when LLC-PK1 cells were co-infected with wtRPV and wtCPV, in contrast to mixed infections between wtRPV and a CPV crmA null mutant where programmed cell death did occur. These results suggest that despite 93% amino acid identity between SPI-2 and crmA, the slight

differences within the serpin reactive site and scaffold regions lead to a variation in inhibitory activity between the two proteins. *In vivo*, crmA does not appear to have an effect on virulence in an mouse intranasal model of infection (123,281).

Serp2. The myxoma virus serpin Serp2 is a 34 kDa cytoplasmic protein which is made at both early and late times during infection. Myxoma Serp2 mutants are severely attenuated in rabbits as judged by the clinical course of the disease as well as the survival rates of the infected rabbits relative wild type infected rabbits (167). Histologically, lesions from animals infected with the myxoma Serp2- virus contained a massive inflammatory response which was not seen following infection with the wild type virus. In addition, lymphocytes in lymph nodes from animals infected with the Serp2 mutant virus which were shown to rapidly undergo apoptosis. Based on these studies, a model proposing that Serp2 is responsible for impairing the inflammatory response and preventing apoptosis in lymphocytes following infection *in vivo* was postulated (167)

Serp2, like crmA, contains aspartic acid at the P1 position, suggesting that Serp2 and crmA may play similar roles during infection. In support of this, Serp2 expressed *in vitro* was reported to have some inhibitory activity against caspase 1 (ICE) (207). However, a second study was unable to demonstrate stable complex formation between Serp2 and caspase 1 (288). In addition, purified, recombinant Serp2 was shown to have some activity against ICE, but inhibition was much less than was seen with crmA produced in the same manner (Serp2 K_i of 80nM compared to 4 pM for crmA). Serp2 was demonstrated to form a stable complex with granzyme B which could be detected following SDS-PAGE. However, enzymatic studies revealed that Serp2 was only a weak inhibitor of granzyme B (K_i = 420 nM) (288). In order to determine whether Serp2 could

function in place of crmA during poxvirus infection, a CPV recombinant was designed which was deleted for crmA but expressed Serp2 (288). The mutant virus was then assayed for the ability to inhibit apoptosis in LLC-PK1 cells, a cell line which has been shown to undergo apoptosis following infection with CPV crmA mutants (146,218). Unlike cells infected with wtCPV, apoptosis was readily observed in cells infected with the CPV Serp2 recombinant, indicating that Serp2 is unable to function in place of crmA during CPV infection.

SPI-7. The 37 kDa SPI-7 protein is the only serpin known to date that is encoded by the suipoxvirus swinepox. It is a cytoplasmic protein which is expressed early during infection (185). Like crmA and Serp2, SPI-7 contains an aspartic acid at its P1 position, suggesting that it too may have some activity against the caspases or granzyme B. However, extensive studies have been unable to detect activity against granzyme B or any of the caspases despite the fact that human caspase 1 is able to cleave SPI-7 in a fashion consistent with cleavage at the P1 residue (N. Thornberry, P.C. Turner, and R.W. Moyer, unpublished results). Replacement of crmA with SPI-7 in CPV generated a recombinant which produced white pocks on the CAM and was unable to prevent apoptosis during infection of LLC-PK1 cells, indicating that SPI-7 is not able to function in place of crmA within the context of CPV infection (185).

Preliminary studies indicate that SPI-7 may play a role in swinepox virulence. Genomic sequencing of two strains of swinepox isolated from wild pigs revealed the presence of identical SPI-7 genes, indicating conservation of the gene in nature and suggesting a possible role in pathogenesis of the virus (185). In addition, an SPV SPI-7 deletion mutant was engineered and assayed for attenuation relative to wild type

swinepox in pigs. The mutant virus caused less extensive gross symptoms as well as histopathology at early times post infection relative to the wild type virus and fewer secondary lesions were seen in animals infected with the mutant (185) Infection with the SPI-7 negative virus was also associated with a trend toward a more vigorous cellular immune response (185). Preliminary studies suggest that SPI-7 may inhibit the function of the proteosome, a protein complex responsible for degrading cellular and foreign antigens for presentation on the cell surface in association with MHC I molecules (185). These *in vitro* results correlate with the appearance of fewer primed SPV-specific lymphocytes in animals infected with the SPI-7 deletion mutant relative to the wild type virus (185).

SPI-3. SPI-3 is found in members of the orthopoxvirus genus, including vaccinia virus, variola, CPV, RPV and raccoonpox virus (260). Unlike the majority of poxvirus serpins, SPI-3 is N-glycosylated and contains three predicted membrane-spanning domains although the exact location of SPI-3 in infected cells is unknown. SPI-3 is not essential for virus growth in cell culture, and does not appear to be necessary for the virulence of CPV, VV or RPV in Balb/c mice following intranasal inoculation (133,281). In addition, VV, RPV and CPV SPI-3 mutants are not attenuated relative to wild type virus following infection of the CAM and pock color was not affected.

Several studies have revealed that SPI-3 is necessary for preventing cell to cell fusion following infection (133,286,323). Infection of tissue culture cells with CPV or VV SPI-3 deletion mutants results in the formation of multinucleated cells, known as syncytia. Though SPI-3 shares homology with members of the serpin superfamily, mutation of the serpin reactive site loop had no effect on the ability of SPI-3 to inhibit

cell fusion, indicating that the ability of SPI-3 to inhibit cell fusion does not rely on its ability to function as a serpin (286).

A recent study has revealed that though the ability of SPI-3 to inhibit cell fusion is not related to serpin function, SPI-3 is able to act as a serine proteinase inhibitor (285). SPI-3 was shown to form strong SDS-stable complexes with several trypsin-like proteinases, including plasmin, urokinase, tissue plasminogen activator (tPA), as well as weaker complexes with thrombin and factor Xa. In addition, SPI-3 protein expressed and purified *in vitro* was able to directly inhibit the enzymatic activity of plasmin, urokinase and tPA. The ability of SPI-3 to react with each of these proteinases was dependent on the serpin motifs of SPI-3, as the RSL site-directed mutant described above was inactive in complex formation and enzymatic assays. Taken together, these results indicate that SPI-3 is a bifunctional protein, with separate domains responsible for serpin activity and inhibition of infected cell fusion.

Serp1. The leporipoxvirus Serp1 gene is found as one copy in malignant rabbit fibroma virus (MRV) and as two copies in myxoma virus (MYX), but is present only as a single fragmented copy in the attenuated shope fibroma virus (SFV) (292). Unlike other poxvirus serpins, Serp1 is expressed late during infection and is the only poxvirus serpin which is secreted (149). Like SPI-3, Serp1 is N-glycosylated and shares a P1 aspartic acid residue. In fact, Serp1 and SPI-3 have nearly identical proteinase inhibitory profiles *in vitro*. Like SPI-3, Serp1 is able to form SDS-stable complexes with and inhibit the proteinases plasmin, urokinase, tPA, thrombin and factor Xa (143,187,285). Because Serp1 is a secreted protein, any one of these extracellular proteinases may be the true target of Serp1 during infection. Indeed, Serp1 has been demonstrated to have both

potent anti-inflammatory activity in animal models of arthritis (151) and to inhibit restenosis following angioplasty (145).

Serp 1 is essential for full virulence of both myxoma and malignant rabbit fibroma viruses in rabbits (292). Infection of rabbits with a MYX Serp1 mutant resulted in significant attenuation of the virus relative to wild type MYX, with more than half of the infected animals recovering from an otherwise lethal infection. Therefore, within the context of MYX infection, Serp1 appears to be necessary for suppressing the inflammatory response.

Because the activities of Serp 1 and SPI-3 are nearly identical *in vitro*, experiments were performed to determine whether the two serpins could substitute for one another in the context of virus infection (307). A CPV derivative, engineered to contain the Serp1 gene in place of SPI-3 and under the control of the SPI-3 promoter was assayed for the ability to inhibit cell to cell fusion in infected tissue culture cells. Unlike cells infected with wt CPV, cells infected with the CPV Serp1 recombinant displayed significant cell to cell fusion indicating that Serp 1 is not able to function as a cell fusion inhibitor. In the same study, a MYX recombinant was generated which contained SPI-3 in place of both copies of Serp1 and under the control of the native Serp1 promoter. Surprisingly, analysis of protein expression in cells infected with the MYX SPI-3 recombinant revealed that SPI-3 was secreted during infection rather than remaining intracellular as is normally observed in orthopoxvirus infections. The MYX SPI-3 recombinant was assayed for virulence in a rabbit model of infection and was found to be as attenuated as a MYX Serp 1 deletion mutant. Taken together, these results indicate that despite a nearly identical reactivity profile *in vitro*, SPI-3 and Serp1 are not able to

substitute for one another in the context of viral infection and implies that the two serpins may have different natural proteinase targets in nature.

Other poxvirus serpin-like genes. A recent article reporting the complete genomic sequence of myxoma virus, strain Lausanne revealed that the virus encodes a third gene with homology to the serpin family which they designate Serp3 (41). The authors of the study propose that Serp3 may function as a serpin during infection, as the predicted amino acid sequence contains conserved serpin structural elements (41). However, analysis of the predicted Serp3 ORF reveals that the carboxy-terminal region of the protein including the serpin RSL is truncated, suggesting that the protein is not likely a functional proteinase inhibitor.

Fowlpox virus, a member of the avipoxvirus genus, has recently been shown to contain five genes with homology to the serpin superfamily (3). However, analysis of the predicted protein sequences of each of the genes demonstrates that only 4 of the 5 proposed FPV serpins are full length (FPV010, FPV040, FPV044, and FPV204) (Table 2). The remaining FPV gene encodes a protein with a predicted molecular weight of 17 kDa that lacks the region corresponding to the serpin reactive site loop. To date, no study has demonstrated any role for the FPV serpins during infection.

The Orthopoxvirus Serpin SPI-1

When the spontaneous white pocks mutants of CPV and RPV were discovered following infection of the CAM nearly forty years ago, it was noted that several of the RPV mutants had a reduced host range and were unable to form plaques on PK-15 pig kidney cell monolayers (75,81). Genetic complementation studies revealed that the gene

necessary for restoration of the plaquing phenotype on PK-15 cells was SPI-1, known as ORF B22R in vaccinia virus (10). Sequencing revealed the presence of the SPI-1 gene in other members of the orthopoxvirus genus, including CPV and variola (123). The SPI-1 and SPI-2/crmA genes are approximately 45% identical, leading some researchers to propose that the two genes were derived from a common ancestral viral serpin gene by duplication and divergence within the virus genome (10). The SPI-1 gene encodes a protein with a predicted molecular mass of 41 kDa that is expressed early during infection and is predicted to remain within the cytoplasm of infected cells (260). Database screening of the predicted SPI-1 amino acid sequence reveals that the protein shares homology to the serpin family of serine proteinase inhibitors.

Studies have shown that deletion of the SPI-1 gene from CPV or VV has no effect on pock color on the CAM or virulence in mice following intranasal inoculation (10,123,281). In contrast, RPV SPI-1 mutants produce white pocks on the CAM, but don't appear to be attenuated in a mouse intranasal model of infection (10,281). In addition, RPV SPI-1 null mutants have a restricted host range and are unable to productively infect the pig kidney PK-15 and LLC-PK1 cell lines or A549 human lung carcinoma and HeLa cervical carcinoma cells (10) and (Kristin Moon, unpublished results). In contrast, the ability of the mutant virus to productively infect and plaque on other cell lines, including CV-1 (African green monkey kidney) and RK-13 (rabbit kidney) cells remains unchanged.

Detailed analysis of A549 and PK-15 cells infected with an RPV SPI-1 null mutant was performed to determine the defect in virus infection (36). The study determined that the growth and spread of the RPV SPI-1 mutant in RK-13 cells was

indistinguishable from wtRPV, but mutant virus production from A549 and PK-15 cell lines was less than 5% of wild type levels in the corresponding cell lines. A comparison of virus protein synthesis and processing in A549 cells revealed no differences following infection with either wtRPV or the RPV SPI-1 mutant. In addition, both the timing and levels of viral DNA production were similar between the wild type and SPI-1 mutant of RPV in A549 cells. However, while the wild type and mutant viruses produced similar numbers of virus particles in RK-13 cells, the RPV SPI-1 mutant virus was found to produce little mature virus in A549 cells when analyzed at 24 hours post-infection, in contrast to wtRPV. Still, transmission electron microscopy of restrictive cell lines infected with the RPV SPI-1 negative virus revealed the presence of immature progeny virions at various stages of development at earlier times post-infection (12 hours post-infection), from the initial membrane crescents to the IMV and IEV forms of the virus, though little mature virus was observed. Thus, it appeared as if the initial stages of virus morphogenesis were taking place, but that virion maturation and release of the virus was somehow impeded in the restrictive cells infected with the SPI-1 mutant virus. The same electron microscopy experiments also revealed that the restrictive A549 and PK-15 cells infected with the RPV SPI-1 mutant displayed many of the morphological features of apoptosis, including chromatin condensation and margination, marked nuclear invagination, and karyohexis. By 24 hours post infection, approximately 94% of the nonpermissive cells infected with the SPI-1 mutant were reported to exhibit the apoptotic morphology. In addition to apoptotic morphology, at least 92% of A549 cells infected with the SPI-1 mutant were demonstrated to contain the DNA fragmentation typical of cells undergoing apoptosis. When nonpermissive cells were infected with the RPV SPI-1

mutant in the presence of cytosine arabinoside, an inhibitor of viral DNA replication and late gene expression, no evidence of apoptosis was seen, suggesting that the infection must proceed beyond the early phase of gene expression before apoptosis is induced. Based on these findings, it was proposed that the inability of the RPV SPI-1 null mutant to form plaques on nonpermissive cell monolayers was due to the induction of apoptosis in the infected cells, which served to degrade progeny virions prior to their release from the cells (36).

A second study has demonstrated a role for SPI-1 in inhibiting apoptosis within the context of a virus infection (147). Cells were infected with wild type CPV or RPV, or CPV or RPV recombinants containing mutations in SPI-1, SPI-2/crmA or both genes. The infected cells were then assayed for their ability to inhibit apoptosis directed via the Fas- or granule-mediated pathways. Both wild type CPV and RPV were able to resist cytolysis employed by either mechanism. Whereas mutation of the crmA/SPI-2 was necessary to relieve inhibition of Fas-mediated cytolysis, in some cell types, mutation of SPI-1 in addition to crmA/SPI-2 was necessary to completely abrogate inhibition. In contrast, viral inhibition of granule-mediated apoptosis was dependent on mutation of both SPI-1 and crmA/SPI-2. These results indicate that, like crmA/SPI-2, SPI-1 also plays a role in inhibiting apoptosis directed by the Fas- and granule-mediated pathways of CTL and suggests that SPI-1 and SPI-2 may work together to inhibit cytolysis of infected cells *in vivo*.

Though SPI-1 has been demonstrated to confer virus host range and to inhibit apoptosis during infection of tissue culture cells, the exact mechanism by which SPI-1 functions is unknown. While SPI-1 shares homology to the serpin family and is

presumed to act as a serine proteinase inhibitor, no biochemical activity has been attributed to SPI-1 to date. In this study, the biochemical properties of SPI-1 were explored by expressing the protein *in vitro* and assaying it for serpin activity. An RPV SPI-1 deletion mutant was constructed, along with RPV recombinants containing site-directed mutations in the SPI-1 RSL, and the ability of each of these viruses to productively infect permissive and nonpermissive cell lines was determined. Finally, RPV variants containing mutations in SPI-1 alone or in parallel with mutations in SPI-2 were assayed in a rabbit model of infection to more completely characterize the effects of serpin mutations on the virulence of RPV *in vivo*.

CHAPTER 2
MATERIALS AND METHODS

Virological Techniques

Cell Culture

CV-1 (ATCC CCL-70), RK-13 (ATCC CCL-37), PK-15 (ATCC CCL-33), A549 (ATCC CCL-185) and Rat-2 (ATCC CRL-1764) cells were routinely grown in GIBCO-BRL minimum essential medium (MEM) with Earle's salts supplemented with 5% fetal bovine serum (FBS), 2 mM glutamine, 50 U penicillin G per ml, 50 ug of streptomycin per ml, 1 mM sodium pyruvate, and 0.1 mM MEM nonessential amino acids (GIBCO BRL, Grand Island, NY). LLC-PK1 cells (ATCC CL-101) were grown in Medium 199 (GIBCO) supplemented with 10% FBS, 2 mM glutamine, 50 U penicillin G per ml, 50 ug of streptomycin per ml, 1 mM sodium pyruvate, and 0.1 mM MEM nonessential amino acids.

Production and Titration of Virus Stocks

RPV-Utrecht (ATCC-VR-157), CPV-Brighton Red (ATCC-VR-302), CPVΔcrmA (10), VV-WR (ATCC VR-119), vTF7.3 (ATCC VR-2153), RPV SPI-1 (-)(10) and their derivatives were grown in either CV-1 or RK-13 cells. Virus stocks were produced by infecting cells at an MOI of 0.01 in medium without serum for 2 hours with constant rocking at 37°C. When cytopathic effect was maximal, infected cells were scraped into medium using a rubber policeman. Cells were pelleted for 5 minutes at 1000

X g. Infected cell pellets were resuspended in medium without serum and stored at –80°C until used.

Virus stocks were titered by plaquing serial ten-fold dilutions on confluent 35 mm dishes of the appropriate cell line under a 1:1 mixture of 1.2% SeaKem LE agarose (FMC Bioproducts, Rockland, ME) and 2X GIBCO MEM. Cells were stained at 72 hours post infection by the addition of 0.11 mg/ml neutral red (GIBCO-BRL) diluted in medium without serum and plaques were counted.

Sucrose Pad Purification of Virus Stocks for Use in Animal Infections

Virus used for animal studies was prepared using the following protocol. Infected RK-13 cells grown in 150 mm dishes were scraped into the medium and collected by centrifugation at 500 X g for 10 minutes. The infected cell pellet was resuspended in TM buffer (10 mM Tris-HCl pH 7.5, 5 mM $MgCl_2$, 0.2 ml per 150 mm dish) and incubated for 10 minutes at room temperature. Cells were then lysed by 20 strokes using a Dounce homogenizer with a tight pestle. The resulting lysate was centrifuged at 500 X g for 10 minutes to pellet nuclei and cell debris. The resulting pellet was then resuspended in TM buffer (0.35 ml per 150 mm dish) and the cells were subjected to two more rounds of Dounce homogenization and centrifugation. Following centrifugation, supernatants were sonicated for 60 seconds using a Vibra-cell probe sonicator (Sonics and Materials, Danbury, CT) set on level 2. The lysates were then layered onto a 36% (w/v) sucrose pad and centrifuged in a Beckman SW28 rotor at 65,000 X g for 90 minutes. The resulting pellet was resuspended in PBS (0.2 ml per 150 mm dish) and the virus stock was divided into 200 ul aliquots which were stored at –80°C until used. Accurate virus titers were

obtained by plating serial dilutions from three separate aliquots of virus as described above. Individual aliquots were thawed once, used, and then discarded.

Construction of RPV SPI-1 Deletion Mutant (RPVΔSPI-1)

Semiconfluent (80%) CV-1 cells grown in 35 mm dishes were infected with wt RPV at an MOI of 0.05 and virus was adsorbed for 2 hours at 37°C. The inoculum was removed and the cells were washed twice with GIBCO MEM medium without serum. 1.5 ml of medium without serum was added to the cells followed by 5-10 ug of the pKMSPI-1-gpt plasmid (described below) conjugated with Lipofectin (GIBCO-BRL). Specifically, the DNA was diluted in water to a volume of 50 ul in an Eppendorf tube, while 12 ul of Lipofectin was diluted with 38 ul of water in a polystyrene tube. The diluted DNA and Lipofectin were then mixed and added dropwise to the infected cells which were incubated at 37°C. At 24 hours post infection, 1.5 ml of GIBCO-MEM supplemented with 5% FBS was added to the cells which were incubated for another 24 hours at 37°C. Transfected cells were harvested at 48 hours post infection by scraping into the media. Crude viral stocks were subjected to three cycles of freezing and thawing and tenfold serial dilutions were plated under a 1:1 mixture of 1.2% agarose and 2X GIBCO MEM on CV-1 cell monolayers which had been pretreated for 6 hours in the presence of 2.5 ug/ml mycophenolic acid, 250 ug/ml xanthine, and 15 ug/ml hypoxanthine. At 72 hours post infection, cell monolayers were stained with neutral red to visualize plaques. Six separate plaques containing virus resistant to mycophenolic acid were picked and placed in 1 ml MEM without serum. Picked plaques were sonicated for 120 seconds and serial dilutions of the picked plaque suspensions were plated under

agarose on CV-1 cell monolayers which had been pretreated with mycophenolic acid, xanthine, and hypoxanthine for 12 hours as described above. In this manner, mycophenolic resistant virus was purified three times before amplification in CV-1 cells. Deletion of the SPI-1 ORF and purity of the final virus stocks were confirmed by PCR and immunoblot assay. A single viral isolate (RPVΔSPI-1) was chosen for expansion and all future work.

Construction of RPV SPI-1 Site-Directed Mutant Viruses

Semiconfluent (80%) CV-1 cells grown in 35 mm dishes were infected with RPVΔSPI-1 at an MOI of 0.05 and virus was adsorbed for 2 hours at 37°C. The inoculum was removed and the cells were washed two times with medium without serum. 1.5 ml of medium without serum was added to the cells followed by 5-10 ug of the appropriate plasmid DNA (pKMSPI-1wt, pKMSPI-1 N321A/F322A/S323A, pKMSPI-1 F322A, pKMSPI-1 T309R) conjugated with Lipofectin in a 100 ul volume. After 24 hours at 37°C, 1.5 ml of medium containing 5% FBS was added to the cells which were further incubated at 37°C for another 24 hours. Transfected cells were harvested at 48 hours post infection.

RPV recombinants containing the wild type or mutant SPI-1 genes in place of the *Escherichia coli* (*E.coli*) *eco-gpt* selectable marker gene at the SPI-1 locus were selected following plaque hybridization using a ^{32}P-labeled randomly primed probe specific for the SPI-1 ORF. Specifically, Rat-2 monolayers grown in 100 mm dishes and infected with approximately 1000-1500 pfu of virus were stained at 72 hours post-infection with neutral red to visualize plaques. Each stained monolayer was then covered with an 82

mm nylon membrane (Magna). Membranes were overlayed with a 3mm Whatman paper saturated in 50 mM Tris-HCl (pH 8.0), 1.5 M NaCl and the monolayer was transferred to the membrane using gloved fingers. A second buffer- saturated nylon membrane was then placed on top of the first membrane, and a dry Whatman paper was placed on top of the filter sandwich. Capillary action allowed the transfer of the monolayer to the second nylon membrane, forming a replica of the original master membrane. Replica filters were wrapped in aluminum foil and stored at -20^{o}C. Master filters were processed for plaque hybridization by incubating first in 0.5 M NaOH, 1.5 M NaCl for 5 minutes, followed by a 5 minute incubation in 0.5 M Tris-HCl (pH 7.4), 1.5 M NaCl. Master filters were air dried after which the DNA was fixed to the membrane by baking in a vacuum oven at 80^{o}C for one hour. Filters were then incubated in hybridization solution (6X SSC, 0.25% (w/v) dried milk) for two hours at 65^{o}C after which time heat denatured, ^{32}P-labeled, randomly primed probe specific for the SPI-1 gene (see DNA techniques for details on probe preparation) was added and the incubation continued overnight. Filters were washed 4 times with 2 X SSC, 0.1% SDS for 5 minutes followed by two washes for 30 minutes with 0.1 X SSC, 0.1% SDS at 60^{o}C with constant agitation. Air dried filters were sandwiched between clear plastic wrap exposed to film. Plaques from replica filters which corresponded to positively hybridizing plaques from the master filters were aseptically removed from the filter and placed in 500 ul MEM without serum. Plaque suspensions were sonicated twice for 60 seconds using a Vibra-Cell probe sonicator on setting 2, and dilutions of 10^{0}, 10^{-1} and 10^{-2} were plated on 100 mm dishes, and the above protocol repeated until a pure virus stock was obtained. Replacement of *eco-gpt*

with the wild type or site-directed SPI-1 genes was confirmed by PCR, sequencing, and immunoblot analysis.

Construction of RPV SPI-2 Insertion Mutant Viruses

CV-1 cells grown in 35 mm dishes were infected with virus (wt RPV, RPVΔSPI-1, or RPV SPI-1 F322A) at an MOI of 0.05 for two hours at 37°C with constant rocking. Cells were washed twice with MEM without serum. 1.5 ml of medium without serum was added to the cells followed by 5-10 ug of RPVΔSPI-2::lacZ DNA conjugated with Lipofectin. At 24 hours post infection, 1.5 ml of MEM supplemented with 5% FBS was added to the cells. At 48 hours post infection, cells were harvested as described previously. Serial tenfold dilutions of the crude virus stocks were plated on CV-1 60 mm dishes under a 1:1 mixture of 1.2 % agarose and 2X MEM. At 48 hours post-infection, cells were stained with X-gal (300 ug/ml, diluted from a 20 mg/ml stock prepared in DMF). Well-isolated blue plaques were picked and resuspended in 1 ml of PBS-AM. Plaque suspensions were sonicated for 120 seconds using a Vibra Cell Sonicator with cup attachment (Sonics and Materials, Danbury, CT), and 10^{-1}, 10^{-2} and 10^{-3} dilutions of the samples were plated on CV-1 60 mm dishes. This procedure was repeated 3-4 times until all of the plaques produced from an isolate stained blue after which time the isolate was expanded to produce a high titer virus stock. Insertional inactivation of the SPI-2 gene was confirmed by PCR and immunoblot analysis.

Virus Host Range Assay

RK-13, A549 and PK-15 cell monolayers grown in 60 mm dishes were infected with approximately 100 pfu of virus in MEM without serum. After two hours of incubation at 37°C, the virus inoculum was removed and the infected cells were overlaid with a 1:1 mixture of 2X GIBCO MEM and 1.2% agarose. At 72 hours post-infection, the agarose overlays were removed and the infected cell monolayers were stained with crystal violet to visualize plaques.

DAPI Staining of Infected Cells

A549 cells were grown in LabTek eight-well chamber slides (Nunc, Naperville, IL) to 60% confluence and infected with virus at an MOI of 10 in 100 ul of MEM without serum. Virus was adsorbed for 2 hours at 37°C. After removal of the inoculum, cells were washed with 300 ul of medium without serum and placed at 37°C. At 18 hours post-infection, medium was removed and cells were washed once with PBS. Cells were fixed by incubating for 20 minutes in PBS containing 3.5% paraformaldehyde at room temperature. Cold methanol was then added to permeabilize the cells which were further incubated for 10 minutes at room temperature. Cells were rinsed twice with PBS followed by the addition of PBS containing 0.5 ug/ml DAPI (4'6-diamidino-2-phenylindole) and incubation for 30 minutes at room temperature. Cells were washed three times with PBS. DAPI-stained DNA was visualized using a fluorescent lamp and DAPI filter and fluorescent cells were photographed using Fuji 400 ASA film.

Intradermal Infection of Rabbits

Adult, ~5 pound female New Zealand White rabbits were obtained from Myrtle's Rabbitry (Thompson Station, TN) and were housed in individual cages in infectious isolation cubicles at the Animal Resource Facility at the University of Florida. Virus inoculums were diluted in 100 ul of PBS and injected intradermally into the shaved right or right and left flanks of each rabbit using a 27-gauge needle and tuberculin syringe. Each animal was weighed on a daily basis and examined for clinical signs of disease. The diameter and induration of the primary site of inoculation was measured daily and photographed periodically. Rectal temperatures were measured using a digital thermometer (Becton-Dickinson, Franklin, New Jersey). Rabbits were sacrificed by intravenous overdose of Xylezene.

Histology of Infected Lesions

Primary lesions were removed following animal sacrifice and placed in 10% buffered formalin. 5 mm sections were made through the center of the lesion, leaving a border of normal skin adjacent to the infected tissue, placed in tissue cassettes, and embedded in paraffin. The embedded lesions were sectioned at 5 μm and stained with hematoxylin and eosin . Each section was examined by two impartial veterinary pathologists.

Recombinant DNA Techniques

Plasmids

pGEM 3ZF::PARP. A cDNA clone of human poly-(ADP-ribose) polymerase (PARP) (kindly provided by Dr. Alexander Burkle, German Cancer Research Center, Heidelberg, Germany) was cloned by M. Teresa Baquero into the plasmid pGEM 3ZF (-) using *Sma* I, oriented such that PARP could be expressed from the P_{T7} promoter.

pALTER Ex1::Lamin A. A cDNA clone of human Lamin A (a gift from Dr. B. Burke, University of Calgary, Calgary, Alberta, Canada) was subcloned into the *Eco* RI and *Xba* I sites of the plasmid pALTER-*Ex1* oriented such that Lamin A could be expressed from the P_{T7} promoter and was kindly provided by M. Teresa Baquero.

pALTER Ex1::SPI-1. This clone was constructed to enable expression of the RPV SPI-1 gene under the control of the P_{T7} promoter. The SPI-1 gene was amplified from RPV genomic DNA by PCR using primers SM 227 (5' ggg gcc atg gat atc ttt aaa gaa cta atc 3') and SM 228 (5' ggg gat cct tat tgc gga tag cag tat ttc 3'). The PCR product DNA was digested with *Nco* I and *Bam* HI and cloned into the corresponding restriction sites in pALTER-*Ex1* plasmid DNA.

pKMSPI-1. The shuttle vector pKMSPI-1 was designed so that the SPI-1 gene of RPV could be replaced by any gene cloned between the SPI-1 left and right flanks contained within the plasmid (Figure 6). Briefly, the 235 base pairs (bp) directly upstream of the SPI-1 ORF (SPI-1 left flank) were amplified from wtRPV genomic DNA

Figure 6. **Construction of the shuttle vector pKMSPI-1.** A) Source of the primers used to amplify the left and right flanking regions of SPI-1 for construction of the shuttle vector pKMSPI-1. The SPI-1 ORF beginning with nucleotide 1 and ending with nucleotide 1074 is designated by a black box. The left flanking sequence of the SPI-1 gene begins at nucleotide –235 and extends to nucleotide 1 of the SPI-1 ORF. The right flanking sequence of SPI-1 begins at the first nucleotide following the SPI-1 ORF and extends to nucleotide +522. SPI-1 left and right flanks are designated by hatched boxes. B) Schematic representation of the pKMSPI-1 shuttle vector. A removable cassette containing either the *E. coli gpt* gene driven by the vaccinia virus $P_{7.5}$ promoter, the wt SPI-1 gene, or each of the three SPI-1 site-directed genes was individually cloned between the left and right flanks of SPI-1. The locations of the relevant restriction sites are shown.

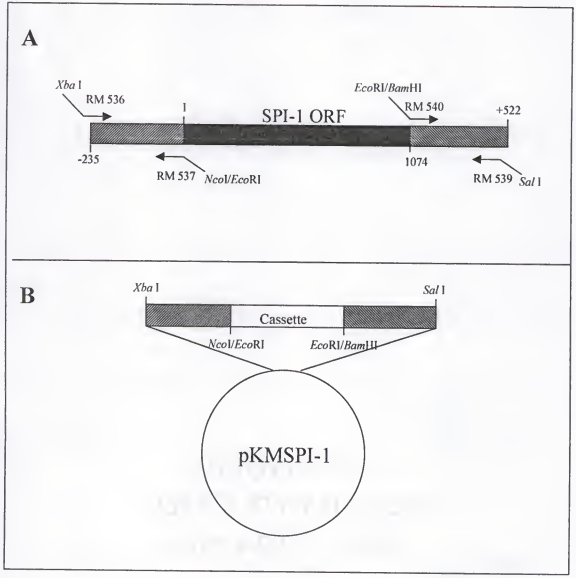
A
Xba I
RM 536
1
SPI-1 ORF
EcoRI/BamHI
RM 540
+522
-235
RM 537
NcoI/EcoRI
1074
RM 539
Sal I
B
Xba I
Sal I
Cassette
NcoI/EcoRI
EcoRI/BamHI
pKMSPI-1

by PCR using the primers RM 536 (5' gct cta gac gat tga ttt tat cat cc 3') and RM 537 (5' cgg aat tcc cat ggt ata gac caa aca at 3') which introduced an *Xba* I site onto the 5' end and an *Nco* I and *Eco* RI site onto the 3' end of the left flank, respectively. The SPI-1 left flank was digested with *Xba* I and *Eco* RI and cloned into pBluescript KS (+) (Stratagene). The 522 bp directly downstream of the SPI-1 ORF (SPI-1 right flank) were amplified from wt RPV genomic DNA by PCR using primers RM 540 (5' cgg aat tcg gat cca tat aaa caa ata gac ttt tat 3') and RM 539 (5' gcg tcg act cta tag aaa cac cta gaa ta 3') which introduced an *Eco* RI and a *Bam* HI site onto the 5' end and a *Sal* I site onto the 3' end of the right flank, respectively. The SPI-1 right flank was digested with *Eco* RI and *Sal* I and cloned into pBluescript KS (+) containing the SPI-1 left flank to create pKMSPI-1.

pKMSPI-1-gpt. A 2081 bp fragment of the *E. coli eco-gpt* gene downstream of the vaccinia virus $P_{7.5}$ promoter was cloned between the SPI-1 left and right flanks into the *Eco* RI site in pKMSPI-1. This plasmid was designed to facilitate deletion of the SPI-1 gene from the RPV genome by providing a selectable marker for homologous recombination.

pKMSPI-1 N321A/F322A/S323A, pKMSPI-1 F322A, pKMSPI-1 T309R. Each of the three SPI-1 site-directed mutant genes (discussed below) were excised from pALTER *Ex1* by digesting with *Nco* I and *Bam* HI and cloned into pKMSPI-1. These plasmids were designed to allow the construction of RPV recombinants containing specific mutations within the putative SPI-1 RSL.

pRPVΔSPI-2::lacZ. This plasmid was designed to aid in the construction of an RPV SPI-2 null virus which contains the *E. coli* gene for the screenable marker β-

galactosidase (lacZ) in place of the central one third of the SPI-2 ORF. The 5' terminal portion of the RPV SPI-2 gene was cloned into pBluescript KS (+) (Stratagene) as a 315 bp *Eco* RV fragment, using the natural restriction sites at nucleotide positions 6 and 321 in the SPI-2 ORF. The desired orientation was verified, and the resulting plasmid, pBS-SPI-2L, was digested with *Xba* I and *Pst* I, and the p11-lacZ fragment from pSC11 (272), which had been excised with *Xba* I and *Pst* I, was inserted to create pBS-SPI-2L-lacZ. Next, the 3' terminal region of the RPV SPI-2 gene was amplified by PCR using the primers RM168 (5' gat cca cta gtt cta gag gac tga cag agg tgt t 3') and SM261 (5' cga att ccg cgg ccg ctg tgg tga aaa gac 3'). The PCR fragment was digested with *Xba* I and *Not* I and cloned into the corresponding *Xba* I and *Not* I sites of pBS-SPI-2L-lacZ. The final plasmid construct, pΔSPI-2::lacZ, contains the RPV SPI-2 gene with a 447 bp internal deletion.

Purification of DNA, Ligation, Transformation, Recovery of Recombinant Plasmids, and Analysis of Transformants

Unless otherwise noted, DNA fragments were isolated following electrophoresis on 1% agarose, Tris-acetate/EDTA (TAE: 40mM Tris-acetate, 1mM EDTA) gels and purified using the Geneclean II kit (Bio 101, Vista, CA) according to the manufacturer's instructions. The resulting DNA was quantified spectrophotometrically for ligations, which were performed using the Rapid DNA ligation kit (Boehringer Mannheim, Germany) according to directions supplied by the manufacturer. The ligated DNA was introduced into competent strains of E. coli using the technique of Sambrook (152). Transformants were grown on LB agar plates (1% tryptone, 0.55 yeast extract, 1% NaCl, 1.5% Difco Bacto-agar) containing the appropriate antibiotic. Plasmid DNA was isolated

using QIAfilter Midi- or Mini-prep kits according to the manufacturer's instructions (QIAGEN, Valencia, CA). All restriction endonuclease digestions were performed using enzymes and buffers supplied by New England Biolabs (Beverly, MA) using conditions supplied by the manufacturer.

PCR

All primers used for amplification of DNA were made by the University of Florida ICBR DNA Synthesis Core Laboratory or were obtained from Genosys (The Woodlands, TX). Reactions were performed using a PTC-100 Thermal Controller (MJ Research Inc., Watertown, MA). PCR to generate products for cloning were performed in a total volume of 100 ul containing 2 U Vent DNA polymerase (New England Biolabs), the manufacturer's recommended buffer, and 200 uM dNTPs. For routine diagnostic PCR, reactions were performed in a 100 ul volume containing 2.5 U Taq Polymerase (Promega), the manufacturer's recommended buffer containing an additional 1.5 mM $MgCl_2$, and 200 uM dNTPs. Typical reactions included an initial denaturation step at 94°C for 4 minutes followed by 30 cycles of denaturation at 94°C for one minute, annealing at 45°C for 1 minute, extension at 72°C (for roughly one minute per kbp of the expected product size), followed by a final extension at 72°C for 8 minutes.

Preparation of Viral DNA

CV-1 monolayers were infected with virus at an MOI of 0.1 to 10. When CPE was maximal, infected cells were scraped into the media with a rubber policeman. Cells were pelleted at 500 X g and the supernatant was transferred to a new tube. EEV was

obtained by pelleting the supernatant at 16,000 X g for 15 minutes. The supernatant was removed and the EEV pellet was resuspended in an appropriate volume of TE. SDS and proteinase K were added to final concentrations of 1% and 1mg/ml, respectively, and the sample was incubated at 50°C overnight. Samples were subjected to phenol chloroform extraction and DNA was precipitated by adding 1/10 volume 3M sodium acetate (pH 5.3) and 2 volumes 95% ethanol. DNA pellets were washed once with 1 ml 70% ethanol, and pellets were dried briefly in a SpeedVac. DNA was resuspended in TE and stored at –20°C until needed. DNA concentrations were determined using a TD700 Fluorometer (Turner Designs, Sunnyvale, CA).

Preparation of SPI-1 Randomly Primed Probe

pAlter-Ex1::SPI-1 was digested using *Nco* I and *Bam* HI and the 1074 bp fragment representing the SPI-1 gene was purified following electrophoresis using the Geneclean II kit according to the manufacturer's instructions. Approximately 50 ng of SPI-1 DNA was denatured by boiling for 10 minutes. ^{32}P-labeled, randomly primed probe was made using the Random Primed DNA Labeling Kit (Boehringer Mannheim, Germany). The probe was diluted 1:1 with 1X NTE (100 mM NaCl, 10 mM Tris-HCl pH 7.4, 1 mM EDTA) and separated from unincorporated nucleotides by passing over a 1.0 ml packed volume Sephadex G-50 column. Radiolabeled probe was stored at 4°C until needed.

Site-Directed Mutagenesis of the SPI-1 RSL

Site-directed mutagenesis of the SPI-1 reactive site loop was performed using the Altered Sites Mutagenesis System (Promega) according to the manufacturer's instructions. The RPV SPI-1 open reading frame was first cloned into the pALTER *Ex1* vector *Nco* I and *Bam* HI sites. The 5' phosphorylated oligonucleotide (RM 538) [5' p-aca gga gta ttt atg act aca gct gcg atg gta tat cgt acg aag 3'] was used to change the predicted P2, P1 and P1' residues at amino acid positions 321, 322 and 323 from asparagine, phenylalanine, serine to alanine, alanine, alanine (N321A/F322A/S323A). The 5' phosphorylated oligonucleotides GM14 [5'p-gga gta ttt atg act aac gcg tcg atg gta tat cgt acg 3'] and RM 543 [5' p-gat gtt aat gag gag tat cgc gaa gca tcg gcc gtt 3'] were likewise used to change the putative P1 residue at position 322 from phenylalanine to alanine (F322A) and the P14 residue at position 309 from threonine to arginine (T309R). In addition to the above amino acid changes, oligonucleotides RM 538, GM 14 and RM 543 were designed to introduce novel *Pst* I, *Mlu* I and *Nru* I sites into the SPI-1 gene, respectively, to enable efficient screening and isolation of mutant clones. The sequences of the site-directed mutant genes were confirmed by sequencing.

Protein Analysis

***In vitro* Expression of Wt SPI-1, His-Tagged SPI-1 and SPI-1 Site-Directed Mutants**

The wild type and site-directed mutant SPI-1 genes had been cloned into the vector pALTER-Ex1 (Promega) using *Nco* I and *Bam* HI, oriented such that the genes could be expressed from the P_{T7} promoter. SPI-1 was likewise cloned into the vector

pTM1-His using *Nco* I and *Bam* HI oriented such that the gene could be expressed from the P_{T7} promoter and allowing the incorporation of a decahistidine tag onto the NH_2-terminus of the protein. *In vitro* expression of ^{35}S-labeled wt SPI-1, His-tagged SPI-1, N321A/F322A/S323A, F322A, and T309R proteins was performed using the TNT T7 Quick Coupled Transcription/Translation System (Promega) according to the manufacturer's instructions.

SDS-PAGE Analysis of SPI-1 Activity

1 ul of ^{35}S-labeled wt SPI-1 or SPI-1 RSL mutant proteins expressed *in vitro* in the TNT system were incubated with varying amounts of the proteinases human pancreas chymotrypsin, human neutrophil cathepsin G (both purchased from Athens Research and Technology, Inc., Athens, GA.), or recombinant mast cell chymase (a generous gift from Dr. Norman Schechter, University of Pennsylvania). Reactions were performed in a total volume of 10 ul containing the appropriate reaction buffer (100 mM Tris-HCl pH 8.0, 10 mM $CaCl_2$ was used with the proteinases chymotrypsin and cathepsin G; 1.5 M Tris-HCl pH 8.0, 9% DMSO was used with mast cell chymase) for 90 minutes at 37°C. Reactions were stopped by the addition of SDS loading buffer and boiling for five minutes. Proteins were separated by electrophoresis for 2 hours at 90 V in an SDS-10% polyacrylamide gel with a discontinuous buffer system. Following SDS-PAGE, gels were fixed for 30 minutes in 25 % methanol, 7 % acetic acid and processed for fluorgraphy using the Amplify system (Amersham). Gels were dried, exposed to film and developed.

His-Tagged Protein Purification

5 ul of ^{35}S-labeled His-tagged SPI-1 expressed in the TNT system was incubated with buffer alone or with 200 nM of cathepsin G or chymotrypsin in a total volume of 20 ul for 15 minutes at 37°C. The reactions were then added to 30 ul of His-Bind Resin (Novagen, Madison, WI) which had been charged with 50 mM $NiSO_4$ for five minutes. The mixtures were incubated at 4°C for 2 hours with constant agitation. The resin was washed with 500 ul of MCAC-50 (20 mM Tris-Cl pH 7.9, 0.5 M NaCl, 10% glycerol, 1 mM PMSF, 50 mM imidazole), then with 500 ul of MCAC-100 (20 mM Tric-HCl pH 7.9, 0.5 M NaCl, 10% glycerol, 1 mM PMSF, 100 mM imidazole) to remove any unbound proteins. His-tagged proteins were removed from the resin by the addition of 2X SDS loading buffer (4% SDS, 20% glycerol, 200 mM DTT, 120 mM Tris-HCl pH 6.8, 0.002% bromophenol blue) and boiling for five minutes. Proteins were separated on SDS-10% polyacrylamide gels and radiolabeled proteins were visualized as described previously.

α_1-Antichymotrypsin Competition Assay

Human plasma α_1-antichymotrypsin was purchased from Athens Research and Technology, Inc.. 1 ul of ^{35}S-labeled wt SPI-1 expressed in the TNT system was reacted with a constant amount of cathepsin G shown to yield complex formation (200 nM) in the presence of increasing amounts of α_1-antichymotrypsin. Reactions were performed in a total volume of 10 ul containing reaction buffer (100 mM Tris-HCl pH 8.0, 10 mM $CaCl_2$) for 90 minutes at 37°C. Reactions were quenched by the addition of 2X SDS

loading buffer, boiled for five minutes, and analyzed by electrophoresis on SDS-10% polyacrylamide gels as described previously.

Time Course of SPI-1: Cathepsin G Complex Decay

15 ul of ^{35}S-labeled wt SPI-1 expressed in the TNT system was incubated with 200 nM cathepsin G in a total volume of 150 ul reaction buffer (100 mM Tris-HCl pH 8.0, 10 mM $CaCl_2$) for 60 minutes at 37°C. A ten-fold molar excess of α_1-antichymotrypsin (2 uM) was then added to prevent further complex formation and the reaction was incubated for up to 24 hours at 37°C. Samples were removed at various times and reactions were quenched by the addition of 2X SDS loading buffer and boiled for five minutes. Proteins were separated on an SDS-10% polyacrylamide gel, ^{35}S-labeled proteins were enhanced with Amplify, and proteins were visualized by autoradiography. High molecular bands representing the SPI-1:cathepsin G complex were quantified with a Model 400S PhosphorImager (Molecular Dynamics, Inc., Sunnyville, CA.).

Production of SPI-1 and SPI-2 Monoclonal Antibodies

The monoclonal antibodies 6H7-364 and 2B12-4B1 were produced by the University of Florida Hybridoma Core (Gainesville, FL). 6H7-364 and 2B12-4B1 were generated by immunizing female BALB/c mice with purified His-tagged RPV SPI-1 or RPV SPI-2 protein, respectively. Splenocytes from immunized animals were fused with a murine myeloma cell line Fused cells were selected and screened for clones producing culture supernatant that was immunopositive for the desired protein by both enzyme-

linked immunoabsorbent assay and immunoblot analysis. The antibodies were column purified prior to use.

Immunoblot Analysis of Infected Cell Extracts

Cells were infected with virus at an MOI of 0.1 to 10. When CPE was maximal, cells were scraped into the medium using a rubber policeman. Infected cells were pelleted by centrifuging for 5 minutes at 500 X g. Cell pellets were washed once in PBS and pelleted as before. Pellets were resuspended in an appropriate volume of cell lysis buffer (100 mM Tris-HCl pH 8.0, 100 mM NaCl, 0.5% Triton X-100) containing 0.2 mM phenylmethylsulfonyl fluoride (PMSF) and cells were placed on ice for 20 minutes. Nuclei and other insoluble material was pelleted by a 15 minute centrifugation at 5,000 X g and the remaining cell lysate was removed to a new tube. Protein concentration was determined according to the method of Bradford (35). Unless otherwise noted, 10 to 15 ug of cell extract was added to an equal volume of 2X SDS loading buffer (0.1 M Tris, 24% (w/v) glycerol, 8% (w/v) SDS, 0.2 M DTT, and 0.02% (w/v) Coomassie blue G-250) and electrophoresed for 2 hours at 90 V in a 10% polyacrylamide/SDS gel with a discontinuous buffer system. Gels were transferred to Nitrobind nitrocellulose membranes (MSI, Westborough, MA) using a semi-dry transfer apparatus (Fisher Scientific, Pittsburgh, PA) in Tris/glycine/methanol transfer buffer at a constant current of 150 mAmps for 2 hours. Membranes were blocked overnight in blocking solution (5% nonfat dry milk, 0.1% Tween in TBS: 150 mM NaCl, 20 mM Tris pH 8.0) at 4°C. Membranes were probed with the appropriate primary antibody diluted in blocking solution for 1.5 hours at room temperature with continuous rocking. Following three ten

minute washes in TBST (0.1% Tween in TBS), membranes were incubated with an appropriate dilution of horseradish peroxidase-conjugated goat anti-mouse secondary antibody (Sigma) in blocking solution for one hour with continuous rocking. After four ten minute washes in TBST, membranes were developed using the ECL-plus system (Amersham Pharmacia Biotech, Inc., Piscataway, NJ) according to the manufacturer's recommended protocol.

Preparation of Infected Cell Extracts for PARP and Lamin A Cleavage Assays

Semiconfluent (80%) monolayers of either A549 or LLC-PK1 cells in 60 mm dishes were either mock infected or infected with wt RPV or RPVΔSPI-1 (A549 cells) or wt CPV or CPVΔcrmA (LLC-PK1 cells) at an MOI of 10. Virus was adsorbed for two hours at 37°C, medium was added, and the infection was allowed to proceed for 14 hours. Cells were harvested by scraping into the medium and were pelleted for five minutes at 200 X g. Cells were washed once with PBS, pelleted, washed once in ice-cold Extract Preparation Buffer [EBP; 50 mM piperazine-N,N'-bis (2-ethanesulfonic acid) (PIPES, pH 7.0), 50 mM KCl, 5 mM EGTA, 2 mM $MgCl_2$, 1 mM dithiothreitol (DTT), 20 uM cytochalasin B], pelleted, and resuspended in 100 to 200 ul of cold EBP containing the proteinase inhibitors phenylmethylsulfonyl fluoride (PMSF; 0.2 mM) and CLAP (containing chymostatin [20 ug/ml], leupeptin [5 ug/ml], antipain [20 ug/ml], and pepstatin A [5 ug/ml].) Cells were lysed by four cycles of freezing and thawing, and the lysates were subjected to centrifugation at 10,000 X g for 15 minutes. The supernatant cytoplasmic extract was either used immediately or stored at –80°C. The protein concentration was determined by Bradford assay.

***In vitro* Expression of PARP and Lamin A and Cleavage Assay**

Plasmid clones containing Lamin A and PARP under the control of the P_{T7} promoter were described previously. ^{35}S-labeled PARP and Lamin A were synthesized using the TNT T7 Quick system according to the manufacturer's instructions. The presence of Lamin A- or PARP-cleaving activity in cell extracts was determined by adding 2 ul of ^{35}S-labeled Lamin A or PARP from a 50 ul transcription/translation reaction mixture to 15 g of extract from either mock or infected cell extracts followed by a 90 minute incubation at 37°C. Proteins were resolved on SDS-10% polyacrylamide gels and radiolabeled proteins were visualized as previously described.

Preparation of Infected Cell Extracts and Caspase 3 Assay

Cells grown in 60 mm dishes were mock infected with wt RPV or RPVΔSPI-1 (A549 cells), wt CPV or CPVΔcrmA (LLC-PK1 cells) at an MOI of 10. Virus was adsorbed for two hours at 37°C, medium was added, and the infection was allowed to proceed for 14 hours at 37°C. Cells were harvested by scraping into the medium and were pelleted for five minutes at 200 X g. Cells were washed once in PBS, pelleted, then resuspended in 100 ul of Caspase Extract Buffer [10 mM HEPES pH 7.5, 2 mM EDTA, 0.1% CHAPS, 1 mM DTT]. Cells were subjected to four cycles of freezing and thawing, followed by centrifugation at 10,000 X g for 15 minutes. Supernatant cytoplasmic extract was used immediately or stored at –80°C. Protein concentration was determined by Bradford assay. 2.5 ug of cell extract was brought to 50 ul with Caspase Extract Buffer in a well of a 96 well microplate. Reactions were started by adding 150 ul of

Caspase Extract Buffer containing 0.1 mM of the fluorogenic Caspase 3 substrate Ac-DEVD-AMC (Calbiochem, La Jolla, CA, diluted 1:1000 from a 10 mM stock prepared in DMSO). Substrate cleavage indicative of Caspase 3-like activity was followed by fluorometry, with an excitation wavelength of 360 nm and an emission wavelength of 465 nm using a Tecan Microplate Reader (Tecan, Durham, NC.).

CHAPTER 3
ANALYSIS OF SPI-1 SERPIN ACTIVITY *IN VITRO*

Introduction. Serpins function as proteinase inhibitors by forming stable 1:1 complexes with their target proteinases. The reactive site loop, or RSL, is an essential component of each inhibitory serpin This stretch of approximately 20 amino acids forms a distorted alpha helix that projects from the surface of the protein and interacts directly with the target enzyme. The RSL closely mimics the substrate site for nucleophilic attack by the active site serine residue of the proteinase. The exact amino acid sequence of the RSL varies among serpins and dictates target enzyme specificity. In fact, mutation of a single amino acid within a serpin RSL is capable of changing the entire inhibitory profile of the serpin.

Proteinase specificity of SPI-1. Although SPI-1 shares homology to serpin superfamily members and is required for growth of RPV in A549 and PK15 cells, SPI-1 has never been demonstrated to act as a proteinase inhibitor either *in vitro* or *in vivo*. The amino acid sequence of the RPV SPI-1 RSL was compared to the analogous residues of cellular inhibitory and noninhibitory serpins as well as other poxvirus serpins (Fig. 7). SPI-1, like most inhibitory serpins, contains a threonine at the P14 position (residue 309), in contrast to the charged arginine

Figure 7. **Comparison of the SPI-1 reactive site loop (RSL) with inhibitory and non-inhibitory serpins.** A diagram of a typical serpin showing the location of the RSL is shown at the bottom of the figure. An alignment of amino acids comprising the reactive site loops of selected cellular or viral serpins is shown, along with the proteinase(s) targeted by each serpin. Sequences begin with the P14 residue of each serpin and terminate with the conserved PF residues at the end of the motif. P1 residues are shown in bold and underlined. Serpin PI-6 is known to have two P1 residues. The predicted P1 amino acid of SPI-1 is also indicated. Critical amino acid motif regions among serpins are boxed. Abbreviations: MYX, myxoma virus; ACT, antichymotrypsin; AT, antitrypsin; OVAL, ovalbumin; ANG, angiotensinogen; tPA, tissue plasminogen activator. Of the serpins shown, only OVAL and ANG are non-inhibitory serpins.

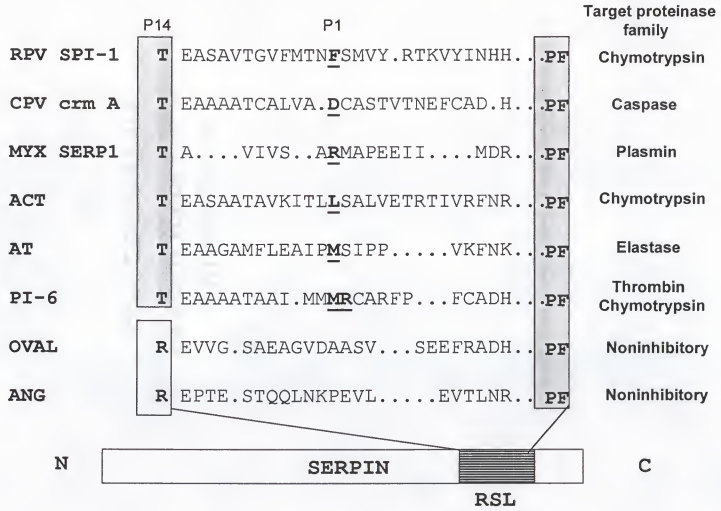
P14
P1
Target proteinase family
RPV SPI-1
T EASAVTGVFMTNFSMVY.RTKVYINHH..PF
Chymotrypsin
CPV crm A
T EAAAATCALVA.DCASTVTNEFCAD.H..PF
Caspase
MYX SERP1
T A....VIVS..ARMAPEEII....MDR..PF
Plasmin
ACT
T EASAATAVKITLLSALVETRTIVRFNR..PF
Chymotrypsin
AT
T EAAGAMFLEAIPMSIPP.....VKFNK..PF
Elastase
PI-6
T EAAAATAAI.MMMRCARFP...FCADH..PF
Thrombin
Chymotrypsin
OVAL
R EVVG.SAEAGVDAASV...SEEFRADH..PF
Noninhibitory
ANG
R EPTE.STQQLNKPEVL.....EVTLNR..PF
Noninhibitory
N
SERPIN
C
RSL

residue present at the P14 position in the noninhibitory serpins ovalbumin and angiotensinogen, which is proposed to prevent RSL strand insertion due to steric hindrance. In addition, the remaining amino acids comprising the serpin proximal hinge (P13-P10) of SPI-1 are all small and uncharged as is seen in other inhibitory serpins. The presence of these uncharged amino acids at the hinge region of SPI-1 suggests that reactive site loop insertion into the serpin backbone could occur following association with its target proteinase, allowing the formation of a stable inhibitory complex. Based on alignment with other serpins, the predicted P1 residue of SPI-1 is the phenylalanine located at position 322. Based on this prediction, SPI-1 may be active against members of the chymotrypsin family of proteinases which share a preference for cleavage after aromatic amino acid residues.

As an initial screen for potential target proteinases of SPI-1, an assay was developed (Fig. 8), designed to exploit the ability of serpins to form SDS-stable complexes with proteinases which they inhibit (211). ^{35}S-labeled SPI-1 prepared in an *in vitro* coupled transcription-translation system (TNT; Promega) was assayed for the ability to form complexes with a panel of proteinases from the chymotrypsin family including chymotrypsin (Fig. 9A), mast cell chymase (Fig. 9B), and cathepsin G (Fig. 9C). ^{35}S-labeled SPI-1 incubated alone is visible as a band of approximately 45 kDa following SDS-PAGE (solid arrow, Fig. 9, lanes 1). Some degree of SPI-1 cleavage was seen in the presence of 6 nM and 20 nM chymotrypsin (Fig. 9A, lanes 3-4), resulting in the formation of an approximately 40 kDa species (dashed arrow) which migrated slightly faster than intact SPI-1 when analyzed on an SDS-10% polyacrylamide gel. Incubation of SPI-1 in the presence of 60 nM or greater of chymotrypsin resulted further cleavage of

Figure 8. ***In vitro* SDS-PAGE bandshift assay for analyzing serpin activity.** The principle behind the SDS-PAGE bandshift assay is depicted kinetically (A) and schematically (B). A) The branched pathway representing the reaction mechanism of serpins is shown. E, proteinase; S_a, active, intact form of the serpin; E'S, the non-covalent Michealis complex; E-S_a, the acyl-enzyme intermediate prior to proteinase translocation; E-S*, the kinetically trapped covalent acyl-enzyme inhibitory complex; S_i, the inactive, cleaved form of the serpin. B) Unreacted ^{35}S-labeled serpin migrates to a certain position following SDS-PAGE (lane 1). During incubation with a non-target proteinase, the ^{35}S-labeled serpin is cleaved within the RSL producing a form of the serpin, S_i ,which migrates slightly faster on an SDS-10% polyacrylamide gel than the unreacted form (lane 2). When reacted with its target proteinase, an inhibitory complex (E-S*) forms between the ^{35}S-labeled serpin and the enzyme which is detected as a slower-migrating radiolabeled species (lane 3). The cleaved S_i form of the serpin is a product of this pathway as well (lane 3).

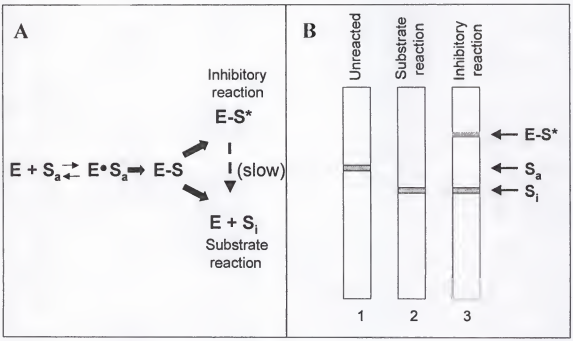
A
Inhibitory reaction
E-S*
E + S_a ⇄ E•S_a ➡ E-S
(slow)
E + S_i
Substrate reaction
B
Unreacted
Substrate reaction
Inhibitory reaction
E-S*
S_a
S_i
1
2
3

the 40 kDa species to smaller degradation products (Fig. 9A, lanes 5-9). Similarly, ^{35}S-labeled SPI-1 incubated in the presence of mast cell chymase was cleaved to produce a form of SPI-1 which migrated slightly faster than intact SPI-1 on an SDS-10% polyacrylamide gel (Fig. 9B). The 40 kDa SPI-1 cleavage product was first detected in the presence of 2 nM mast cell chymase (Fig. 9B, lane 2) and was seen in the presence of increasing enzyme concentrations from 2 nM to 6 μM (Fig. 9B, lanes 2-9). At higher concentrations of chymase, further degradation of the 40 kDa SPI-1 species occurred (Fig. 9B, lanes 6-9). When reacted with cathepsin G in concentrations ranging from 60 nM to 6 μM, SPI-1 cleavage to produce the 40 kDa SPI-1 species was seen (Fig. 9C, lanes 5-9). Once again, in the presence of large amounts of proteinase, the initial 40 kDa SPI-1 species was further degraded to smaller molecular weight products (Fig. 9C, lanes 6-9). In addition, reaction of SPI-1 with cathepsin G resulted in the formation of two novel high molecular weight bands (Fig. 9C, lanes 5-8). The sizes of the high molecular weight species (65 kDa and 70 kDa) are consistent with the expected size of SDS-stable complexes between SPI-1 (~45 kDa) and cathepsin G (~25 kDa). Both novel high molecular weight bands were present at approximately equal intensity in the presence of 60 and 200 nM cathepsin G (lanes 5 and 6). The amount of the 65 kDa form increased greatly at 600 nM and 2 uM cathepsin G, while that of the 70 kDa form decreased (lanes 7 and 8). These results suggest that an initial 70 kDa complex is formed between SPI-1 and cathepsin G which then decays to form the 65 kDa species. This decay is probably the result of enzymatic degradation of the 70 kDa complex to the smaller form by excess unreacted cathepsin G. A similar observation has been reported for interactions between the inhibitory serpin α_1-antichymotrypsin and cathepsin G (201)

Figure 9. **SDS-PAGE analysis of SPI-1 activity.** ^{35}S-labeled SPI-1 prepared in an *in vitro* coupled transcription/translation system was incubated with three-fold increasing concentrations of A) human pancreas chymotrypsin, B) recombinant mast cell chymase or C) human neutrophil cathepsin G (lanes 1, no enzyme; lanes 2, 2 nM enzyme; lanes 3, 6 nM enzyme; lanes 4, 20 nM enzyme; lanes 5, 60 nM enzyme; lanes 6, 200 nM enzyme; lanes 7, 600 nM enzyme; lanes 8, 2 μM enzyme; lanes 9, 6 μM enzyme). Reaction mixtures were incubated at 37°C for 90 minutes. Radiolabeled proteins were visualized following SDS-PAGE and autoradiography. The intact form of SPI-1 (solid arrow) as well as SPI-1 cleaved at or near the RSL (dashed arrow) is shown. High molecular weight protein bands representing complex formation between SPI-1 and cathepsin G are indicated by brackets.

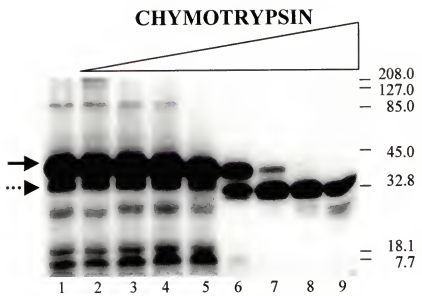
CHYMOTRYPSIN
208.0
127.0
85.0
45.0
32.8
18.1
7.7
1 2 3 4 5 6 7 8 9

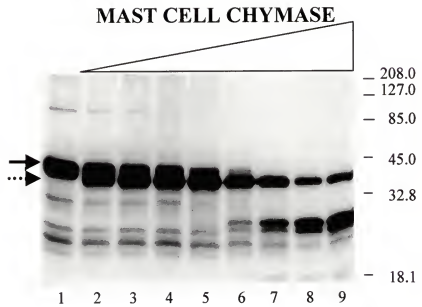
MAST CELL CHYMASE
208.0
127.0
85.0
45.0
32.8
18.1
1 2 3 4 5 6 7 8 9

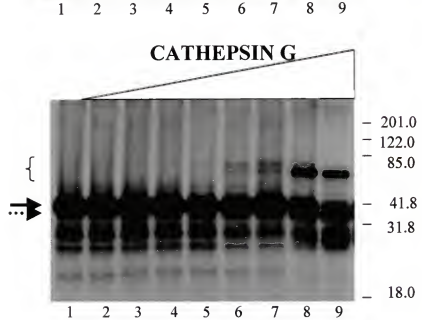
CATHEPSIN G
201.0
122.0
85.0
41.8
31.8
18.0
1 2 3 4 5 6 7 8 9

or chymotrypsin (234). In each of these studies, it was determined that to obtain a stable irreversible complex between the serpin and cathepsin G or chymotrypsin, a high molecular weight intermediate form of the complex must be cleaved by free enzyme to produce a final lower molecular weight product. Thus, SPI-1 produced *in vitro* is an efficient substrate for the chymotrypsin family members chymotrypsin and mast cell chymase. In addition, ^{35}S-labeled SPI-1 incubated with cathepsin D, thrombin, and elastase was cleaved to produces similar 40 kDa product, but no SDS-stable complexes were formed (data not shown). However, SPI-1 is able to form SDS-stable, high molecular weight complexes with cathepsin G.

Proteinase interaction occurs at SPI-1 RSL. Incubation of SPI-1 with all of the enzymes tested resulted in the formation of a 40 kDa cleavage product (Fig. 9, dashed arrow). A 40 kDa cleavage product is consistent with the expected size of SPI-1 cleaved within the RSL followed by the release of an ~ 4 kDa product representing the carboxy-terminus of the protein. To test this hypothesis, ^{35}S-labeled SPI-1 protein containing a decahistidine tag at the amino-terminus (His-tagged SPI-1) was generated using the TNT system. The protein was incubated alone or with the proteinases cathepsin G or chymotrypsin (Fig. 10) for 15 minutes to allow enzymatic cleavage to occur. His-tagged protein products were then purified using a His-Bind resin column and were analyzed following SDS-PAGE and autoradiography. Intact his-tagged SPI-1 protein migrated as a ~ 49 kDa band on an SDS-10% polyacrylamide gel (solid arrow, Fig. 10, lane 1). A high molecular weight band representing the complex between His-tagged SPI-1 and cathepsin G was seen (Fig. 10, lane 2, brackets).

Figure 10. **SPI-1 is cleaved at or near the RSL by the proteinases chymotrypsin and cathepsin G.** ^{35}S-labeled His-tagged SPI-1 prepared in the TNT system was incubated with buffer alone (lane 1) or with 200 nM cathepsin G (lane 2) or 200 nM chymotrypsin (lane 3) for 15 minutes at 37°C. His-tagged products were purified by binding to His-Bind resin and purified products were detected following SDS-PAGE and autoradiography. The intact form of His-tagged SPI-1 is shown by a solid arrow, while the form of His-tagged SPI-1 cleaved at or near the RSL is indicated by a dashed arrow. High molecular weight complexes between His-tagged SPI-1 and cathepsin G are shown (brackets).

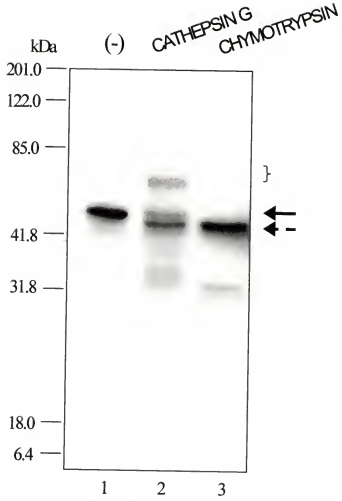
kDa
(-)
CATHEPSIN G
CHYMOTRYPSIN
201.0
122.0
85.0
41.8
31.8
18.0
6.4
}
1
2
3

Following incubation with cathepsin G (lane 2) or chymotrypsin (lane 3), a His-tagged product of approximately 45 kDa was visible (dashed arrow). The finding that the 45 kDa cleavage products retained their amino-terminal decahistidine tags and were visible following purification over the nickel column is consistent with the proposed model of proteolytic cleavage occurring at the carboxy-termini within the SPI-1 RSL.

α_1-antichymotrypsin inhibits SPI-1 complex formation with cathepsin G. The inhibitory mechanism of serpin action relies on nucleophilic attack on the serpin P1-P1' scissile bond within the RSL by the catalytic serine of the target proteinase. To prove that complex formation between cathepsin G and SPI-1 is dependent on the presence of the cathepsin G active site, ^{35}S labeled SPI-1 was incubated with cathepsin G in the presence of the serpin α_1-antichymotrypsin, a competing natural inhibitor of cathepsin G (Fig. 11). Radiolabeled SPI-1 prepared in the TNT system was incubated alone (Fig. 11, lane 1) or with cathepsin G (200 nM) under conditions demonstrated to yield complex formation as shown in Fig. 9C. The reactions were performed in the absence (Fig. 11, lane 2) or presence (lanes 3 to 9) of increasing amounts of α_1-antichymotrypsin. The formation of complexes between cathepsin G and SPI-1 was again reflected by the presence of 65kDa and 70 kDa protein bands following separation of the reactants by SDS-PAGE (lanes 2 to 4). Radiolabeled complex formation was inhibited in the presence of 200 nM α_1-antichymotrypsin (lane 5) as expected, consistent with the ability of α_1-antichymotrypsin to compete with SPI-1 for complex formation with cathepsin G at a 1:1 molar ratio of the proteinase to α_1-antichymotrypsin. SPI-1 did not form a complex with cathepsin G when incubated under conditions where the concentration of α_1-antichymotrypsin was in excess of the target proteinase (600 nM

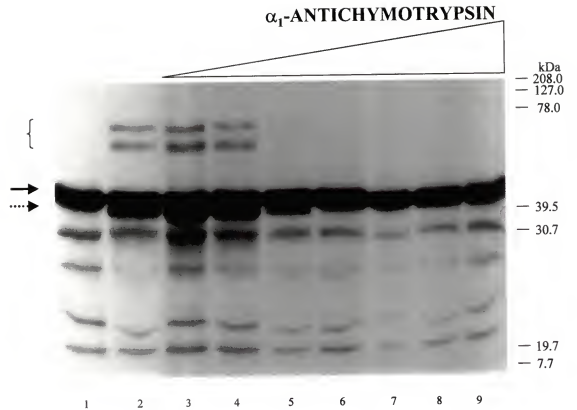

Figure 11. **Reaction of SPI-1 with cathepsin G in the presence of the competing serpin α_1-antichymotrypsin.** ^{35}S-labeled SPI-1 prepared in the TNT system was incubated with buffer alone (lane 1) or with 200 nM cathepsin G in the absence (lane 2) or presence of three-fold increasing concentrations of α_1-antichymotrypsin ranging from 20 nM (lane 3) to 20 μM (lane 9). Reactions were performed at 37°C for 90 minutes. Proteins were resolved on SDS-10% polyacrylamide gels, and radiolabeled proteins were visualized by autoradiography. Uncleaved SPI-1 is visible as a ~45 kDa band in lane 1 (solid arrow). SPI-1 cleaved within the RSL appears as a ~40 kDa band (dashed arrow), while higher molecular weight bands representing SDS-stable complexes with cathepsin G (brackets) are present in lanes 2 to 4.

[lane 6] to 200 μM [lane 9] of α_1-antichymotrypsin). These results indicate that SPI-1 and α_1-antichymotrypsin compete for the same active site serine residue of cathepsin G and that active cathepsin G is required for complex formation with the virus protein, consistent with the proposed model of SPI-1 inhibitory serpin function.

Stability of the SPI-1:cathepsin G complex. Inhibitory complexes between serpins and their target proteinases are stable for hours to even days before hydrolyzing (211). An experiment was performed to determine whether the complex formed between SPI-1 and cathepsin G is stable, as would be expected following reaction of an inhibitory serpin with its target proteinase (Fig. 12). ^{35}S-labeled SPI-1 expressed in the TNT system (Fig. 12, lane 1) was incubated with 200 nM cathepsin G for 60 minutes at 37°C to allow complex formation. A sample was removed after the one hour preincubation period to ensure that complex formation had occurred (lane 2). Then, a ten-fold molar excess of α_1-antichymotrypsin (2μM) was added to the reaction mixture to inactivate any remaining cathepsin G and prevent further reaction of cathepsin G with SPI-1. The reaction mixture was further incubated for up to 24 hours at 37°C, and samples were removed for analysis at 1, 2, 3, 4, 5, 6, 7, 8, 9, and 24 hours after the addition of α_1-antichymotrypsin and subjected to SDS-PAGE (Fig. 12, lanes 3 to 12). Complex formation had occurred following the initial preincubation of SPI-1 and cathepsin G (lane 2). The complex remained visible throughout the experiment, decreasing in intensity by 24 hours after the addition of α_1-antichymotrypsin. High molecular weight bands representing complexes between SPI-1 and cathepsin G in lanes 3 to 12 were measured with a PhosphorImager. PhosphorImager measurements from three separate experiments were averaged and expressed graphically as log units

Figure 12. **Stability of the SPI-1-cathepsin G complex.** ^{35}S-labeled SPI-1 prepared in the TNT system (lane 1) was preincubated in the presence of 200 nM cathepsin G for 60 minutes at 37°C (P.I., lane 2) to allow complex formation. Following the one hour incubation, α_1-antichymotrypsin was added in excess to a final concentration of 2 uM to quench any unreacted cathepsin G and the reaction was further incubated for another 24 hours at 37°C. Samples were removed at 1 (lane 3), 2 (lane 4), 3 (lane 5), 4 (lane 6), 5 (lane 7), 6 (lane 8), 7 (lane 9), 8 (lane 10), 9 (lane 11), and 24 (lane 12) hours after the addition of α_1-antichymotrypsin, and the proteins were resolved on an SDS-10% polyacrylamide gel. Radiolabeled proteins were visualized by autoradiography. High molecular weight bands representing the complex between SPI-1 and cathepsin G are indicated by brackets. After exposure to film, the counts in the high molecular weight bands representing the complex between SPI-1 and cathepsin G in lanes 3 to 12 of the gel were measured with a PhosphorImager. PhosphorImager measurements from three separate experiments were averaged and expressed graphically in log units versus time (inset).

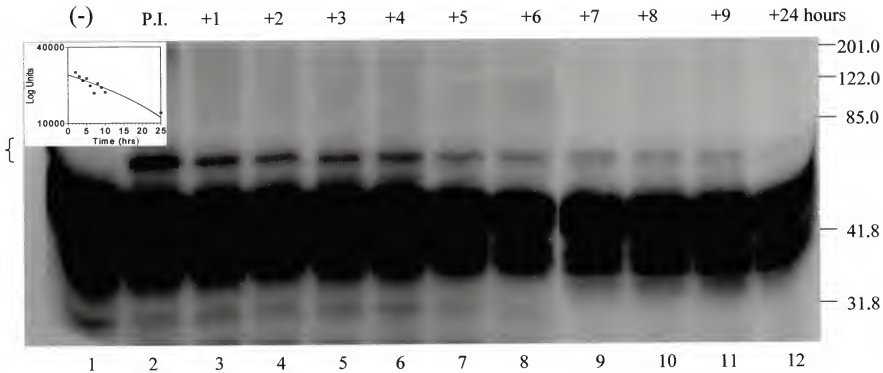
(-)
P.I.
+1
+2
+3
+4
+5
+6
+7
+8
+9
+24 hours
40000
10000
Log Units
0 5 10 15 20 25
Time (hrs)
201.0
122.0
85.0
41.8
31.8
1 2 3 4 5 6 7 8 9 10 11 12

versus time (Fig. 12, inset). Based on the graph, the half-life of the complex between SPI-1 and cathepsin G was estimated to be 22.5 hours. The relatively long half-life of complexes formed between SPI-1 and cathepsin G is consistent with a model whereby SPI-1 functions as an inhibitory serpin active against cathepsin G.

Effects of RSL mutations on SPI-1 activity *in vitro*. The mechanism of serpin action relies heavily on the identity of amino acids within the serpin reactive site loop, with proteinase specificity being highly dependent on the P1 residue. To determine whether the predicted SPI-1 reactive site loop region is required for complex formation with cathepsin G, site-directed mutagenesis of the SPI-1 RSL was performed (Fig. 13). The first mutant, N321A/F322A/S323A, was designed to alter not only the predicted P1 residue of the RSL but the adjacent P2 and P1' residues as well (Fig. 13A). ^{35}S-labeled wild type and mutant SPI-1 proteins were prepared in the TNT system and added to cathepsin G (Fig. 14A and B). Mutant SPI-1 protein was cleaved within or near the RSL, as indicated by the presence of a ~ 40 kDa band that migrated slightly faster than the uncleaved protein following SDS-PAGE (Fig. 14B). However, no SDS-stable complex was visible between the mutant SPI-1 protein and cathepsin G. Thus, it appears that the putative P1 residue of SPI-1 resides within the three mutated amino acid residues, most likely at position 322.

To test this prediction, a second mutant, F322A, was made, with only the phenylalanine at the predicted P1 position (amino acid 322) changed to alanine. ^{35}S-labeled F322A synthesized in the TNT system was incubated with increasing concentrations of cathepsin G (Fig. 14C). Cleavage within the RSL was seen when the

Figure 13. **Diagram of SPI-1 site-directed mutants**. Amino acids comprising the reactive site loop of A) wt SPI-1, B) N321A/F322A/S323A, C) F322A and D)T309R are shown. The location of the P14, P2, P1 and P1' residues are shown at the top of the figure. Within each amino acid sequence, mutated residues are designated by bold type

		P14	P2P1P1'
A	WT SPI-1	...EEYTEASAVTGVFMTNFSMVYRTKVYI...	
B	N321A/F322A/S323A	...EEYTEASAVTGVGMTAAAMVYRTKVYI...	
C	F322A	...EEYTEASAVTGVGMTNASMVYRTKVYI...	
D	T309R	...EEYREASAVTGVGMTNFSMVYRTKVYI...	

Figure 14. **Effects of RSL mutations on the ability of SPI-1 to form a complex with cathepsin G.** ^{35}S-labeled A) wild type SPI-1, B) N321A/F322A/S323A, C) F322A and D) T309R were prepared in the TNT system and assayed alone (lanes 1) or with three-fold increasing concentrations of cathepsin G ranging from 2 nM (lanes 2) to 6 μM (lanes 9). Reaction mixtures were incubated at 37°C for 90 minutes and radiolabeled proteins were visualized following SDS-PAGE and autoradiography. High molecular weight complexes between SPI-1 and cathepsin G are indicated by brackets. The intact form of SPI-1 is shown with a solid arrow, while SPI-1 cleaved at or near the RSL is indicated by a dashed arrow.

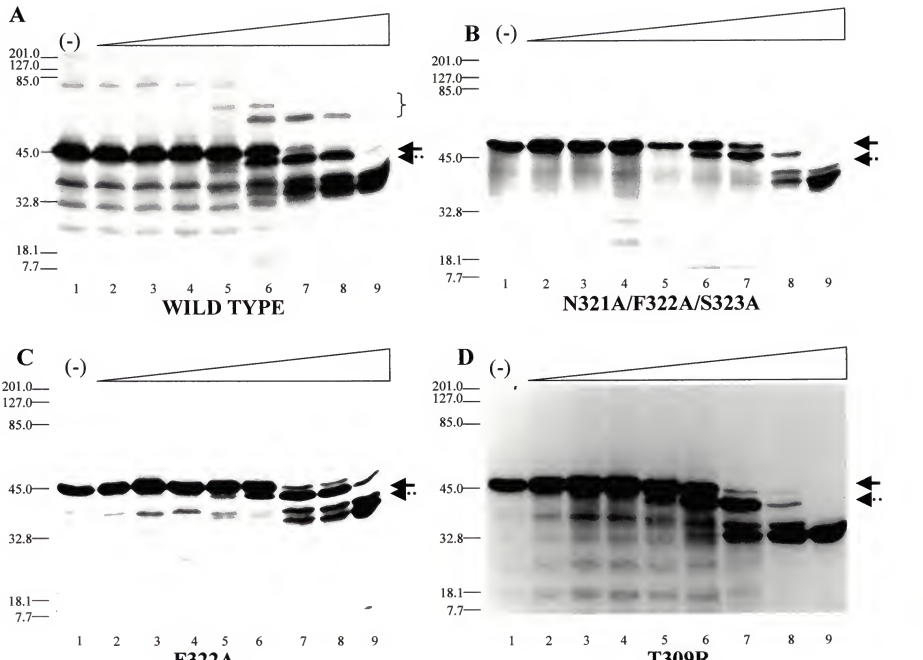
A
(-)
201.0
127.0
85.0
45.0
32.8
18.1
7.7
1 2 3 4 5 6 7 8 9
WILD TYPE
B
(-)
201.0
127.0
85.0
45.0
32.8
18.1
7.7
1 2 3 4 5 6 7 8 9
N321A/F322A/S323A
C
(-)
201.0
127.0
85.0
45.0
32.8
18.1
7.7
1 2 3 4 5 6 7 8 9
F322A
D
(-)
201.0
127.0
85.0
45.0
32.8
18.1
7.7
1 2 3 4 5 6 7 8 9
T309R

mutant protein was assayed with cathepsin G at concentrations of 60 nM or greater, but no SDS-stable complexes were formed. This strongly indicates that the P1 residue responsible for complex formation with cathepsin G is the phenylalanine at position 322. RSL cleavage of N321A/F322A/S323A and F322A in the absence of the proposed P1 phenylalanine at residue 322 likely occurs at the nearby phenylalanine, tryosine, or methionine residues in the exposed RSL at amino acid residues 318, 319, 324, and 326 (Fig. 13).

A third mutant, T309R, was constructed to contain an arginine in place of threonine at the critical predicted P14 hinge region of SPI-1 (Fig. 13D). It has been proposed that the presence of an arginine residue such as is seen in the hinge region of the noninhibitory serpins ovalbumin and angiotensinogen prevents RSL insertion into the serpin backbone, a step important for complex formation and the inhibitory activity of serpins (84,135). ^{35}S-labeled T309R synthesized in the TNT system was assayed for complex formation with cathepsin G (Fig. 14D). As with the other mutant proteins, complex formation with cathepsin G did not occur. The inability of the T309R mutant containing an arginine at the P14 site to form a complex with cathepsin G suggests that strand insertion is necessary for complex formation to occur, consistent with the model of SPI-1 inhibitory serpin activity.

CHAPTER 4
DISCUSSION OF SPI-1 SERPIN ACTIVITY *IN VITRO*

Poxvirus serpins. While members of the serpin superfamily of serine proteinase inhibitors are found throughout nature, the large DNA poxviruses are the only virus family known to encode functional serpins. A gene with homology to the serpin superfamily has been discovered in gammaherpesvirus 68 by routine sequencing (300). However, the predicted protein sequence of the gene indicates that key serpin motifs including the reactive site loop are missing from the open reading frame, suggesting that the herpesvirus gene product is not a functional serpin. Members of four different poxvirus genera, including the orthopoxviruses, leporipoxviruses, avipoxviruses and suipoxviruses, have been demonstrated to contain genes with homology to the serpin family.

Each of the poxvirus serpins can be roughly grouped by target proteinase specificity based on sequence similarity and proposed function. Excluding the newly discovered myxoma Serp3 and the fowlpox serpins which have yet to be characterized, three major poxvirus serpin groups are proposed (Table 3). The orthopoxvirus serpin SPI-2/crmA, the leporipoxvirus serpin Serp2, and the suipoxvirus serpin SPI-7 each contain aspartic acid PI residues. In the case of SPI-2/crmA and Serp2, the aspartic acid P1 residues are associated with inhibition of one or more members of the caspase family

Table 3.
Proposed Poxvirus Serpin Groups Based on RSL P1 Identities

Group	Genus	Serpin	Amino acid sequence of RSL
I.	Orthopoxvirus	CPVcrma	…yidvn eey*teaaaat calvad**cast vtn.efcadh pfiyvirhv…
	Orthopoxvirus	RPVspi2	…yidvn eeyteaaaat svlvadcast vtn.efcadh pfiyvirhv…
	Leporipoxvirus	MYXserp2	…yievt efgttaasct ygcvtdfggt mdpvvlkvnk pfifiikhd…
	Suipoxvirus	SPVspi7	…vievn edgttasast cccvad...s vsnkefyays pfifyikdn…
	Avipoxvirus	FPV010	…vikvd eygteaasvt escttd..gi kkipivkanv pfmflvadv…
		FPV251	…vikvd eygteaasvt escttd..gi kkipivkanv pfmflvadv…
II.	Leporipoxvirus	MYXserp1	…kiead ergttassdt aitliprnal ...taivank pfmfliyhk…
	Orthopoxvirus	VVspi3	…kidvd eggtvaeast imvatarssp ...eklefnt pfvfiirhd…
III.	Orthopoxvirus	RPVspi1	…fidvn eeyteasavt gvfmtnfsmv yrt.kvyinh pfmymikdn…
Unclassified	Avipoxvirus	Fpv204	…iiev. qy..dkvktt kplnv..... .rcssfyvnk pfifivtdv…
	Avipoxvirus	Fpv044	…qvdfi nnkivlgdq. .....kkwek isnnnyhinr pfifvikyn…
	Leporipoxvirus	MYXserp3	…dgdtc tehdttastc tiiikttgld flfmgkl…
	Avipoxvirus	Fpv040	…eleft nneypkinc. sscset... vvgk pfifilq…

* RSL P14 amino acid residue is underlined.
** When known, the RSL P1 residue is highlighted.

of cysteine proteinases (207,217,265,274,288,324) as well as inhibition of apoptosis (34,63,78,146,147,167,218,278,279,306). While SPI-7 shares a P1 aspartic acid residue, it has never been shown to have activity against caspase family members. However, the studies of SPI-7 activity were performed with human caspase enzymes and therefore lack of inhibition by SPI-7 may be due to differences in species specificity of the enzyme. The conservation of SPI-7 among laboratory and field isolates of swinepox virus, the attenuation of swinepox virus SPI-7 deletion mutants in animals, and the ability of SPI-7 to be cleaved within the RSL by caspase 1 (185) suggests that the swinepox virus serpin may function in a manner analogous to SPI-2/crmA and Serp1 within the context of a natural infection. The protein products of the recently discovered FPV010 and FPV251 genes are also tentatively included in this group (3). Based on amino acid alignment of the FPV ORFs with other known poxvirus inhibitory serpins, conservation of important serpin structural motifs is seen. Both FPV010 and FPV251 appear to possess small, uncharged threonine residues at the P14 hinge position in addition to aspartic acid at the putative P1 residue suggesting that the proteins may function to inhibit a similar class of proteinases as other poxvirus serpins in the group. However, while the FPV010 gene is predicted to encode a full-length 38 kDa protein, the product of FPV251 is predicted to be a truncated 17 kDa protein that shares 90% amino acid identity with FPV010. FPV251 likely arose following duplication of the FPV010 gene during replication and is not expected to be a functional serpin.

Members of the second group of poxvirus serpins include the orthopoxvirus SPI-3 and leporipoxvirus Serp1 and contain arginine at the P1 position. Members of this group of poxvirus serpins have been demonstrated to inhibit members of the trypsin family of

serine proteinases, including plasmin, urokinase, and tissue plasminogen activator (tPA) (143,187,285), suggesting that these two serpins may play a similar role during infection of their natural hosts. However, while Serp1 is the only example of a secreted poxvirus serpin (149), SPI-3 is proposed to remain cell-associated during orthopoxvirus infections (307). While Serp1 was unable to prevent cell fusion when expressed from the SPI-3 locus in CPV, SPI-3 was likewise unable to functionally replace Serp1 during myxoma virus infection of rabbits (307). Still, given the fact that the two serpins have nearly identical proteinase inhibitory profiles *in vitro*, it remains possible that SPI-3 and Serp1 play similar roles in the context of a natural infection and that it is differences in the timing of expression and localization of the serpins that prevents them for substituting for one another during infection of the recombinant myxoma and cowpox viruses.

SPI-1. While SPI-1 is found in members of the orthopoxvirus genus, including cowpox, vaccinia, variola and rabbitpox virus, a corresponding serpin is absent from all other poxvirus genera making SPI-1 the only member of this third poxvirus serpin group. Of all of the poxvirus serpins, SPI-1 is most closely related to SPI-2/crmA, sharing 47% amino acid identity to the protein. However, amino acid comparison of SPI-1 and SPI-2/crmA reveals that the two serpins differ at the crucial RSL, making it unlikely that the two proteins inhibit the same family of proteinases. When the amino acid sequence of the SPI-1 RSL was compared with similar residues from other viral and cellular inhibitory serpins, SPI-1 appeared to have all of the structural motifs necessary to function as an inhibitory serpin. However, the ability of SPI-1 to function as an inhibitory serpin had never been explored and was the subject of this study.

Based on spatial alignment of conserved serpin motifs, the amino acid at the P1 residue of SPI-1 was predicted to be the phenylalanine at position 322. Based on this assumption, SPI-1 was assayed for the ability to form SDS-stable complexes with members of the chymotrypsin family of serine proteinases which share a preference for cleavage following aromatic residues. While SPI-1 was cleaved within the RSL by the enzymes chymotrypsin and mast cell chymase, it formed an SDS-stable, high molecular weight complex with cathepsin G consistent in size with an inhibitory serpin complex (Fig. 9). The fact that complex formation was seen only with cathepsin G and not with other closely related members of the chymotrypsin family or with serine proteinases from other families indicates that the reaction between SPI-1 and cathepsin G is highly specific. Complex formation between SPI-1 and cathepsin G was prevented in the presence of α_1-antichymotrypsin, an inhibitory serpin active against chymotrypsin family members, indicating that active proteinase is necessary for complex formation to occur and that SPI-1 and α_1-antichymotrypsin compete for the same active site serine residue of cathepsin G (Fig. 11). Once formed, the complex between SPI-1 and cathepsin G was shown to be stable, with an estimated half-life of 22.5 hours at 37°C (Fig. 12). The ability to form a specific, long-lived, SDS-stable complex with cathepsin G is consistent with the ability of SPI-1 to inhibit enzyme activity.

Further evidence that complex formation with cathepsin G is dependent on the serpin activity of SPI-1 was achieved by performing site-directed mutagenesis on amino acids essential for serpin activity. Both N321A/F322A/S323A and F322A contain mutations at the predicted P1 residue (amino acid 322) and were unable to form a complex with cathepsin G (Fig. 14 B and C). Likewise, T309R, which contains a

charged arginine in place of threonine at the P14 position, was unable to complex with cathepsin G, suggesting that RSL insertion into the serpin backbone is necessary for complex formation to occur consistent with SPI-1 serpin activity (Fig. 14 D). These data strongly suggest that SPI-1 possesses the properties of a functional inhibitory serpin with a P1 residue of phenylalanine and is able to form a specific, long-lived, SDS-stable complex with cathepsin G.

These *in vitro* studies investigating the serpin activity of SPI-1 were performed using radiolabeled SPI-1 prepared in a coupled *in vitro* transcription/translation system. Using this system, evidence for proteinase inhibition is seen by the ability of the serpin to form an SDS-stable, high molecular weight complex with a suspected target proteinase. This same *in vitro* system has been used in our laboratory as well as by other researchers to demonstrate inhibitory serpin activity. In every instance, the ability of a given serpin to form an SDS-stable complex with a target proteinase *in vitro* is associated with the ability of the serpin to directly inhibit enzyme activity (143,187,285). Still, attempts have been made to purify SPI-1 protein in order to more fully prove direct inhibition of cathepsin G by SPI-1. Recombinant SPI-1 protein containing either an amino-terminal decahistidine or calmodulin binding peptide (CBP) affinity tag was expressed in bacteria and purified over the appropriate affinity resin. In both cases, the purified protein was smaller than the expected size, consistent with nonspecific proteolytic cleavage by bacterial proteases. Not surprisingly, the cleaved purified proteins were inactive in inhibition assays with cathepsin G. Furthermore, decahistidine or CBP-tagged SPI-1 prepared *in vitro* using the TNT system formed much weaker complexes with cathepsin G in SDS-PAGE assays than untagged SPI-1 (data not shown), suggesting that SPI-1

protein containing an N-terminal tag may be intrinsically less stable or less reactive than untagged protein. Utilization of carboxy-terminal tags for SPI-1 protein purification were avoided due to the fact that any steric hindrance induced by the tag may restrict the mobility of the carboxy-terminal portion of SPI-1 which is essential for serpin activity. In addition, several attempts were made to express untagged SPI-1 in infected cells using the vaccinia T7 overexpression system. However, the absence of a SPI-1 affinity tag required the use of whole cellular extracts in cathepsin G inhibition assays which often contained endogenous proteases that cleaved the cathepsin G chromagenic substrate used in the assays and made interpretation of the results difficult. Currently, other methods of purifying SPI-1 protein are being investigated.

Importance of Cathepsin G activity *in vivo.* Cathepsin G, neutrophil elastase, and proteinase 3 are the major proteolytic enzymes in the azurophil granules of polymorphonuclear leukocytes (neutrophils), mast cells, and monocytes and are involved in the degradation of foreign organisms and dead tissues within the phagolysosome during inflammatory reactions (14,18,309). Cathepsin G is a member of the chymotrypsin family of serine proteinases, and cleaves substrates at peptide bonds on the carboxy-terminal side of phenylalanine, methionine, and leucine residues (18). In mammals, cathepsin G is involved in regulating many processes such as vasodilation, degradation of the extracellular matrix, and platelet activation (18). Known cathepsin G substrates include laminin, type IV collagen, fibronectin, elastin, proteoglycans, and immunoglobulins G and M (15,18,115). Proteolytic processing of the complement components C3 and Factor V and clotting factors by cathepsin G has been demonstrated to lead to their activation *in vivo* (150). Cathepsin G has also been demonstrated to

cleave the pro-forms of several cytokines including interleukin-8 and interleukin-1β leading to their activation(196). In addition, cathepsin G released from neutrophils during the acute inflammatory response has been shown to be chemotactic for monocytes and likely plays a role in the transition of the constituents within an inflammatory exudate from neutrophil to mononuclear cells (48). Cathepsin G also has a role in enhancing the cytotoxicity of T cells and natural killer (NK) cells by binding to the cells activating them (319). While the enzymatic activity of cathepsin G is essential for each of the above activities, the bactericidal properties that are attributed to cathepsin G are not mediated by the catalytic domain (247,263).

Given the many biological processes in which the proteinase plays a role, stringent regulation of cathepsin G activity is essential. Increased levels of cathepsin G due to chronic inflammation or because of genetic or acquired deficiencies of its natural inhibitors can result in the uncontrolled digestion of most proteins of the extracellular matrix (141). Indeed, excess levels of cathepsin G have been demonstrated to play a role in the development of connective tissue diseases such as emphysema, rheumatoid arthritis and perionditis (100,103). In addition, uncontrolled release of cathepsin G from PMNs and degradation of structural and elements and humoral factors has been shown to be a major cause of multiple organ failure in septic shock (116).

Several mammalian serpins are capable of inhibiting cathepsin G activity. The serpin α_1-antichymotrypsin is synthesized and secreted mainly by hepatocytes, although it can also be produced by alveolar macrophages, cells of epithelial origin, and some tumor cells (50,227). α_1-antichymotrypsin is thought to be the major inhibitor of secreted cathepsin G in human plasma. In addition to its role in protecting host tissues from

proteolytic damage caused by cathepsin G, α_1-antichymotrypsin has recently been demonstrated to neutralize the chemotactic activity of cathepsin G, preventing the influx of monocytes to the site of inflammation (48). The importance of α_1-antichymotrypsin in regulating cathepsin G activity is emphasized by the fact that no homozygous deficient α_1-antichymotrypsin conditions have been reported and it is thought that such a phenotype would be incompatible with normal development (227).

Recently, a second major inhibitor of cathepsin G activity has been discovered. PI-6, also referred to as Cytoplasmic Antiproteinase (CAP) or Placental Thrombin Inhibitor (PTI), is a serpin which localizes exclusively to the cytoplasm. PI-6 is an unusual serpin, in that it is capable of inhibiting more than one class of serine proteinases using distinct amino acid residues. Inhibition of the trypsin-like proteinases thrombin and urokinase is achieved using the arginine at position 341 as the P1 residue, while inhibition of chymotrypsin family members occurs following interaction with the nearby methionine residue at position 340 (220). While PI-6 was first discovered as a major proteinase inhibitor in placental tissue, it has only recently been found to be present in monocytes, granulocytes and myelomonocytic cell lines (243). Within these cells, PI-6 is present in an SDS-stable inhibitory complex with cathepsin G (243). It has been proposed that PI-6 acts as a natural inhibitor of cathepsin G that leaks into the cytoplasm of monocytes or granulocytes during phagocytosis or during synthesis of the proteinase.

In addition to α_1-antichymotrypsin and PI-6, a third mammalian serpin has been demonstrated to inhibit cathepsin G activity. The squamous cell carcinoma antigen (SCCA) is normally expressed on the surface of some cells within the squamous epithelia of the skin and mucous membranes, but also serves as a marker for advanced tumors of

the cervix, lung and oropharnyx (235). Neutral and acidic forms of the antigen exist, termed SCCA1 and SCCA2, respectively, and both forms possess serpin activity. SCCA1 has been demonstrated to inhibit the papain-like cysteine proteinases cathepsins S, K and L in a manner analogous to serpin inhibition of serine proteinases (236,275). SCCA2 has been shown to inhibit the chymotrypsin family members mast cell chymase and cathepsin G (235). While studies of the inhibitory profiles of SCCA1 and SCCA2 were performed *in vitro* and little is known about the role of the serpins in proteinase inhibition *in vivo*, it has been proposed that SCCA2 may function to inhibit inflammation mediated by cathepsin G or related proteinases at the site of tumor growth.

Possible role of SPI-1 in inhibiting cathepsin G activity during poxvirus infection. Because the cell-mediated arm of the immune response is important in countering a poxvirus infection (38), it is interesting that members of the orthopoxvirus genus encode a gene product which is potentially capable of targeting and inhibiting cathepsin G as a possible means of preventing inflammation and lymphocyte activation. Because SPI-1 remains intracellular during infection (123), it is unlikely that the serpin functions to inhibit cathepsin G that has been exocytosed during an inflammatory response. Instead, SPI-1 may play a role in inhibiting intracellular cathepsin G. Little is known regarding the cell types which become infected by poxviruses *in vivo*, however several studies have demonstrated poxvirus infection of lymphocytic and mononuclear cells (30,69,77). SPI-1 may play a role analogous to PI-6 in inhibiting cathepsin G present in the cytoplasm of cells of the myelocytic lineage. This would allow inhibition of cathepsin G prior to its release from the azurophil granules, thus preventing inflammation to the site of infection and activation of lymphocytes and natural killer

cells. In addition, SPI-1 may act to inhibit cathepsin G released into the cytoplasm of infected cells by professional phagocytes in order to prevent intracellular damage and delay cell death until completion of the virus life cycle.

Conclusions. This study is the first to demonstrate that SPI-1 has the properties of an inhibitory serpin *in vitro*. Though SPI-1 was screened for inhibitory activity against a panel of serine proteinases of the chymotrypsin family, the serpin formed an SDS-stable inhibitory complex only with cathepsin G. However, it remains possible that cathepsin G is not the true target proteinase of SPI-1 *in vivo*. Given that the P1 residue of SPI-1 is the phenylalanine at position 322 and that no evidence of complex formation was seen when SPI-1 was assayed with cathepsin D, thrombin, or elastase, it is likely that the natural target of SPI-1 is a member of the chymotrypsin family of serine proteinases. Because like most poxvirus serpins, SPI-1 remains intracellular during infection, the target proteinase of SPI-1 likely resides within infected cells. The function of SPI-1 during infection of tissue culture cells and a discussion of potential target proteinases of SPI-1 within those cells follows in Chapters 5 and 6.

CHAPTER 5
ANALYSIS OF SPI-1 FUNCTION IN INFECTED TISSUE CULTURE CELLS

Introduction. Previous work has demonstrated that SPI-1 gene expression is necessary for RPV growth in certain nonpermissive cell lines and that infection of the restrictive cells with an RPV SPI-1 null mutant results in some of the features of apoptosis (10,36). After demonstrating that the SPI-1 protein has the potential to function as an inhibitory serpin *in vitro*, experiments were performed to determine if the serpin activity of SPI-1 was necessary for its role in mediating the host range of RPV.

Recombinant virus construction. To perform these studies, it was first necessary to construct an RPV mutant containing a complete deletion of the SPI-1 open reading frame. pKMSPI-1 was designed so that any gene cloned between the SPI-1 left and right flanking sequences within the vector could be introduced in place of the wild type SPI-1 gene in the virus genome by homologous recombination as depicted in Figure 15. To create the RPV SPI-1 deletion mutant, the *Escherichia coli* (*E.coli*) eco-gpt gene encoding the selectable marker guanine phosphoribosyl transferase under the control of the vaccinia $P_{7.5}$ early/late promoter was cloned between the SPI-1 left and right flanks of pKMSPI-1 to create pKMSPI-1-gpt. Wt RPV infection of CV-1 cells was followed by transfection with pKMSPI-1-gpt and selection of the RPV SPI-1 deletion mutant

Figure 15. **Scheme for creating RPV SPI-1 recombinants**. The plasmid pKMSPI-1 contains a multiple cloning site (MCS) between the left and right flanking sequences of SPI-1 (SPI-1_L and SPI-1_R, respectively). Following infection, transfection, and the appropriate selection, any gene cloned between the SPI-1 left and right flanking sequence within the plasmid will replace the wild type SPI-1 gene within the RPV genome.

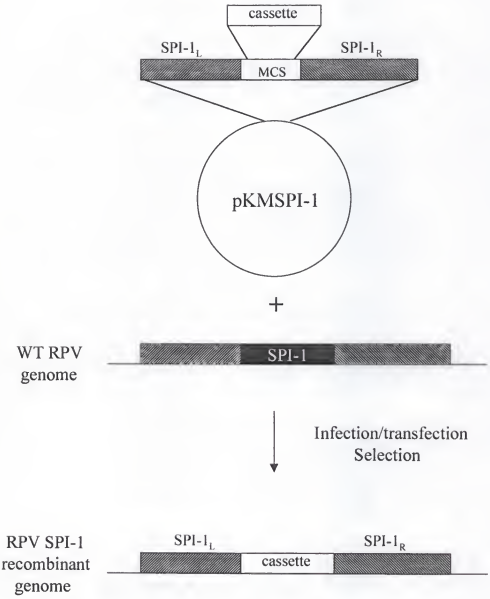
cassette
SPI-1L
SPI-1R
MCS
pKMSPI-1
+
WT RPV genome
SPI-1
Infection/transfection
Selection
RPV SPI-1 recombinant genome
SPI-1L
SPI-1R
cassette

(RPVΔSPI-1) was performed in the presence of mycophenolic acid. To confirm the absence of the SPI-1 gene in the recombinant virus, PCR was performed using primers specific for the SPI-1 gene on virus genomic DNA (Fig. 16A). In addition, immunoblot analysis was performed on extracts from cells infected with wt RPV or RPVΔSPI-1 using SPI-1-specific antisera to ensure that no SPI-1 protein was expressed from the RPV deletion mutant (Fig. 16B). To ensure that no unintended mutations had been introduced into the viral genome during the construction of RPVΔSPI-1, the wild type SPI-1 gene was re-inserted in place of eco-gpt at the SPI-1 locus in RPVΔSPI-1. Utilizing a similar strategy as was used in the construction of the RPV SPI-1 deletion mutant, cells were first infected with RPVΔSPI-1 and then transfected with the pKMSPI-1 shuttle vector containing the wild type SPI-1 gene between the SPI-1 flanking sequences (pKMSPI-1wt). The RPV SPI-1 reconstructed virus (RPVΔSPI-1 Rec.) was isolated following the appropriate selection, and the presence of the SPI-1 gene was confirmed by PCR and Western blot analysis (Fig. 16A and B, lanes 3). In addition, wt RPV, RPVΔSPI-1, and the RPV SPI-1 reconstructed virus were assayed for the ability to form plaques on RK-13, A549 and PK15 cell lines. Consistent with published results, wt RPV was able to plaque on each cell line tested, while the SPI-1 deletion mutant was able to plaque only on the permissive RK-13 cell line (10). The RPV SPI-1 reconstructed virus was indistinguishable from wt RPV and was able to plaque on permissive and nonpermissive cell lines, indicating that no unintended mutations affecting host range were introduced into the RPV genome during construction of the RPV SPI-1 deletion mutant virus (data not shown).

Figure 16. **PCR analysis of RPVΔSPI-1 DNA and immunoblot screening of infected cell extracts**. CV-1 cells were infected with wt RPV (lanes 1), RPVΔSPI-1 (lanes 2) and RPVΔSPI-1 Rec. (lanes 3). At 12 hours post infection, viral DNA was isolated from infected cell supernatants and assayed for the presence of the SPI-1 gene by PCR analysis using primers specific for SPI-1 (A). In addition, cytoplasmic cell extracts were made from the infected cells and were used to assay for SPI-1 protein expression by Western blot analysis using SPI-1 specific antisera (B). The location of SPI-1 DNA (A) and protein (B) are indicated by arrows.

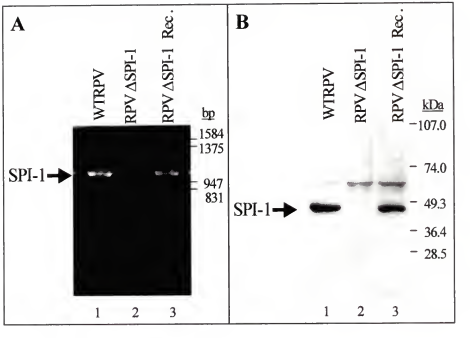
A
WTRPV
RPV ΔSPI-1
RPV ΔSPI-1 Rec.
bp
1584
1375
947
831
SPI-1
1
2
3
B
WTRPV
RPV ΔSPI-1
RPV ΔSPI-1 Rec.
kDa
107.0
74.0
49.3
36.4
28.5
SPI-1
1
2
3

RPVΔSPI-1 was then used to create recombinant viruses containing the SPI-1 RSL mutations that abolished the ability of SPI-1 to form inhibitory complexes with cathepsin G *in vitro* (Fig. 13). Each of the genes was cloned into pKMSPI-1 between the SPI-1 upstream and downstream flanking sequences, and the resulting vectors were used to replace the eco-gpt gene at the SPI-1 locus within the RPVΔSPI-1 genome. Because the SPI-1 site-directed mutant genes were introduced in place of the wild type SPI-1 gene, expression of the RSL mutants was under the control of the native SPI-1 gene promoter. The SPI-1 promoter was used to ensure that each of the mutant genes were expressed at the same time and at the same levels as the wild type SPI-1 gene during infection.

SPI-1 is modified *in vivo*. In the recombinant viruses, designated RPV SPI-1 N321A/F322A/S323A, RPV SPI-1 F322A, and RPV SPI-1 T309R, the presence of the mutant SPI-1 genes was confirmed by PCR analysis using primers specific for the SPI-1 gene and sequencing of viral DNA (data not shown). In addition, experiments were performed to confirm the expression of the mutant SPI-1 proteins during infection. Extracts prepared from CV-1 cells infected with wt RPV or each of the RPV SPI-1 RSL mutants were assayed for SPI-1 expression by Western blot analysis using antisera directed against the SPI-1 protein (Fig. 17). Unlabeled SPI-1 protein expressed *in vitro* using the TNT system was used as a positive control for the assay. SPI-1 protein was detected following infection of CV-1 cells with each of the viruses tested. Surprisingly, SPI-1 protein expressed during infection of CV-1 cells with wt RPV (Fig. 17, lane 1)

Figure 17. **SPI-1 protein expression by wt RPV and RPV SPI-1 RSL mutant viruses.** Immunoblot analysis of extracts prepared from CV-1 cells infected with wt RPV (lane 1), RPV SPI-1 N321A/F322A/S323A (lane 2), RPV SPI-1 F322A (lane 3)or RPV SPI-1 T309R (lane 4)or from wt SPI-1 prepared in the TNT system (lane 5) using antisera specific for SPI-1. The unmodified form of SPI-1 is designated by a solid arrow while modified SPI-1 is indicated by a dashed arrow.

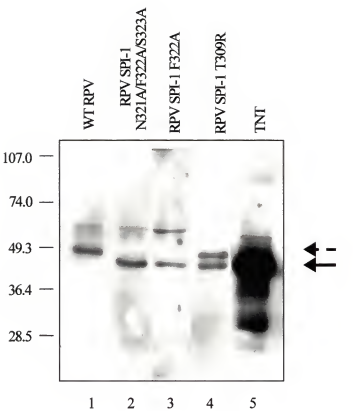
WT RPV
RPV SPI-1 N321A/F322A/S323A
RPV SPI-1 F322A
RPV SPI-1 T309R
TNT
107.0
74.0
49.3
36.4
28.5
1
2
3
4
5

appeared larger than SPI-1 protein made in the TNT system based on the relative mobility of the proteins during SDS-PAGE (Fig. 17, lane 5) (~ 49 kDa verses ~ 45 kDa, respectively). Furthermore, SPI-1 protein expressed from the RPV SPI-1 N321A/F322A/S323A (lane 2) and RPV SPI-1 F322A (lane 3) recombinant viruses migrated to the same position as wt SPI-1 prepared in the TNT system. Two immunopositive protein bands were seen in lysates from cells infected with RPV SPI-1 T309R (lane 4). The uppermost protein band appears to be the same size as SPI-1 protein expressed from wt RPV, while the lowermost protein species migrated to the same position as SPI-1 made in the TNT system. These results suggest that the SPI-1 protein is somehow modified during infection of CV-1 cells with wt RPV, but not with RPV SPI-1 N321A/F322A/S323A or RPV SPI-1 F322A. The presence of two SPI-1 protein species following infection of CV-1 cells with RPV SPI-1 T309R suggests that partial modification of the mutant protein may be taking place.

These results suggest that wt SPI-1 becomes modified during infection of the permissive CV-1 cell line, but that mutation of amino acids within the RSL either partially (P14) or completely (P1) inhibits the modification from occurring. To determine whether the modification is cell line-specific, wt RPV, RPV SPI-1 F322A, or RPV SPI-1 T309R were used to infect the permissive CV-1 and RK13 cell lines as well as the restrictive A549 and PK15 cell lines and immunoblot analysis using SPI-1-specific antisera was performed on infected cell extracts using wt SPI-1 prepared in the TNT system as a control for unmodified SPI-1 protein (Fig. 18). In addition, SPI-1 F322A and T309R RSL proteins were expressed *in vitro* using the TNT system and subjected to

Figure 18. **Cellular modification of SPI-1 protein is not cell line-specific.** Immunoblot analysis of SPI-1 expression in cytoplasmic extracts prepared from CV-1 (lanes 1-3), A549 (lanes 4-6), RK13 (lanes 7-9) or PK15 (lanes 10-12) cells infected with wt RPV, RPV SPI-1 F322A, or RPV SPI-1 T309R and comparison with wild type and RSL mutant forms of SPI-1 prepared *in vitro* using the TNT system and subjected to SDS-PAGE on the same gel. The unmodified form of SPI-1 is designated by a solid arrow while modified SPI-1 is indicated by a dashed arrow.

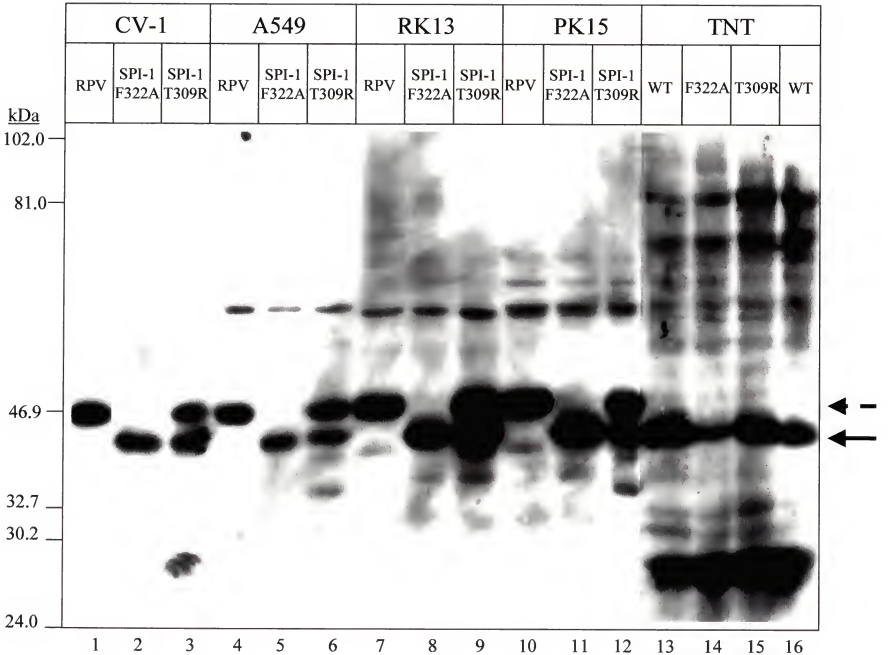
CV-1
A549
RK13
PK15
TNT
RPV
SPI-1 F322A
SPI-1 T309R
WT
F322A
T309R
kDa
102.0
81.0
46.9
32.7
30.2
24.0
1 2 3 4 5 6 7 8 9 10 11 12 13 14 15 16

SDS-PAGE and immunoblot analysis to determine the relative electrophoretic mobilities of the mutant proteins. Interestingly, both of the SPI-1 RSL mutant proteins expressed *in vitro* migrated to the same position as wild type protein prepared in the TNT system following electrophoresis through an SDS/10% polyacrylamide gel (Fig. 18, lanes 13-16). Wt SPI-1 prepared in all cell lines assayed migrated more slowly than SPI-1 protein expressed in the TNT system (Fig. 18, lanes 1, 4, 7, 10 and 13-16). In contrast, SPI-1 protein expressed following infection of both permissive and nonpermissive cells with RPV SPI-1 F322A migrated to the same position as the TNT SPI-1 protein following electrophoresis through an SDS/10% polyacrylamide gel (Fig. 18, lanes 2, 5, 8, 11 and 13-16). Following infection of all cell lines tested, SPI-1 protein expressed from RPV SPI-1 T309R was evident as two immunopositive species (Fig. 18, lanes 3, 6, 9, 12, and 13-16). The uppermost band of the doublet migrated to the same position as SPI-1 expressed during wt RPV infection while the lower protein band migrated to the same position as SPI-1 expressed *in vitro* using the TNT system following SDS-PAGE. These results indicate that the modification that takes place to SPI-1 protein following wt RPV infection is not cell line specific and occurs following infection of both permissive and nonpermissive cell lines. Furthermore, mutation of the SPI-1 P1 and P14 residues appears to adversely affect the ability of the serpin to become modified during infection of all cell lines tested, but the RSL mutations do not alter the electrophoretic mobility of SPI-1 protein expressed *in vitro*.

Host range of RPV SPI-1 recombinants. Because SPI-1 is necessary for mediating the complete viral host range of RPV and the protein has been shown to

Figure 19. **Host range of wild type RPV and RPV SPI-1 RSL mutants.** Plaque formation of wtRPV and RPV SPI-1 RSL mutants on RK13, A549 and PK15 cell lines is shown.

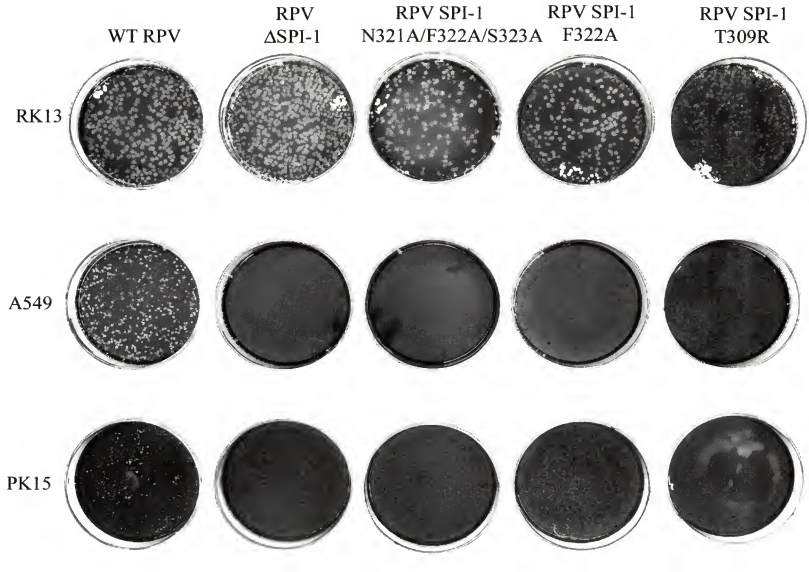
WT RPV
RPV ΔSPI-1
RPV SPI-1 N321A/F322A/S323A
RPV SPI-1 F322A
RPV SPI-1 T309R
RK13
A549
PK15

function as an inhibitory serpin *in vitro*, studies were performed to examine the effects of the SPI-1 RSL mutations which abolished the ability of SPI-1 to form complexes with cathepsin G *in vitro* on RPV host range. Permissive RK13 and nonpermissive A549 and PK15 cell monolayers were infected with approximately 100 pfu of wt RPV, RPVΔSPI-1, RPV SPI-1 N321A/F322A/S323A, RPV SPI-1 F322A and RPV SPI-1 T309R (Fig. 19). Consistent with published results, wt RPV was able to form plaques on all cell lines, while RPVΔSPI-1 was unable to form plaques on the two restrictive A549 and PK15 cell lines (10). The mutant viruses RPV SPI-1 N321A/F322A/S323A, RPV SPI-1 F322A, and RPV SPI-1 T309R were each able to form plaques on RK13 cells but were unable to do so on A549 or PK15 cells. The inability of the RPV SPI-1 RSL mutants to productively infect cell lines restrictive for SPI-1 null mutants strongly suggests that it is the ability of SPI-1 to function as an inhibitory serpin which is essential for its role in conferring viral host range.

Apoptotic features of A549 cells infected with RPV SPI-1 recombinants.

Previous work has demonstrated that the reduced host range of RPV SPI-1 null mutants is associated with the induction of the morphological features of apoptosis in infected nonpermissive cell lines (36). Since the RPV recombinants containing site-directed mutations within the SPI-1 RSL displayed the same reduced host range as the RPV SPI-1 deletion mutant, experiments were performed to determine if the host range restriction of these recombinant viruses correlated with the apoptotic-like morphology observed in restrictive cell lines infected with SPI-1 null mutants. A549 cells were mock infected or infected with wt RPV, RPVΔSPI-1, RPV SPI-1 N321A/F322A/S323A, RPV SPI-1

Figure 20. **DAPI staining of A549 cells infected with wtRPV and RPV SPI-1 RSL mutants.** A549 cells were mock infected with medium alone or infected with wtRPV, RPVΔSPI-1, RPV SPI-1 N321A/F322A/S323A, RPV SPI-1 F322A, or RPV SPI-1 T309R at an MOI of 10. Cells were stained with the DNA-specific dye DAPI at 18 hours post infection to display nuclear morphology. Arrows indicate condensed nuclei.

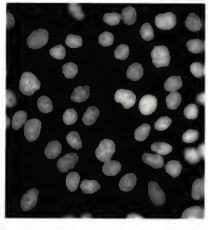

MOCK

WT RPV

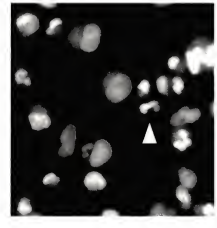

RPVΔSPI-1

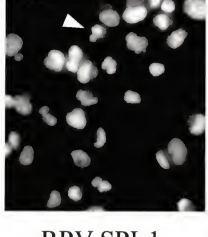

RPV SPI-1
N321A/F322A/S323A

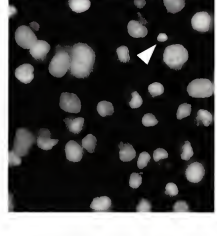

RPV SPI-1
F322A

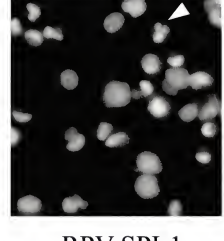

RPV SPI-1
T309R

F322A, or RPV SPI-1 T309R at an MOI of 10. At 18 hours post-infection, cells were fixed, permeabilized, and stained with the fluorescent DNA-specific dye DAPI (Fig. 20). Unlike mock- or wt RPV-infected cells, nuclei from A549 cells infected with either of the three recombinants containing SPI-1 RSL mutations displayed the same apoptotic morphological features as seen in the RPVΔSPI-1 infected cells, including chromatin condensation and nuclear invagination. Thus, the infection of nonpermissive cells with any of the RPV mutants expressing a SPI-1 protein lacking serpin activity results in an abortive infection associated with a form of cell death displaying the morphological features of apoptosis.

While previous work from our laboratory has demonstrated that restrictive cell lines infected with RPV SPI-1 null mutants display the morphological features of apoptosis, studies have not been performed to determine whether the biochemical changes that normally accompany the apoptotic morphological features such as caspase activation and cleavage of death substrates also take place in the infected cells. Therefore, experiments were performed to determine whether cleavage of the DNA repair enzyme poly(ADP- ribose) polymerase (PARP) or the nuclear structural protein lamin A, two major caspase death substrates, takes place during the nonpermissive infection of restrictive cell lines with RPV SPI-1 mutants. A549 cells were mock infected or infected with wt RPV or RPVΔSPI-1 at an MOI of 10, and infected cell extracts were prepared at 14 hours post infection. As a control for the assay, LLC-PK1 pig kidney cells were mock infected or infected with wt CPV or CPVΔcrmA as previous work has shown that LLC-PK1 cells infected with CPVΔcrmA but not with wt CPV undergo apoptosis

Figure 21. **Cleavage of death substrates PARP and lamin A by infected cell extracts.** Extracts prepared from A549 or LLC-PK1 cells at 14 hours post infection were mixed with ^{35}S-labeled A) PARP or B) human lamin A prepared in the TNT system and incubated for 90 minutes at 37°C. Proteins were separated on SDS-10% polyacrylamide gels, and radiolabeled proteins were visualized by autoradiography. The solid arrows indicate intact PARP or lamin A, while dashed arrows indicate PARP or lamin A cleavage products.

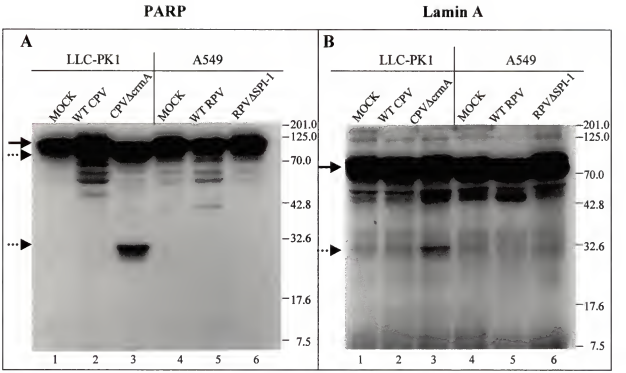
PARP
Lamin A
A
B
LLC-PK1
A549
MOCK
WT CPV
CPVΔcrmA
WT RPV
RPVΔSPI-1
201.0
125.0
70.0
42.8
32.6
17.6
7.5
1
2
3
4
5
6

Figure 22. **Induction of caspase 3 activity in infected cell extracts.** LLC-PK1 cells were mock infected or infected with wtCPV or CPVΔcrmA and A549 cells were mock infected or infected with wt RPV or RPVΔSPI-1. Extracts prepared from infected cells were harvested 14 hours post infection and incubated with a fluorogenic substrate specific for caspase 3 (Ac-DEVD-AMC). Fluorescence readings were taken at the indicated times and plotted as relative fluorescence units over time.

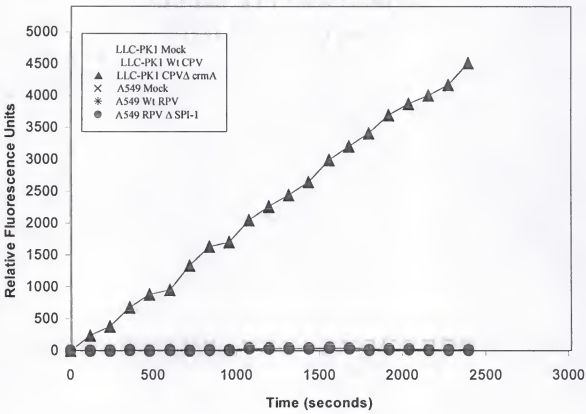
LLC-PK1 Mock
LLC-PK1 Wt CPV
LLC-PK1 CPVΔ crmA
A549 Mock
A549 Wt RPV
A549 RPV Δ SPI-1
Relative Fluorescence Units
5000
4500
4000
3500
3000
2500
2000
1500
1000
500
0
0
500
1000
1500
2000
2500
3000
Time (seconds)

accompanied by caspase activation and cleavage of death substrates (146). ^{35}S-labeled PARP (Fig. 21A) or lamin A (Fig. 21B) prepared *in vitro* using the TNT system were incubated with infected cell extracts for 90 minutes at 37°C, and the reacted products were analyzed following SDS-PAGE and autoradiography. Only extracts prepared from LLC-PK1 cells infected with CPVΔcrmA cleaved PARP (116 kDa) to the expected 85 and 30 kDa fragments (Fig. 21A, lane 3). Likewise, extracts prepared from LLC-PK1 cells infected with CPVΔcrmA cleaved lamin A from its native form to a 30 kDa product (Fig. 21B, lane 3), again consistent with previous studies (146). In contrast, no PARP or lamin A cleavage was seen when the ^{35}S-labeled death substrates were incubated with any other cell extract, including the lysate harvested from RPVΔSPI-1 infected A549 cells. As a further assay to examine caspase activity in the infected cells, cell extracts were directly tested for activation of the major effector apoptotic proteinase, caspase 3. Extracts prepared from LLC-PK1 cells infected with CPVΔcrmA possessed caspase 3-like activity as determined by cleavage of the fluorogenic caspase 3 substrate Ac-DEVD-AMC (Fig. 22), whereas all other extracts, including the lysate prepared from A549 cells infected with RPVΔSPI-1 did not. Thus, while A549 cells infected with RPV SPI-1 null mutants undergo the morphological changes associated with apoptosis, these changes occur in the absence of terminal effector caspase activation and cleavage of the major death substrates PARP and lamin A. These results suggest that during infection, SPI-1 expression may be necessary for inhibition of a caspase-independent form of cell death.

CHAPTER 6
DISCUSSION OF SPI-1 FUNCTION IN INFECTED TISSUE CULTURE CELLS

Previous work has demonstrated that SPI-1 gene expression is essential for the full host range of RPV (10). Furthermore, infection of cells nonpermissive for SPI-1 null mutations with an RPV SPI-1 negative virus was shown to trigger the morphological features of apoptosis (36). Because SPI-1 shares homology with members of the serpin family of serine proteinase inhibitors it was assumed that the ability of SPI-1 to function as a serpin was essential for its role in mediating viral host range. However, this assumption had remained untested until now.

The role of SPI-1 serpin activity in regulating RPV host range and infected cell apoptosis. In order to determine the importance of SPI-1 serpin function *in vivo*, three RPV recombinants were created containing the same specific SPI-1 RSL mutations which abolished inhibitory complex formation with cathepsin G *in vitro*. All three recombinants were shown to have the same reduced host range as an RPV SPI-1 deletion mutant, indicating for the first time that it is the ability of SPI-1 to function as a serpin that is crucial for its role during infection of certain cell lines. *In vitro* studies revealed that SPI-1 is able to form inhibitory complexes with the chymotrypsin family member cathepsin G, and that mutation of the P1 phenylalanine at position 322 abolished the interaction (Fig. 14). Mutation of the identical phenylalanine residue in RPV SPI-1 N321A/F322A/S323A and RPV SPI-1 F322A resulted in the same host range restriction

as RPVΔSPI-1, strongly suggesting that the inhibition of a chymotrypsin-like proteinase by SPI-1 is essential for virus growth in nonpermissive cells. Furthermore, the inability of RPV SPI-1 T309R to plaque on A549 and PK15 cell lines indicates that RSL insertion into the SPI-1 backbone is necessary for SPI-1 activity in restrictive cells, and provides additional evidence that the ability of SPI-1 to function as an inhibitory serpin is essential for productive RPV infection (Fig. 19).

Previous research established that the reduced host range of an RPV SPI-1 null mutant was due to the induction of apoptosis in restrictive cells that served to degrade progeny virions prior to their release from the cytoplasm (36). In the present study, RPV SPI-1 N321A/F322A/S323A, RPV SPI-1 F322A, and RPV SPI-1 T309R infections of A549 cells were each shown to induce the same changes in nuclear morphology that were seen following RPVΔSPI-1 infection of restrictive cell lines (Fig. 20). These are the first observations that demonstrate that it is the serpin activity of SPI-1 that is necessary to prevent the morphological changes. However, this study also reveals that although many of the morphological indications of apoptosis are present in A549 cells infected with RPV mutants lacking SPI-1 serpin activity, three of the biochemical changes that normally accompany apoptosis are absent in the infected cells. While cleavage of the death substrates PARP and lamin A occurred in the presence of control apoptotic extracts, the proteins remained intact following incubation with lysates prepared from A549 cells infected with RPVΔSPI-1 (Fig. 21). Furthermore, activation of the terminal apoptotic effector protease caspase 3 did not take place in nonpermissive cells infected with the SPI-1 deletion mutant (Fig. 22). In addition to the results of this study, a second study published during the writing of this manuscript challenges the current model of

SPI-1 anti-apoptosis activity. In the study, a vaccinia virus recombinant was constructed containing a 585 bp deletion within the SPI-1 open reading frame (251). Like RPVΔSPI-1, the VV SPI-1 mutant had a restricted host range and was unable to form plaques in several cell lines including A549 cells. However, while previous studies from our laboratory demonstrated that 94% of A549 cells infected with RPVΔSPI-1 exhibited nuclear morphology characteristic of apoptosis (36), Shisler and co-workers reported that only 7.5% of A549 cells infected with the vaccinia virus SPI-1 mutant displayed apoptotic morphology and that no evidence of DNA fragmentation, caspase 3 activation, or cleavage of apoptotic death substrates was present in the infected cells. Furthermore, infection of A549 cells with the VV SPI-1 mutant was characterized by reduced levels of viral intermediate and late mRNAs, viral late proteins, and viral late protein processing products (251). The authors speculate that instead of inhibiting the induction of apoptosis, SPI-1 functions to allow efficient expression of viral intermediate and late genes during infection of restrictive cell lines. However, previous studies of A549 cells infected with wt RPV or an RPV SPI-1 null mutant determined that the levels of virus gene expression and protein synthesis and processing were equivalent during both infections (36). The discrepancies in the two sets of results may stem from the use of different viruses in each study. Though SPI-1 is expressed by many orthopoxvirus members, the relative importance of the protein may vary during infection with each virus due to differences in the specific array of "non-essential" genes encoded by the viruses. For example, while inactivation of the SPI-1 gene results in the reduced host range of RPV, CPV SPI-1 null mutants have no host range restriction indicating that SPI-1 does not fulfill equivalent roles in each virus (10). Thus, while SPI-1 may serve to

allow efficient expression of vaccinia intermediate and late genes during infection of A549 cells, the protein does not appear to perform a similar role during RPV infection of the same cells. However, it is clear that SPI-1 acts to confer the complete host range of both RPV and VV, and this study demonstrates that the ability of SPI-1 to function as an inhibitory serpin is an essential property of the protein in this regard.

When the first study demonstrating a role for SPI-1 in regulating apoptosis during infection was published, many of the techniques and reagents necessary for the detailed analysis of apoptotic events were not available (36). Here, a more thorough examination of the nonproductive infection of A549 cells with RPVΔSPI-1 revealed that several hallmarks of apoptosis are absent in the cells. Remarkably, no evidence of caspase activation was observed. There are at least two possible explanations for these results. The first is that despite the morphological features of apoptosis, cell death occurs through another mechanism unrelated to apoptosis. The second is that death occurs through a novel apoptotic pathway not involving caspase activation. A third possibility is that apoptotic cell death is triggered following infection of restrictive cells with RPV SPI-1 null mutants, but that in the presence of viral crmA/SPI-2, a serpin known to function as an effective caspase inhibitor (265,274,324), the apoptotic cascade is blocked and cell death occurs through the alternative necrotic pathway. Cell death has been shown to occur in cells induced to undergo apoptosis in the presence of z-VAD, a general inhibitor of all caspases, as well as the baculovirus p35 protein which is an effective inhibitor of caspases 1,2, 6, 7, 8, and 10 (40,61,194,318). In each of these studies, many but not all hallmarks of apoptotic death were demonstrated, suggesting early abortion of the apoptotic cascade after some of the associated phenotypic changes had taken place.

Some researchers have proposed that when apoptosis is induced under conditions where caspase activation is blocked, mitochondrial permeability transition occurs unabated resulting in the loss of mitochondrial inner transmembrane potential, uncoupling of the respiratory chain, and hyperproduction of reactive oxygen species that lead to the unavoidable necrotic demise of the cell (94,129,138,139,232,317). A recent study examined the fate of cells exposed to CTL-generated granzyme B in the absence of activated caspases 3 or 8, effector enzymes known to control many of the processes essential for apoptosis induced by the granule proteinase (19). The study demonstrated that in situations in which caspases 8 or 3 were inhibited or absent, respectively, granzyme B was able to bypass the block in the cell death program by directly cleaving the pro-apoptotic molecule Bid, leading to mitochondrial collapse. However, in the absence of the endogenous effector proteinase caspase 3, completion of the apoptotic cascade was prevented and the cells died by a form of death resembling necrosis. In a similar manner, RPV infection of restrictive cell lines in the absence of SPI-1 may trigger the initial steps of apoptosis leading to the mitochondrial permeability transition and the accompanying early hallmarks of apoptosis such as chromatin condensation and nuclear invagination. However, in the presence of the RPV caspase inhibitor crmA/SPI-2, activation of effector caspases is unable to take place and the apoptotic cascade is arrested. In this scenario, the irreversible cytotoxic damage associated with mitochondrial collapse results in rapid cellular necrosis which degrades progeny virions prior to completion of the virus life cycle. If this model is correct, one would expect that the combined inactivation of both SPI-1 and SPI-2/crmA in RPV would result in the successful execution of the apoptotic cascade in infected nonpermissive cells,

accompanied by caspase activation and cleavage of apoptotic death substrates. Future experiments will address whether this model is correct.

It is interesting to speculate what causes certain cell lines to be nonpermissive for infection with RPV SPI-1 mutants. The expression of several poxvirus genes have been demonstrated to be essential for the productive infection of certain cell lines, and in many cases, the differential expression of a cellular protein has been proposed to determine the permissivity of the cell line. E3L has been shown to function by binding dsRNA and inhibiting activation of the interferon-sensitive PKR thereby inhibiting the kinase from phosphorylating eIF-2α and blocking mRNA translation (46). While vaccinia virus E3L mutants have a reduced host range and are unable to grow in HeLa cells, the mutants are able to productively infect RK13 cells. A comparison of the endogenous levels of PKR produced by each cell line revealed that the permissive cells express very low levels of the kinase, while the restrictive cell line produces very high levels of the protein (124), leading some to propose that the endogenous level of PKR within a cell may dictate whether the cell line is permissive for infection by E3L mutants. The protein product of the vaccinia virus K1L gene has been implicated in the regulation of viral gene transcription and contains ankyrin repeats, motifs known to facilitate protein-protein interactions. VV mutants deleted for the K1L gene have a reduced host range and can not productively infect RK13 cells. Infection of the restrictive cell lines with VV K1L mutants results in the premature inhibition of viral and host protein synthesis (214). Studies have shown that while the cellular vaccinia virus intermediate transcription factor VITF-2 can be isolated from the nuclei of uninfected cells permissive for infection with VV K1L mutants, the factor can not be isolated from nonpermissive RK13 cells (224).

Current models propose that VITF-2 exists in a latent form in restrictive cell lines, and that K1L serves to activate and recruit VITF-2 from the host cell nucleus early during infection. In the absence of K1L, VV intermediate gene expression can not take place in RK13 cells and the infection is aborted. In a similar manner, RPV SPI-1 may function to govern the activity of a host proteinase that is differentially expressed in permissive verses nonpermissive cell lines. While the data presented in this study does not exclude the possibility that the target enzyme of SPI-1 is present in both permissive and nonpermissive cell lines, it does suggest that SPI-1 inhibition of the proteinase is essential for productive RPV infection of restrictive cell lines. In the absence of SPI-1 inhibitory serpin activity, RPV infection of nonpermissive cells results in activation of the target proteinase which ultimately leads to the abortive virus infection accompanied by altered nuclear morphology and a caspase-independent form of cell death.

The fact that the altered morphology of nonpermissive cells infected with RPV SPI-1 RSL mutants is confined to nuclei suggests that the serine proteinase target of SPI-1 in restrictive cells may function to regulate nuclear structure. While it is not yet known if cathepsin G is the natural target of SPI-1 in infected animals, it is unlikely to be the target proteinase in the infected tissue culture cells used in this study, since immunoblot analysis of RK13, PK-15 and A549 cell extracts indicates that cathepsin G is absent in these cells (data not shown). A calcium-regulated serine proteinase with chymotryptic activity is associated with the nuclear scaffold (NS-associated protease) (51). Inhibition of the proteinase with AAPFcmk, a peptide inhibitor of chymotrypsin-like proteinases, has been shown to prevent lamin B1 breakdown and chromatin cleavage in nuclei incubated in the presence of apoptotic cell extracts (321,322). Inhibition of the protease

was also shown to prevent lamin B1 degradation in thymocytes and lamin degradation, histone B1 cleavage, and DNA fragmentation in thymocyte nuclei incubated with calcium, all of which could also be inhibited by Bcl-2 (159). In light of the fact that RPV SPI-1 mutant infections of restrictive cells are characterized by chromatin condensation and nuclear invagination, SPI-1 inhibition of the NS-associated protease is an attractive hypothesis and predicts that SPI-1 may localize to the nucleus. This model is currently being tested.

The nature of the SPI-1 modification. This study also provides the first evidence that wt SPI-1 becomes modified during RPV infection of tissue culture cells, resulting in a protein with a slower electrophoretic mobility than SPI-1 produced *in vitro* using the TNT coupled transcription/translation system (Fig. 17). The difference in size between wt SPI-1 prepared *in vitro* verses that expressed during infection was judged to be approximately 4-7 kDa, based on comparison of the relative electrophoretic mobilities of the two proteins with molecular weight standards following SDS-PAGE. Although the SPI-1 modification was shown to occur regardless of the cell type in which the protein was expressed, mutations within the SPI-1 RSL adversely affected the ability of the protein to become modified during infection (Fig. 18). The combined mutations of the P2, P1 and P1' residues in RPV SPI-1 N321A/F322A/S323A as well as the single amino acid change at the P1 residue in RPV SPI-1 F322A completely prevented the modification from taking place *in vivo*. Furthermore, changing the single P14 amino acid in RPV SPI-1 T309R from threonine to arginine at the distal end of the RSL appeared to partially inhibit the modification from occurring in infected tissue culture cells. However, the same RSL mutations had no affect on the migration of the corresponding

SPI-1 proteins expressed *in vitro*, indicating that altered electrophoretic mobilities of the virally-expressed proteins is the direct result of their intracellular expression and is not due to any inherent protein conformational changes resulting from the mutations themselves. Two models are consistent with these results. The first is that the slower electrophoretic mobility of wild type SPI-1 expressed *in vivo* is due to a post-translational modification of the protein that takes place in infected cells. This model predicts that the amino acid mutations within the SPI-1 RSL in the viruses RPV SPI-1 N321A/F322A/S323A, RPV SPI-1 F322A, and RPV SPI-1 T309R prevent the modification from being added to the mutant proteins either because the sequence motif necessary for the modification to occur is within the serpin RSL, or that the mutations lead to protein conformational changes which prevent the modification from taking place. Aside from the serpin signature, sequence motif databases predict that the SPI-1 open reading frame contains several potential sites for N-glycosylation, including a region within the RSL from amino acids 321 to 324 (Prosite PDOC00001). However, experiments studying the effects of N- and O-linked glycosylation inhibitors on viral protein expression in cells infected with the highly related vaccinia virus strain Western Reserve concluded that SPI-1 is not glycosylated during infection (123) In addition, the SPI-1 open reading frame contains several regions with homology to protein kinase C (Prosite PDOC00005) and casein kinase II phosphorylation motifs (Prosite PDOC00006). If wild type SPI-1 is phosphorylated *in vivo* and mutation of the SPI-1 P1 prevents the modification from occurring, incubation of cells infected with wt RPV or RPV SPI-1 F322A in the presence of ^{32}P-orthophosphate should only radiolabel the wild type

protein. Only the radiolabeled phosphorylated wild type protein would be detected following immunoprecipitation with antisera directed against SPI-1 and SDS-PAGE.

The second model proposes that instead of a post-translational modification, the discrepancy in size between SPI-1 expressed *in vivo* and that prepared in the TNT system is due to the formation of an inhibitory complex between the serpin and its natural target proteinase in infected cells. If this model is correct, the inability of recombinant wt SPI-1 protein prepared using overexpression systems to inhibit cathepsin G in enzymatic assays (data not shown) is likely due to the absence of SPI-1 inhibitory serpin activity while complexed with the target proteinase. While the molecular weight of the modified protein is smaller than what would be predicted for an inhibitory complex between SPI-1 and its target, the relatively small increase in size following complex formation (approximately 4-7 kDa) could be due to degradation of the serpin:proteinase complex by intracellular enzymes. In agreement with this model, mutation of the P1 residue rendered SPI-1 protein expressed from either RPV SPI-1 N321A/F322A/S323A or RPV SPI-1 F322A unable to become modified, presumably because the proteins no longer possess the RSL substrate cleavage site necessary for recognition by the target proteinase (Figs. 17 and 18). Following infection of cells with RPV SPI-1 T309R, two immunopositive SPI-1 species were observed, consistent in size with expression of both the modified and unmodified forms of the protein. This model predicts that because the SPI-1 P14 mutant contains the wild type P1 phenylalanine residue it is recognized by and able to form an initial complex with the target proteinase, identical in size to the complex formed between the enzyme and wild type SPI-1 protein expressed *in vivo*. However, due to the mutation within the hinge region which prevents RSL strand insertion into the serpin

backbone, the complex is not stabilized by proteinase translocation and the enzyme quickly dissociates releasing the second, smaller form of SPI-1. Alternatively, mutation of the SPI-1 P14 residue may somehow occlude the SPI-1 substrate site and render the mutant protein less recognizable by the target proteinase so that not all of the T309R protein within the infected cell associates with the enzyme to become modified. While mutation of the P14 residue in T309R completely abolished the ability of T309R to complex with cathepsin G *in vitro*, it remains possible that the affinity of the natural target proteinase for SPI-1 is stronger than that of cathepsin G allowing the target enzyme to form a complex with the mutant serpin protein in the presence of mutations within the hinge region, albeit less efficiently than with the wild type SPI-1. In further favor of this model, an RPV SPI-1 T309R variant was recently isolated that had regained the ability to productively infect and form plaques on the restrictive A549 cell line (RPV SPI-1 R309C) (Ben Luttge, personal communication). Sequencing of the mutant virus genomic DNA exposed changes in the SPI-1 open reading frame that resulted in an arginine to cysteine mutation at residue 309, corresponding to the P14 position within the serpin RSL (Ben Luttge, personal communication). Immunoblot analysis revealed that in contrast to SPI-1 expressed from the parental RPV SPI-1 T309R virus, SPI-1 containing the cysteine P14 residue migrated to the same position as modified SPI-1 following electrophoresis through an SDS/10% polyacrylamide gel (Ben Lutge, personal communication). Like threonine, the amino acid found at the P14 position of most inhibitory serpins including wild type SPI-1, cysteine is a small uncharged amino acid, a requirement for RSL insertion into the serpin backbone during the formation of inhibitory complexes. The ability of the arginine to cysteine mutation at the P14 site to not only restore virus growth

in A549 cells but also to allow the protein to become modified strongly suggests that the modification represents the remnants of an inhibitory complex between SPI-1 and its natural target proteinase within the infected cell. Experiments are underway to determine whether the SPI-1 R309C protein is able to form inhibitory complexes with cathepsin G *in vitro*.

Future work will address the nature of the SPI-1 modification. In collaboration with Dr. Donald Hunt from the University of Virginia, mass spectrometry analysis will be performed on SPI-1 protein derived from infected cells. First, samples of both modified and unmodified SPI-1 isolated from cells infected with wt RPV and RPV SPI-1 F322A, respectively, will be analyzed and compared to more accurately determine the exact molecular mass change supplied by the SPI-1 modification. Techniques are also available to fragment the purified wt SPI-1 and F322A proteins and compare the relative molecular masses of selected peptide products in order to determine where within the SPI-1 amino acid sequence that the modification occurs as well as the nature of the alteration if due to simple post-translation modification. If the SPI-1 modification is demonstrated to result from the generation of an inhibitory complex rather than the addition of a post-translational modification, mass spectrometry techniques may also enable the identification of the interacting protein. This would require the isolation of the region corresponding to the modified form of SPI-1 from a polyacrylamide gel transferred to a PVDF membrane. Following *in situ* digestion of the membrane-bound protein with trypsin, the peptide matching the SPI-1 RSL can be preferentially selected for further analysis. Comparison of the total peptide sequence array of the modified SPI-1 sample with the expected SPI-1 amino acid sequence should allow the detection of any

novel sequence(s) corresponding to the target proteinase which can then be identified using protein databases.

An alternate and more tedious approach to identify the target proteinase would make use of His-tagged SPI-1 prepared using the vaccinia/T7 overexpression system, which also becomes modified in infected cells (Lauren Morges, personal communication). The modified His-tagged protein can be purified from infected cell extracts and used to raise rabbit polyclonal antisera which will likely contain antibodies which will react with the 4-7 kDa peptide of the interacting enzyme. If the target proteinase is cellular, immunoprecipitation of uninfected cell extracts should allow detection and isolation of the protein. However, if the target of SPI-1 is a viral protein, infection of cells with an RPV variant expressing the unmodified form of SPI-1 (such as RPV F322A) followed by immunoprecipitation should detect the interacting protein.

Conclusions. This study is the first to directly link the ability of SPI-1 to function as an inhibitory serpin with its role in mediating the complete viral host range of RPV. *In vitro* experiments investigating the target proteinase specificity of SPI-1 revealed that the protein is active against cathepsin G, a member of the chymotrypsin family, and that the phenylalanine at residue 322 serves as the serpin P1 residue in this regard. Taken together with studies demonstrating the inability of the RPV SPI-1 F322A mutant to productively infect cell lines restrictive for SPI-1 null mutations, these results strongly imply that the target proteinase of SPI-1 within infected cells has chymotrypsin-like activity. Data presented in this study also questions the current model of SPI-1 as a negative regulator of apoptosis in infected cells, although infection of restrictive cell lines with RPV mutants lacking SPI-1 serpin activity is associated with the induction of

morphological changes characteristic of apoptotic cell death. While SPI-1 clearly is involved in the host range of RPV in tissue culture cells and may even directly interact with components of the cell death pathway, little is known regarding the role of SPI-1 during infection of animal hosts. Experiments addressing the role of SPI-1 during rabbit infection are discussed in Chapters 7 and 8.

CHAPTER 7
ANALYSIS OF THE ROLE OF SPI-1 IN INFECTED ANIMALS

Introduction. Poxviruses are the only virus family known to encode functional serpins, several of which have been shown to function as virulence factors *in vivo* (166,209,292). The conservation of the SPI-1 gene among all members of the orthopoxvirus genus, including vaccinia, rabbitpox, cowpox, and variola viruses implies that SPI-1 expression may function to mediate viral pathogenesis during infection of animal hosts. However, while preliminary studies reporting that RPV SPI-1 null mutants produce white pocks on the CAM suggests that SPI-1 may play a role in preventing the influx of inflammatory cells to the site of infection, mutation of the SPI-1 gene had no effect on RPV virulence in a mouse intranasal model of infection (10,281). The mouse intranasal model of infection allows some indication of RPV virulence, but it is not the host in which RPV displays its full spectrum of pathogenesis. For this reason, studies were performed to determine the effect of RPV SPI-1 mutations in rabbits. In addition to studying the effects of a complete deletion of the SPI-1 gene from RPV, infections were also performed using RPV SPI-1 F322A which expresses a SPI-1 protein lacking serpin activity in order to determine if the role of SPI-1 during animal infection is related to its ability to function as a proteinase inhibitor

Virus strain construction. Because previous work has demonstrated that expression of both SPI-1 and SPI-2 is necessary to inhibit CTL-mediated apoptosis of

RPV-infected target cells *in vivo* (147), the effects of SPI-1 mutations on RPV pathogenesis were examined alone or in combination with mutations in the SPI-2 gene. In order to achieve the desired SPI-2 gene disruption in the RPV recombinants, the vector pΔSPI-2::lacZ was designed containing the gene for the screenable marker β-galactosidase in place of the central one third of the SPI-2 open reading frame . Infection of CV-1 cells with the viruses wt RPV, RPVΔSPI-1, or RPV SPI-1 F322A was followed by transfection with the pΔSPI-2::lacZ DNA and selection of isolates with the ability to form blue plaques when grown in the presence of the β-galactosidase substrate X-gal. After pure isolates of the recombinants were obtained, designated RPVΔSPI-2, RPV SPI-1 (F322A)ΔSPI-2, and RPVΔSPI-1ΔSPI-2, insertional mutation of the SPI-2 gene was confirmed by PCR analysis of viral genomic DNA using SPI-2-specific primers (Fig. 23). Because the SPI-1 and SPI-3 genes contain sequence similarity to SPI-2, it was important to confirm that the genes remained intact following inactivation of the SPI-2 gene. Therefore, PCR was also used to amplify these genes using the appropriate primers (Fig. 23). Genomic DNA isolated from the wt RPV, RPVΔSPI-1 and RPV SPI-1 F322A virus stocks to be used in the animal experiments served as controls for the assay. As expected, SPI-3 was amplified from each control virus while SPI-1 was amplified only from wt RPV and RPV SPI-1 F322A. While the 1035 bp SPI-2 gene was amplified from viral DNA isolated from wt RPV, RPV SPI-1 F322A, and RPVΔSPI-1, the insertion of the lacZ gene at the SPI-2 locus in the viruses RPVΔSPI-2, RPV SPI-1(F322A)ΔSPI-2 and RPVΔSPI-1ΔSPI-2 added an additional 2.1 kbp of DNA to the central portion of the SPI-2 gene. Therefore, the disrupted gene in the SPI-2 mutant viruses was too large to be

Figure 23. **PCR analysis of virus constructs used in animal experiments**. Viral DNA isolated from wt RPV, RPV SPI-1(F322A), RPVΔSPI-1, RPVΔSPI-2, RPV SPI-1 (F322A)ΔSPI-2, or RPVΔSPI-1ΔSPI-2 was analyzed by PCR using primers specific for SPI-1 (lanes 1-6), SPI-2 (lanes 8-13) or SPI-3 (lanes 5-20). Plasmid DNA containing the appropriate serpin gene was used as a positive control for the PCR reactions (+, lanes 7, 14, and 21).

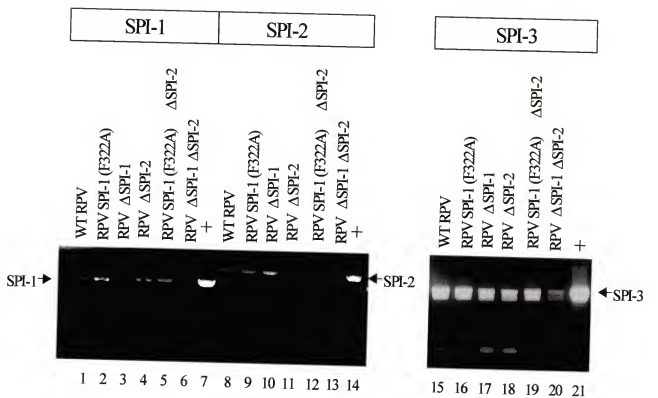
SPI-1
SPI-2
SPI-3
WT RPV
RPV SPI-1 (F322A)
RPV ΔSPI-1
RPV ΔSPI-2
RPV SPI-1 (F322A) ΔSPI-2
RPV ΔSPI-1 ΔSPI-2
+
SPI-1
SPI-2
SPI-3
1 2 3 4 5 6 7 8 9 10 11 12 13 14
15 16 17 18 19 20 21

amplified utilizing the PCR conditions used to amplify the wild type gene. As expected, SPI-1 was amplified only from RPVΔSPI-2 and RPVSPI-1 (F322A)ΔSPI-2 while SPI-3 was detected in all of the recombinants, indicating that mutation of the SPI-2 gene in each of the viruses took place without affecting the similar SPI-1 and SPI-3 genes.

In addition to confirming the presence or absence of the SPI genes in the recombinant viruses, experiments were performed to ensure that the appropriate serpin proteins were expressed during infection (Fig. 24). Cell lysates prepared from CV-1 cells infected with wt RPV, RPVΔSPI-1, RPV SPI-1 F322A, RPVΔSPI-2, RPV SPI-1 (F322A)ΔSPI-2, or RPVΔSPI-1ΔSPI-2 were subjected to SDS-PAGE followed by immunoblot analysis using antisera recognizing either SPI-1 (Fig. 24A) or SPI-2 (Fig. 24B) proteins. As expected, SPI-1 protein was detected in extracts prepared from wt RPV, RPVΔSPI-2, RPV SPI-1 F322A and RPV SPI-1 (F322A)ΔSPI-2 but was absent in all other infected cell lysates (Fig. 24A). Consistent with previous findings, SPI-1 protein expressed from RPV SPI-1 F322A migrated faster during electrophoresis through an SDS/10% polyacrylamide gel than protein expressed from wt RPV (Fig. 24A, lanes 6-7). Furthermore, SPI-1 protein expressed during infection with RPV SPI-1 (F322A)ΔSPI-2 migrated faster than SPI-1 produced in RPVΔSPI-2-infected cells, demonstrating that SPI-2 expression has no effect on the ability of SPI-1 to become modified during infection. SPI-2 protein was produced following infection of CV-1 cells with wt RPV, RPVΔSPI-1, and RPV SPI-1 F322A but was absent in RPVΔSPI-2, RPV SPI-1 (F322A)ΔSPI-2 and RPVΔSPI-1ΔSPI-2 infected cell lysates indicating the successful inactivation of SPI-2 gene expression in the recombinant viruses.

Figure 24. **Immunoblot analysis of virus constructs used in animal experiments.** CV-1 cells were infected with wtRPV (lanes 1 and 7), RPVΔSPI-1 (lanes 2), RPVΔSPI-2 (lanes 3), RPVSPI-1(F322A)ΔSPI-2 (lanes 4), RPVΔSPI-1ΔSPI-2 (lanes 5), or RPVSPI-1(F322A) (lanes 6). Cytoplasmic cell extracts were harvested at 18 hours post infection and immunoblotted using antisera against A) SPI-1 or B) SPI-2 proteins. Immunopositive proteins were detected using chemiluminescence. The location of the SPI-2 and the modified form of SPI-1 proteins are indicated by solid arrows. The location of the unmodified SPI-1 species is designated by a dashed arrow.

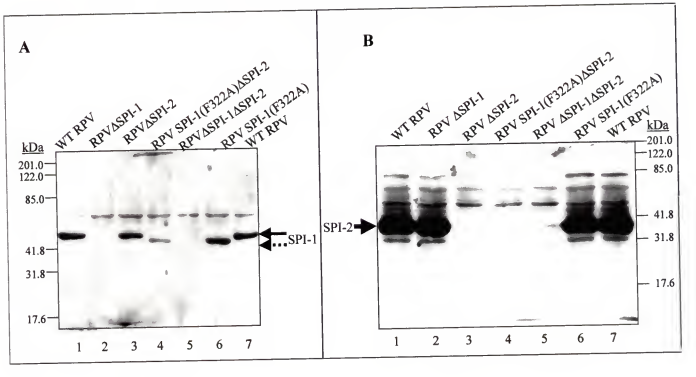
A
WT RPV
RPVΔSPI-1
RPVΔSPI-2
RPV SPI-1(F322A)ΔSPI-2
RPVΔSPI-1ΔSPI-2
RPV SPI-1(F322A)
WT RPV
kDa
201.0
122.0
85.0
41.8
31.8
17.6
SPI-1
1 2 3 4 5 6 7
B
WT RPV
RPV ΔSPI-1
RPV ΔSPI-2
RPV SPI-1(F322A)ΔSPI-2
RPV ΔSPI-1ΔSPI-2
RPV SPI-1(F322A)
WT RPV
kDa
201.0
122.0
85.0
41.8
31.8
17.6
SPI-2
1 2 3 4 5 6 7

Host range of virus constructs. It has been well established that SPI-1 plays an important role in the host range of RPV (10,36), which this study has shown may involve inhibition of a caspase-independent form of cell death. In addition, other studies have demonstrated that crmA, and to some extent SPI-2, prevents apoptosis triggered by infection of LLC-PK1 cells with CPV and RPV, respectively(146,218). Because available data suggests that both serpins may function to inhibit premature cell death thereby extending the duration of a productive poxvirus infection, experiments were conducted to determine whether the combined mutations of both SPI-1 and SPI-2 in RPV SPI-1 (F322A)ΔSPI-2 and RPVΔSPI-1ΔSPI-2 affected the ability of the recombinants to successfully infect tissue culture cells. RPV SPI-1 (F322A)ΔSPI-2 and RPVΔSPI-1ΔSPI-2 were assayed for the ability to form plaques on a variety of cell lines. Representative results from one experiment in which the viruses were assayed for host range using wt RPV, RPVΔSPI-1, RPV SPI-1 F322A and RPVΔSPI-2 as controls are shown in Figure 25. As expected, wt RPV was able to form plaques on all cell lines tested, while RPVΔSPI-1 was able to grow only during infection of the permissive RK13 cell line. Consistent with previous observations made in this study, mutation of the SPI-1 P1 residue in RPV SPI-1 F322A resulted in host range restriction, rendering the recombinant unable to plaque on the restrictive A549 and PK-15 cell lines. As demonstrated previously (10), insertional inactivation of the SPI-2 gene in RPVΔSPI-2 had no effect on virus host range in any cell line tested. Furthermore, while RPV SPI-1 (F322A)ΔSPI-2 and RPVΔSPI-1ΔSPI-2 were unable to form plaques on cell lines restrictive for SPI-1 mutations, no additional host range restrictions were observed in any cell line assayed.

Figure 25. **Host range of virus constructs used in animal experiments.** Plaque formation of wtRPV and the RPV recombinants used in the animal experiments on A549, PK-15 and RK13 cells is shown.

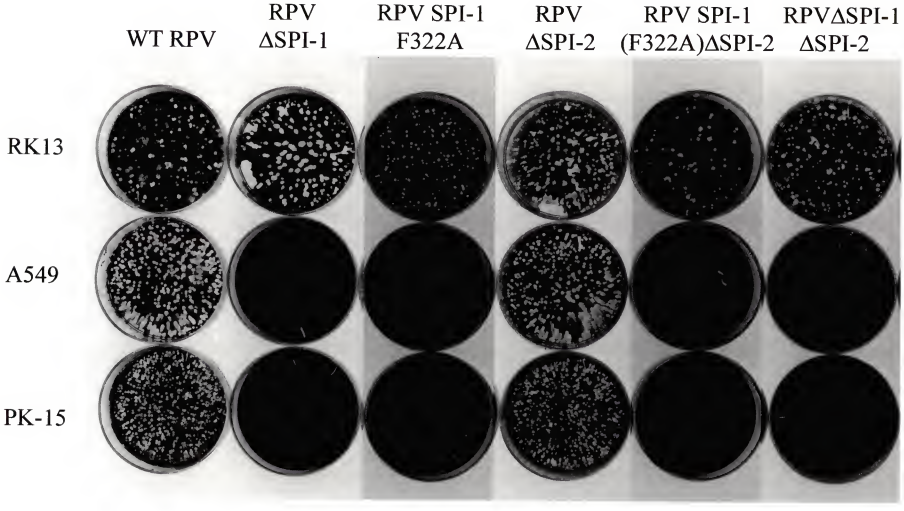
WT RPV
RPV ΔSPI-1
RPV SPI-1 F322A
RPV ΔSPI-2
RPV SPI-1 (F322A)ΔSPI-2
RPVΔSPI-1 ΔSPI-2
RK13
A549
PK-15

Therefore, it appears that mutation of both serpins has no more effect on virus host range in tissue culture cells than mutation of SPI-1 alone.

Rabbit infections. After the thorough characterization of the viruses just described, crude virus stocks of wt RPV, RPVΔSPI-1, RPVΔSPI-2, RPV SPI-1 F322A, RPV SPI-1 (F322A)ΔSPI-2 and RPVΔSPI-1ΔSPI-2 were purified over a sucrose cushion to remove any cellular proteins present in the stocks, thus minimizing the risk of nonspecific inflammation in infected animals due to the introduction of cellular antigens. Purified stocks were dispensed into 1 ml aliquots and stored at –80°C. To ensure accurate titers, single aliquots of each virus were chosen at random and titered in triplicate on RK13 cell monolayers. 100 pfu of each virus were used to inject female New Zealand White rabbits intradermally in each flank for a final dose of 200 pfu per rabbit. Each virus was used to infect a group of three rabbits and animals were monitored daily for signs of disease including fever, weight loss, nasal and/or occular discharge, dyspnea, and the development of secondary lesions. An additional rabbit was mock-infected with PBS buffer using identical inoculation methods. The animal was housed with the other rabbits and examined daily for symptoms to serve as a control for virus cross-contamination within the group. Symptoms were recorded and are summarized in Table 4. In addition, variations in animal body temperatures and degree of weight change over the course of the experiment are depicted graphically in Figures 26 and 27, respectively.

As shown in Table 4, disease symptoms varied little among rabbits infected with wt RPV, RPVΔSPI-1, RPV SPI-1 F322A, RPVΔSPI-2, RPV SPI-1 (F322A)ΔSPI-2 and RPVΔSPI-1ΔSPI-2. Animals infected with each of these viruses developed fevers reaching maximum temperatures of 105.2°F to 107.6°F (average 106.1°F) that lasted from

1 to 7 days in duration (average 4.6 days) (Table 4 and Fig. 26). All but one rabbit developed nasal discharge which ranged from mild to severe in gravity. At least one rabbit from each virus group suffered from dyspnea, which varied among rabbits from slight wheezing to extreme difficulty in breathing. Nearly all infected rabbits experienced some degree of occular discharge which completely obstructed the vision of the most affected animals. Every infected rabbit developed secondary lesions, indicating spread of the virus from the primary inoculation site to other regions of the body.

While many rabbits survived the infection and several showed signs of recovery by day 14 post-infection, at least one rabbit from each virus group succumbed prior to termination of the experiment. Seven of the original 18 infected rabbits died on day 8 post-infection, including one rabbit from the wt RPV, RPVΔSPI-1, RPV SPI-1 F322A, and RPVΔSPI-2 virus groups. Surprisingly, the highest mortality was associated with RPVΔSPI-1ΔSPI-2 infection, as all rabbits infected with this virus died on day 8 post-infection. Several of the rabbits that died on day 8 displayed a rapid decrease in body temperature characteristic of terminal rabbitpox on day 7 post-infection (Fig. 26). All rabbits in the study lost weight over the course of the experiment, but the percent weight change seen in the animals which died on day 8 post-infection was not significantly more than that seen in the surviving animals (Fig. 27). As summarized in Table 4, while the presence of secondary lesions indicates that each of the infected animals were viremic, many of the animals which expired on day 8 post-infection had exhibited only mild signs of illness just prior to their death. Due to the number of largely asymptomatic rabbits that died on day 8 of the experiment, the animals were necropsied and primary lesions were removed and processed for histology. Necropsy revealed that only some of the animals

Table 4.
Virulence of RPV SPI-1 and SPI-2 Mutants in Rabbits

Virus (Animal#)	Max. Temp. (°F)	Fever Duration (Days)	Nasal Discharge	Dyspnea	Occular Discharge	Secondary Lesions	Death (Day)
WT RPV							
(9H103)	106.4	5	++*	+	++	+	no
(9H105)	105.7	2	-	-	-	+	no
(9H104)	105.5	6	+++	++	++	+	yes(8)
RPVΔSPI-1							
(9H106)	106.6	3	+	-	++	+	no
(9H108)	105.2	4	+	-	+	+	yes(8)
(9H127)	106.2	7	+++	+++	+++	+	yes(11)
RPV SPI-1 F322A							
(9H125)	105.9	5	+	-	+	+	no
(9H126)	106.8	8	+++	+++	+++	+	no
(9H124)	105.6	6	+	-	+	+	yes(8)
RPVΔSPI-2							
(9H124)	106.1	2	++	-	-	+	no
(9H123)	106.4	6	+++	++	++	+	no
(9H122)	105.4	1	+	-	++	+	yes(8)
RPV SPI-1 (F322A)ΔSPI-2							
(9H115)	105.8	6	++	-	++	+	no
(9H117)	107.6	7	+	-	-	+	no
(9H116)	106.4	4	+++	+++	+	+	yes(10)
RPVΔSPI-1 ΔSPI-2							
(9H118)	106.9	5	+	-	+	+	yes(8)
(9H119)	106.2	4	++	-	++	+	yes(8)
(9H120)	106.3	3	++	+++	+++	+	yes (8)
PBS							
(9H107)	103.6	0	-	-	-	-	no

* Each symptom was ranked from absent (-) to severe (+++)

Figure 26. **Rabbit rectal temperature changes following infection with wtRPV or RPV constructs containing serpin mutations.** Rabbits were infected with A) wt RPV, B) RPVΔSPI-2, C) RPVΔSPI-1, D) RPV SPI-1(F322A), E) RPVΔSPI-1ΔSPI-2, or F) RPV SPI-1(F322A)ΔSPI-2. Rectal temperatures were measured daily and are expressed graphically as degrees Fahrenheit over time.

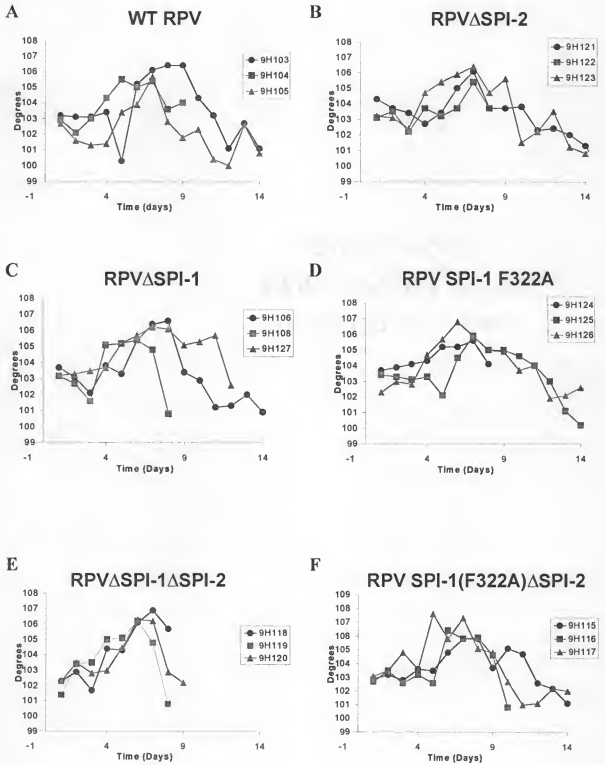
A
WT RPV
B
RPVΔSPI-2
C
RPVΔSPI-1
D
RPV SPI-1 F322A
E
RPVΔSPI-1ΔSPI-2
F
RPV SPI-1(F322A)ΔSPI-2
Degrees
Time (days)
Time (Days)
9H103
9H104
9H105
9H121
9H122
9H123
9H106
9H108
9H127
9H124
9H125
9H126
9H118
9H119
9H120
9H115
9H116
9H117

Figure 27. **Rabbit body weight changes following infection with wtRPV or RPV constructs containing serpin mutations.** Rabbits were infected with either A) Wt RPV, B) RPVΔSPI-2, C) RPVΔSPI-1, D) RPV SPI-1 (F322A), E) RPVΔSPI-1ΔSPI-2 or F) RPV SPI-1 (F322A)ΔSPI-2. Rabbits were weighed daily and measurements are expressed graphically as percent weight change over time.

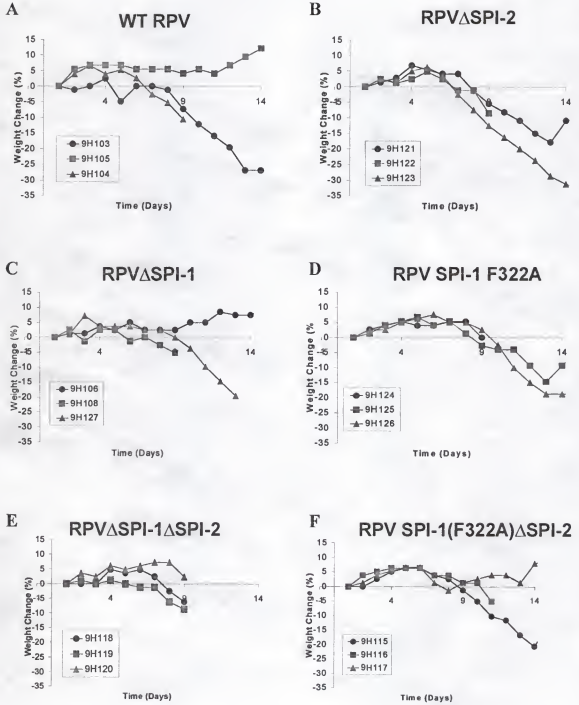
A
WT RPV
Weight Change (%)
Time (Days)
9H103
9H105
9H104
B
RPVΔSPI-2
9H121
9H122
9H123
C
RPVΔSPI-1
9H106
9H108
9H127
D
RPV SPI-1 F322A
9H124
9H125
9H126
E
RPVΔSPI-1ΔSPI-2
9H118
9H119
9H120
F
RPV SPI-1(F322A)ΔSPI-2
9H115
9H116
9H117

had the classical gross internal lesions characteristic of rabbitpox, and no correlation could be made between a particular virus and the ability to cause internal lesions (Trenton R. Schoeb, DVM, PhD., personal communication). In contrast, the histology of primary lesions from each of the expired rabbits were nearly identical, regardless of the virus used to infect the rabbits (data not shown). The lesions exhibited severe edema and necrosis of the dermis, subcutis, and epidermis. Extreme degeneration of hair follicles and blood vessels was also present within the lesions. Only a mild inflammatory response was seen within the deep dermis of the primary infection sites, consisting of heterophils (neutrophils), macrophages and lymphocytes (Trenton R. Schoeb, DVM, PhD., personal communication). It is important to note that evidence of a gastrointestinal disorder including diarrhea and the presence of a thick anal discharge was seen during examination of many of the animals which died on day 8 post-infection. The possibility that the expired animals were suffering from an unknown enteric illness at the time of inoculation which compounded the effects of the poxvirus infection can not be excluded.

Aside from the animals that succumbed on day 8 post-infection, only one animal died over the course of the experiment. The RPV SPI-1 (F322A)ΔSPI-2-infected rabbit (9H116) died on day 10 and exhibited the classical symptoms of rabbitpox disease prior to its death. These symptoms included pyrexia for approximately 4 days followed by a dramatic drop in body temperature on day 9 post-infection (Fig. 26 F), nasal and occular discharge, large numbers of secondary lesions on all parts of the body, and severe dyspnea which caused the animal to gasp for air. Although the animal showed signs of anorexia including decreased stool output just prior to death, the animal lost only 9.49% of its original body weight over the course of the experiment (Fig. 27). While many of

the remaining animals displayed the same grave symptoms (Table 4), each animal survived through day 14. As seen in Figure 26, the majority of the surviving rabbits experienced fever followed by a drop in body temperature in addition to a significant decrease in body weight (Fig. 27). By day 14 post-infection, several of the remaining animals began to display signs of recovery including weight gain and the normalization of body temperature (Figs. 26 and 27), while other rabbits continued to deteriorate and likely would have succumbed to the infection if the experiment had been allowed to continue. Still other rabbits exhibited elevated temperatures and the secondary lesions which are the hallmark of viremia but lacked any other overt signs of disease. No correlation could be made between a particular virus and the ability to cause either the terminal or asymptomatic disease phenotype in this experiment.

In addition to the rabbits infected to examine the overall effects of serpin mutations on the progression of gross rabbitpox disease, a second group of rabbits was infected in parallel in order to examine the results of serpin mutations on the inflammatory response at the primary site of inoculation. Individual rabbits were infected with 100 pfu of either wt RPV, RPVΔSPI-1, RPV SPI-1 F322A, RPV ΔSPI-2, RPV SPI-1 (F322A)ΔSPI-1 or RPVΔSPI-1ΔSPI-2 in each flank. Animals were sacrificed and primary lesions were removed and processed for histology on day 4 post-infection, a timepoint at which the greatest contrast among primary lesions caused by different poxvirus variants is seen (307). The histopathology of each of the lesions were independently examined by two impartial investigators, and the results of their analysis are summarized in Table 5. While histology from the primary lesions excised from the rabbits that died at day 8 were remarkably similar (described above), clear differences

were seen in the lesions isolated from rabbits sacrificed at day 4 post-infection (Fig. 28, Table 5). The primary lesion isolated from the wt RPV-infected rabbit at day 4 shared striking similarities with the lesions isolated from the animals that died on day 8. Severe edema and necrosis was present as well as degeneration and necrosis of structures within the lesion, including blood vessels and hair follicles (Fig. 28). As in the lesions from the rabbits which expired on day 8 post-infection, the inflammatory response was minimal and was evident only in the deep dermis. Inflammatory cells within this portion of the lesion were a mixture of heterophils (neutrophils), monocytes/macrophages, and lymphocytes.

Primary lesions from each of the animals infected with viruses bearing serpin mutations exhibited a greater influx of inflammatory cells than the lesion isolated from the wt RPV infected rabbit which was evident at the surface of the lesions as well as within the deep dermal layers (Fig. 28). While an overall trend toward greater levels of inflammation relative to wt RPV was observed for the serpin mutant viruses as a group, closer examination revealed differences in the nature of the inflammatory response caused by each virus. The lesion isolated from the rabbit infected with RPVΔSPI-2 displayed increased edema relative to the other lesions. The lesion tissue also appeared more hyperplastic than the corresponding tissue in the other rabbits. The RPVΔSPI-2 lesion displayed significant levels of hydropic degeneration within the basal layer of the epidermis which was not appreciated in the lesions caused by wt RPV, RPVΔSPI-1 or RPV SPI-1 F322A This form of degeneration is usually associated with apoptosis. However, because the techniques necessary to accurately detect apoptotic cells were not used in these experiments, the number of apoptotic cells within the lesion could not

Figure 28. **Histology of rabbit primary lesions following infection with wtRPV or RPV serpin mutant viruses.** Rabbits were infected with 100 pfu of either A) wt RPV, B) RPVΔSPI-2, C) RPVΔSPI-1, D) RPV SPI-1 F322A, E) RPV SPI-1 (F322A)ΔSPI-2 or F) RPVΔSPI-1ΔSPI-2 in each flank. Rabbits were euthanized at day 4 post-infection and primary lesions were excised and processed for histology as described in the Materials and Methods. Representative regions of both the deep dermis (left) and superficial (right) areas of each lesion were chosen and photographed.

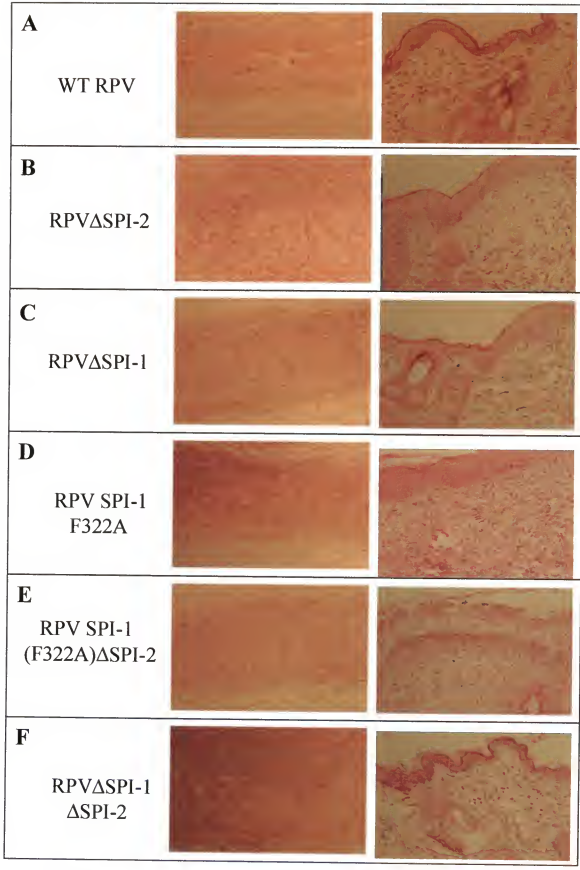
A
WT RPV
B
RPVΔSPI-2
C
RPVΔSPI-1
D
RPV SPI-1
F322A
E
RPV SPI-1
(F322A)ΔSPI-2
F
RPVΔSPI-1
ΔSPI-2

Table 5.
Summary of Rabbit Primary Lesion Histology
Following Infection with Wt RPV and RPV Serpin Mutants

Virus	Epidermis	Deep Dermis
WT RPV	Significant edema present Necrosis Degeneration of structural elements within the lesion Minimal inflammation	Minimal inflammatory infiltrate consisting of heterophils, monocytes/ macrophages and lymphocytes
RPVΔSPI-2	Significant edema present Necrosis Hyperplastic tissue within lesion Hydropic degeneration Minimal to moderate inflammation	Moderate inflammatory infiltrate consisting of heterophils, monocytes macrophages and lymphocytes
RPVΔSPI-1	Significant edema present Necrosis Severe inflammation associated with a large number of mononuclear cells but few heterophils	Significant inflammatory infiltrate consisting of heterophils, monocytes/ macrophages and lymphocytes
RPV SPI-1 F322A	Significant edema present Necrosis Some degeneration of structural elements within lesion Severe inflammation associated with a large number of mononuclear cells and few heterophils	Significant inflammatory infiltrate consisting of heterophils, monocytes/ macrophages and lymphocytes
RPV SPI-1 (F322A) ΔSPI-2	Significant edema present Severe necrosis and degradation of lesion tissue Severe hydropic degeneration Severe inflammation	Necrosis Significant inflammatory infiltrate consisting of heterophils, monocytes/ macrophages and lymphocytes
RPVΔSPI-1 ΔSPI-2	Significant edema present Severe necrosis and degradation of lesion tissue Severe hydropic degeneration Severe inflammation	Necrosis Significant inflammatory infiltrate consisting of heterophils, monocytes/ macrophages and lymphocytes

determined. The amount of inflammation within the deep dermis of the lesion was significantly greater than that seen in the wt RPV infected animal. The inflammatory cell infiltrate was an evenly mixed population of heterophils (neutrophils), lymphocytes, and cells of the monocyte/macrophage lineage (Trenton R. Schoeb, DVM, PhD., personal communication).

Examination of the primary lesion harvested from the rabbit infected with RPVΔSPI-1 revealed a massive influx of inflammatory cells within the superficial area of the lesion which was not observed in the other rabbit tissues. While the inflammatory infiltrate observed in the other lesions was an even mix of lymphocytes, heterophils (neutrophils), and monocytes/macrophages, the inflammatory response within the superficial layer of the RPVΔSPI-1 lesion was nearly devoid of heterophils. In addition, there was a major inflammatory response within the deep dermis that was significantly greater than that present in the lesion isolated from the wt RPV infected animal. Within this region, the inflammatory infiltrate was a mixed population of lymphocytes, heterophils (neutrophils) and mononuclear cells similar to that seen in the RPVΔSPI-2 infected rabbit lesion.

The histology of the lesion isolated from the RPV SPI-1 F322A infected rabbit was nearly identical to the corresponding lesion from the rabbit infected with RPVΔSPI-1. As with all of the lesions caused by the serpin mutant viruses, a significantly greater number of inflammatory cells were present in the lesion relative to the wtRPV infected animal. Within the deep dermis, a mixed population of inflammatory cells was observed. In addition, an inflammatory infiltrate comprised of monocytes/macrophages and

lymphocytes was present in the superficial area of the lesion. As seen in the RPVΔSPI-1 lesion, the cell population within this section of the lesion contained a significant reduction in the number of heterophils/neutrophils present. The fact that mutation of the putative SPI-1 P1 residue in RPV SPI-1 F322A resulted in the same primary lesion phenotype as that caused by the RPV SPI-1 deletion mutation strongly suggests that the ability of SPI-1 to function as an inhibitory serpin is important for its role during infection *in vivo*.

The histopathology of the primary lesions caused by infection with RPVΔSPI-1ΔSPI-2 and RPV SPI-1 F322AΔSPI-2 was nearly identical. While some inflammation was present in the superficial epidermis of the lesions, much of this region was affected by extensive necrosis. In fact, the necrosis was so severe that much of the epidermis within the central regions had disintegrated. Not surprisingly, many of the structural components of the affected tissue, including blood vessels and hair follicles, had been damaged. The extensive tissue destruction seen in the lesions did not appear to have resulted from an increased inflammatory response, as no real differences in the levels of inflammation in these samples relative to the remaining lesions caused by the RPV serpin mutants were appreciated. The inflammatory response in these lesions was similar to that seen in the lesions caused by the single mutant viruses and consisted of a mixed population of monocytes/macrophages, heterophils (neutrophils) and lymphocytes. The hydropic degeneration which was present in the lesion caused by RPVΔSPI-2 was also evident in these lesions. While this form of tissue destruction is often associated with apoptotic cell death, the assays needed to accurately measure the levels of apoptosis within the affected tissues were not performed.

Taken together, these results imply that while no real contrast exists in the ability of wt RPV and the RPV serpin mutants to cause systemic disease in rabbits under these conditions, the early inflammatory response at the primary infection site differs between the viruses suggesting that the serpins may function to modulate components of the host innate immunity. In contrast, previous observations made in our laboratory demonstrated that mutation of either the RPV SPI-1 or SPI-2 genes caused a mild degree of attenuation *in vivo*, whereas mutation of both genes resulted in significant attenuation with no accompanying nasal or occular discharge, dyspnea, or secondary lesions in infected rabbits (M. Brooks, R. Stern, and R. Moyer, unpublished results). However, while the methods used to disrupt the SPI-2 gene were identical in both sets of experiments, the previous study utilized an RPV SPI-1 mutant, designated RPV SPI-1 (-), that contained the gene for the selectable marker *eco-gpt* inserted within the serpin open reading frame without concomitant deletion of any SPI-1 gene sequence (Fig. 29). Furthermore, a lower infectious dose of virus was used in the previous study and infections were given in a single inoculation. Because minor variations in the infection protocols and/or the differences in the mutant virus strain constructions may have resulted in the discrepancies in these two sets of results, a third experiment was performed. This experiment utilized the lower inoculation dose used by the previous researchers and compared the ability of the two RPV SPI-1 mutant viruses, RPVΔSPI-1 and RPV SPI-1 (-), to cause disease in rabbits relative to wtRPV. However, due to time and budgetary constraints, the effects of combined SPI-1 and SPI-2 mutations on virulence were not examined.

Twelve New Zealand White rabbits were randomly assigned into three groups of four animals and infected in the right flank with 50 pfu of either wt RPV, RPVΔSPI-1 or

Figure 29. **Schematic representation of the genomic SPI-1 locus in the viruses wtRPV, RPVΔSPI-1 and RPV SPI-1 (-).** A diagrammatic comparison of a portion of the genomes of wtRPV, RPVΔSPI-1 and RPV SPI-1 (-) is shown. The SPI-1 ORF is depicted by a black box, while the gene for the selectable marker Eco-gpt cloned under the control of the $P_{7.5}$ promoter is shown by a stippled box. The left flanking sequence of SPI-1 beginning 235 nucleotides upstream of the SPI-1 ORF (L) is shown, as well as the right flanking sequence of SPI-1 (R) which begins at nucleotide 1074 of the SPI-1 ORF and extends 522 nucleotides.

WT RPV

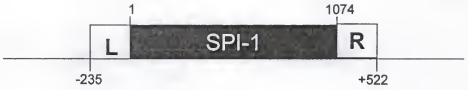

RPVΔSPI-1

RPV SPI-1 (-)

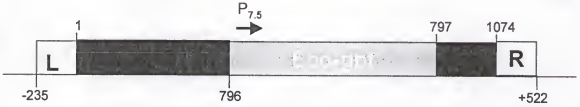

RPV SPI-1 (-). Once again, an additional rabbit was mock-infected with PBS buffer using identical inoculation methods and was housed in the same unit to serve as a control for virus cross-contamination. As before, animals were monitored daily and symptoms are summarized in Table 6 while changes in animal body temperature and total body weight are depicted graphically in Figures 30 and 31, respectively. During this experiment, individual symptom severity scores were assigned based on the extent of each rabbit's disease. Each day, rabbits were examined by an impartial observer for the presence of nasal and occular discharge, dyspnea, and secondary lesions and each symptom was given a numerical value from 0 (absent) to 3 (severe). Using this system, an asymptomatic animal received zero points, while a maximum score of 9 points was assigned to an animal with severe nasal and occular discharge, great difficulty breathing, and the presence of a large number of secondary lesions. At the end of the experiment, the daily scores for each animal were averaged to determine individual mean symptom severity scores which are listed in Table 6. Primary lesions were observed daily and photographed in order to document any differences in the lesions caused by the infecting viruses. Photographs from a single representative lesion caused by each virus were selected and are shown in Figure 32.

No difference was seen in the ability of RPVΔSPI-1, RPV SPI-1 (-) and wt RPV to cause pyrexia in rabbits as all animals developed fevers following infection (Fig.30). In contrast, other disease symptoms varied dramatically between groups of rabbits infected with wt RPV versus those infected with the SPI-1 mutant viruses. As seen in

Table 6.
Virulence of Wt RPV, RPVΔSPI-1 and RPV SPI-1 (-) in Rabbits

Virus (Animal#)	Max. Temp (°F)	Fever Duration (Days)	Nasal Discharge	Dyspnea	Ocular Discharge	Secondary Lesions	Death (Day)	Symptom Severity Score
Wt RPV								
(9J16)	106.4	4	+++*	+++	+++	++	yes(8)	8.0**
(9J25)	106.3	5	+++	+++	+++	+++	yes(9)	7.0
(9J24)	106.6	5	+++	+++	+++	++	yes(9)	8.0
(9J17)	106.6	10	+++	+++	+++	++	no	7.0
RPVΔSPI-1								
(9J15)	107.2	6	+	-	+	++	no	3.8
(9J22)	106.1	8	+	+	+	++	no	4.0
(9J23)	106.8	5	+++	+++	+++	+++	yes(9)	8.0
(9J14)	107.1	8	+	-	+	++	no	5.2
RPVSPI-1(-)								
(9J20)	106.7	6	+	-	-	+	no	3.2
(9J19)	106.3	7	-	-	-	+	no	2.4
(9J18)	106.8	8	+	-	-	+	no	2.4
(9J21)	107.0	8	+	+	+	++	no	2.4
PBS	103.8	-	-	-	-	-	no	0.0

* Each symptom was ranked from absent (-) to severe (+++)
** Criteria used to determine severity scores:

	0	1	2	3
Dyspnea	none	mild	moderate	severe
Nasal/occular discharge	none	slight	moderate	heavy
Number of secondary lesions	0	1-10	11-20	21-30

Figure 30. **Rabbit rectal temperature changes following infection with wtRPV, RPVΔSPI-1 or RPV SPI-1 (-).** Rabbits were infected with A) wt RPV, B) RPVΔSPI-1, or C) RPV SPI-1 (-). Animal rectal temperatures were measured daily and are expressed graphically as degrees Fahrenheit over time.

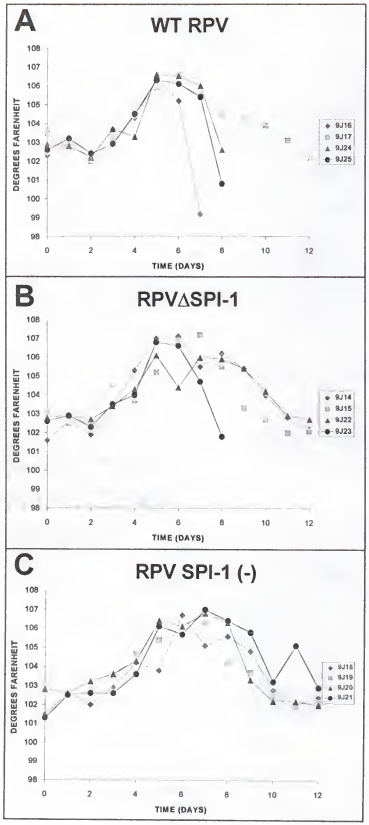
A
WT RPV
DEGREES FARENHEIT
TIME (DAYS)
9J16
9J17
9J24
9J25
B
RPVΔSPI-1
DEGREES FARENHEIT
TIME (DAYS)
9J14
9J15
9J22
9J23
C
RPV SPI-1 (-)
DEGREES FARENHEIT
TIME (DAYS)
9J18
9J19
9J20
9J21

Figure 31. **Rabbit body weight changes following infection with wtRPV, RPVΔSPI-1 or RPV SPI-1 (-).** Rabbits were infected with either A) Wt RPV, B) RPVΔSPI-1, or C) RPV SPI-1 (-). Animals were weighed daily and measurements are expressed graphically as percent weight change over time.

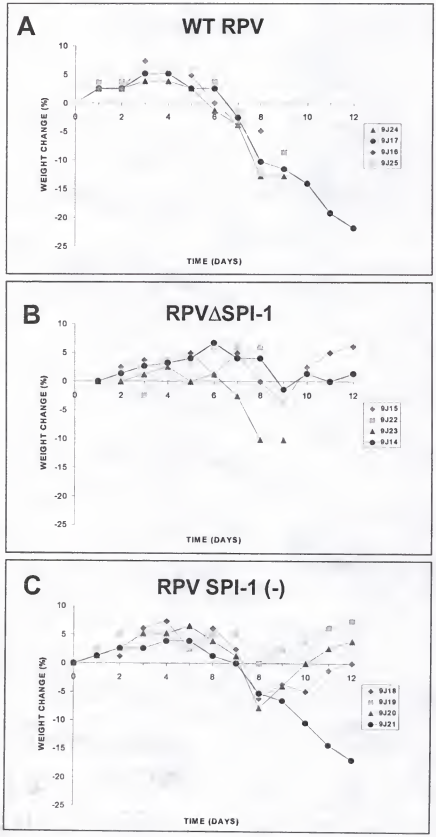
A
WT RPV
WEIGHT CHANGE (%)
TIME (DAYS)
9J24
9J17
9J16
9J25
B
RPVΔSPI-1
WEIGHT CHANGE (%)
TIME (DAYS)
9J15
9J22
9J23
9J14
C
RPV SPI-1 (-)
WEIGHT CHANGE (%)
TIME (DAYS)
9J18
9J19
9J20
9J21

Table 6, rabbits infected with wt RPV displayed severe nasal and occular discharge and all suffered from extreme dyspnea which caused the animals to arch their backs to gasp for air. Moderate to maximal numbers of secondary lesions were present on the animals indicating efficient spread of the virus from the primary inoculation site. Rabbits infected with wt RPV suffered from anorexia which resulted in significant weight loss in each animal in the virus group (Fig. 31). In contrast, many of the rabbits infected with the RPV SPI-1 mutant viruses suffered little or no weight loss over the course of the experiment and when weight loss did occur, the weight change was minimal and transient (Fig. 31). Two animals infected with the SPI-1 mutant viruses lost significantly more weight than other rabbits in the corresponding virus groups. The RPVΔSPI-1 infected rabbit (9J23) lost approximately 10% of its original body weight and was the only animal infected with the virus which died prior to termination of the experiment. Rabbit 9J21, which was infected with RPV SPI-1 (-), suffered anorexia that resulted in the loss of nearly 20% of its original body weight but the animal survived until termination of the experiment on day 12 post-infection.

Three out of four rabbits infected with the wild type virus died prior to termination of the experiment. The surviving wtRPV-infected animal (9J17) had lost over 20% of its original body weight by day 12 post-infection (Fig. 32), exhibited severe disease symptoms (Table 6), and likely would have succumbed to the infection if the experiment had been allowed to continue. Likewise, a single rabbit infected with RPVΔSPI-1 (9J23) suffered a similar pattern of disease over the course of the experiment accompanied by severe nasal and occular discharge, dyspnea, and a large number of secondary lesions, and the animal died on day 9 of the experiment. However, all

remaining animals infected with the RPV SPI-1 mutant viruses displayed a much milder form of disease than the wild type infected animals. In rabbits infected with RPVΔSPI-1 and RPV SPI-1 (-), discharge from the nares and eyes was minimal or absent, and any difficulty breathing was minor.

Although a separate infection was not performed in order to determine histological differences in the inflammatory response caused by infection with the viruses used in this experiment, the primary lesions were examined daily and differences were observed at the gross level (Fig. 32). Each of the primary lesions caused by infection with wt RPV, RPVΔSPI-1 and RPV SPI-1 (-) appeared similar through day 4 post-infection. A white inflammatory cell infiltrate could be seen beneath the surface of the skin surrounding a darkening central region of necrosis in each of the lesions by day 5 post-infection. While no differences were appreciated between the lesions caused by RPVΔSPI-1 and RPV SPI-1 (-) at this time, the lesion formed by wt RPV appeared larger than both mutant virus lesions and was associated with a greater degree of inflammation and necrosis. On day 7, an increased inflammatory infiltrate was observed in the lesions formed by wt RPV and RPVΔSPI-1. However, the wild type lesion was characterized by a massive zone of inflammation surrounding a central dark region of necrosis, whereas the lesion formed by RPVΔSPI-1 appeared to be comprised almost entirely of an inflammatory cell infiltrate. In addition, differences between the lesions formed by the two SPI-1 mutant viruses were appreciated at this time. The RPV SPI-1 (-) lesion was significantly smaller than the lesions caused by the other viruses, and appeared to be localized to a minute region of necrosis at the site of inoculation. Little additional change was observed in the primary lesions formed by either of the two SPI-1 mutant viruses

Figure 32. **Comparison of the primary lesions formed following infection of animals with wt RPV, RPVΔSPI-1 or RPV SPI-1 (-).** Twelve rabbits were separated into three groups of four animals each and were intradermally inoculated with 50 pfu of either wtRPV, RPVΔSPI-1, or RPV SPI (-) as described in the text. A representative primary lesion from each virus group was selected and photographed at days 3, 5, 7, 10, and 12 post-infection as indicated.

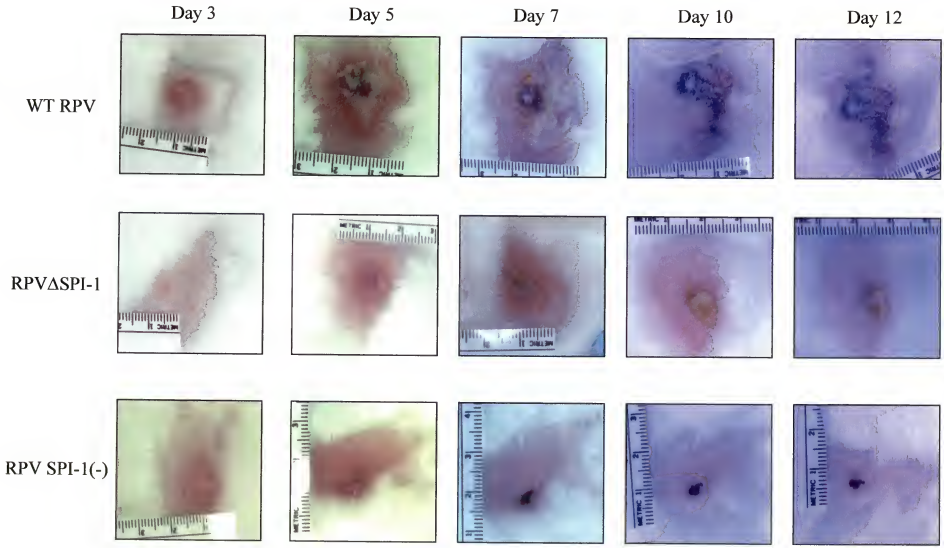
Day 3
Day 5
Day 7
Day 10
Day 12
WT RPV
RPVΔSPI-1
RPV SPI-1(-)

through day 10 post-infection. In contrast, the tissue surrounding the primary site of inoculation with wtRPV continued to undergo necrosis, resulting in bleeding at the site of infection. Upon termination of the experiment on day 12 post-infection, clear differences in the primary lesions caused by each of the viruses were easily appreciated. The wild type lesion exhibited considerable necrosis and oozing and was tender to the touch. The lesion formed by RPVΔSPI-1 was smaller and appeared to be composed almost entirely of an inflammatory cell infiltrate. The RPV SPI-1 (-) lesion was significantly smaller than the other two lesions and no inflammatory infiltrate was noticed. In fact, a scab had formed at the injection site and the infection seemed to be resolving.

Close examination of the results of this experiment suggest that while animals infected with both RPV SPI-1 mutant viruses as a group were attenuated relative to wt RPV, the disease caused by RPV SPI-1 (-) appeared to be even milder than that caused by RPVΔSPI-1. As shown in Table 6, the mean severity scores of rabbits infected with RPV SPI-1 (-) were consistently lower than the RPVΔSPI-1 infected animals. Though animals infected with all of the viruses developed fevers that reached similar maximum temperatures (Fig. 30), while several of the RPVΔSPI-1 infected rabbits exhibited nasal and occular discharge and dyspnea, the vast majority of the rabbits infected with RPV SPI-1 (-) were largely asymptomatic (Table 6). While primary lesions suggest that the damage caused by infection with both RPVΔSPI-1 and RPV SPI-1 (-) was not as extensive as that caused by wt RPV, the RPV SPI-1 (-) lesion was smaller than the RPVΔSPI-1 lesion and less inflammation was seen. In addition, fewer secondary lesions were present on RPV SPI-1 (-) animals than on rabbits in any other infection group including those infected with RPVΔSPI-1. Furthermore, while at least one rabbit from

the wt RPV and RPVΔSPI-1 infection groups died prior to day 12, all animals infected with RPV SPI-1 (-) survived until termination of the experiment. Taken together, these results suggest that at low infectious doses, RPV SPI-1 mutant viruses are attenuated relative to wt RPV in rabbits. Furthermore, it appears that in this animal model RPV SPI-1 (-) causes a more attenuated disease than RPVΔSPI-1.

CHAPTER 8
DISCUSSION OF THE ROLE OF SPI-1 IN INFECTED ANIMALS

Virus Immunomodulatory Proteins. In nature, viruses can cause either acute or persistent infections of their hosts. Virus evasion of the host immune response is important for successful replication in both types of infections, but different elements of the host defense are targeted in each case. Viruses that cause persistent infections must encode factors that allow continued virus replication in the presence of specific anti-viral components of the host immune system. In contrast, viruses that cause acute, systemic infections must avoid the early nonspecific or innate elements of host immunity in order to replicate to the high titers necessary for efficient spread to another susceptible host.

Like other large DNA viruses, poxviruses encode more factors than are strictly necessary for the replication and packaging of progeny virions. Recently, the complete genomic sequences of several chordopoxvirus members have been reported (3,41,246,315). These advances have allowed for the first time the comparison of the total gene arrays encoded by the members of each diverse genera, and have led to the identification of the minimal set of genes which are deemed essential for vertebrate poxvirus replication in tissue culture. In addition, the complete genomes of two entomopoxviruses have recently been sequenced which allow the further delineation of the minimal shared set of genes which are
necessary for replication of both vertebrate and insect poxviruses (2,22). While it is striking to note the impressive array of factors which poxviruses produce to allow

autonomous replication in the host cell cytoplasm, equally remarkable is the vast number of open reading frames which have been conserved over time by the viruses though not strictly essential for replication. Though deletion of many of these "nonessential" virus genes has no effect on virus growth in tissue culture cells, the mutant viruses are often attenuated in their ability to infect and cause disease in animals. In contrast to the "housekeeping" genes shared by poxviruses of both vertebrate and insect hosts, considerable variation exists in the factors encoded by the remainder of the virus genomes across virus subfamilies and genera. Almost certainly, the variation within these regions of the genome arose over time allowing specific adaptation of each virus to its natural host.

Many tactics for countering the host response to infection are shared across virus families. For example, in addition to members of the poxvirus family, human cytomegalovirus, human T-cell leukemia virus type 1 and human immunodeficiency virus (HIV) have each been shown to incorporate host RCA proteins on the surface of progeny virions as a mechanism of complement evasion (226). Members of both the herpesvirus and poxvirus families have been demonstrated to produce cell-associated chemokine receptors as well as secreted cytokine receptors (160). Viral inhibitors of apoptosis have been demonstrated in many viruses, including those belonging to the poxvirus, adenovirus, baculovirus, and herpesvirus families [see references (54,189,277,284) for recent reviews]. However, poxviruses are unique in that they are the only virus family known to encode functional members of the serpin class of serine proteinase inhibitors, indicating a novel form of virus anti-host defense. Genes encoding serpins have been found in members of the orthopoxvirus, leporipoxvirus, avipoxvirus

and suipoxvirus genera. While several of these poxvirus serpins have yet to be characterized, studies on the remaining virus serpins indicate that each protein serves an important function during infection *in vivo*.

Effects of SPI-1 mutation on RPV pathogenesis *in vivo*. During the analysis of spontaneous RPV and CPV mutants which formed white pocks on infected chorioallantoic membranes of embryonated chicken eggs, it was noted that several of the RPV mutants had a reduced host range and were unable to productively infect pig kidney cell lines (75,81,182). Later studies demonstrating that SPI-1 gene expression was necessary for relief of the RPV host range restriction were the first to imply a possible role for the protein as a virulence factor during natural infection (10,36). However, two independent studies revealed no apparent defect in the ability of RPV, CPV or vaccinia SPI-1 null mutants to cause disease in a murine intranasal model of infection (123,281). Still, published reports suggesting a role for RPV SPI-1 in preventing infected cell apoptosis (36) as well as the recent finding that SPI-1 expression is necessary to inhibit granule-mediated lysis of RPV-infected cells by CTL (147) prompted further examination of the function of SPI-1 during animal infections. In this study, the ability of a complete SPI-1 deletion mutant of RPV (RPVΔSPI-1) to cause disease in rabbits relative to wt RPV was examined. Furthermore, because this study is the first to directly demonstrate that SPI-1 has properties consistent with inhibitory serpin activity both *in vitro* and during infection of tissue culture cells, the importance of SPI-1 serpin function during animal infections was also addressed. Studies were performed using RPV viruses bearing mutations in the SPI-1 gene alone, as well as with viruses carrying combined

mutations in both SPI-1 and SPI-2 genes in order to evaluate any additive effects of the serpin mutations.

The first rabbit infection performed in this study revealed no appreciable difference in the ability of the RPV serpin mutants to cause disease in rabbits relative to wild type virus. Rabbits infected with 100 pfu of wt RPV, RPV ΔSPI-1, RPV SPI-1 F322A, RPV ΔSPI-2, RPV SPI-1 (F322A)ΔSPI-2 and RPV ΔSPI-1ΔSPI-2 in both the right and left hind flanks developed similar symptoms, including pyrexia, weight loss, dyspnea, nasal and/or occular discharge, and viremia (Figs. 26 and 27, Table 4). Furthermore, at least one rabbit from each virus group died prior to termination of the experiment on day 14 post-infection, implying that the serpin mutations did not result in any significant virus attenuation relative to wt RPV. Similarly, two previous studies using a mouse intranasal model of infection reported that inactivation of the RPV, CPV or VV SPI-1 gene had no adverse affect on the ability of the mutant viruses to cause disease (123,281). However, the same studies reported conflicting results regarding the effect of SPI-2 inactivation in the viruses. While Thompson and co-workers demonstrated that mutation of the SPI-2 gene in both RPV and CPV resulted in disease attenuation and alteration of pulmonary pathology in infected mice relative to wild type virus, Kettle et al. reported no difference in the disease phenotypes caused by murine infection with either wild type vaccinia virus or a SPI-2 deletion mutant. Surprisingly, in this latest study, the highest mortality was associated with RPVΔSPI-1ΔSPI-2 infection, as all rabbits infected with the virus died on day 8 post-infection. However, these results are in direct contrast with previous unpublished results from our laboratory which demonstrated that RPV SPI-1 and SPI-2 single serpin mutants were mildly attenuated and

did not cause death in infected rabbits and that an RPV SPI-1/SPI-2 double mutant was dramatically attenuated relative to wt RPV and resulted in a largely asymptomatic infection (M. Brooks, R. Stern, and R. Moyer, unpublished results).

It is difficult to reconcile these seemingly conflicting results in the absence of additional experiments. While both studies demonstrating little ((281) or no (123) effect on virus pathogenesis in the presence of serpin mutations were performed in the same inbred strain of Balb/c mice, the current study only examined the ability of RPV SPI-1 and SPI-2 mutants to cause disease in an outbred population of rabbits. Thus, some of the discrepancies may be due to the difference in animal models used. In addition to using different animal models to study the contribution of SPI-1 and SPI-2 to orthopoxvirus virulence, here the viruses were introduced intradermally in two separate injections for a final dose of 200 pfu per animal, while previous work in mice utilized the intranasal route of inoculation to introduce much higher doses of virus (10^2-$10^{7.6}$ pfu/mouse and 10^4-10^6 pfu/mouse, (281) and (123), respectively). It is possible that these differences alone are sufficient to produce the divergent results. Indeed, the route of inoculation utilized has been shown to profoundly affect the outcome of poxvirus infection. For example, intracranial inoculation of mice with a vaccinia mutant lacking expression of the viral secreted IL-1β receptor B15R was shown to result in a 100-fold greater lethal dose 50 (LD_{50}) relative to wild type virus (264). In contrast, a separate study demonstrated that mice intranasally infected with a VV B15R deletion mutant actually displayed an accelerated and significantly more severe disease than wt VV (7). The dramatic variation in the results reported from these two studies have been proposed to stem from the distinct effects of IL-1β action in the brain verses the lungs in the

absence of the viral cytokine receptor. However, the same rabbit strain and inoculation route were shared between the present study and the previous work from Brooks and co-workers (M. Brooks, R. Stern, and R. Moyer, unpublished results), making the differences in these latter two set of experimental results harder to explain. However, the limited number of rabbits used in both experiments and the relatively large number of animals in the current study that died on day 8 post-infection displaying few, if any, signs of poxvirus disease but exhibiting some evidence of a gastrointestinal disorder, which decreased the number of animals infected with each virus that could be evaluated require that further experiments be performed before a model can be proposed.

Because some variation did exist in both the infection methods utilized and the viruses used in the two rabbit experiments exploring the effects of SPI-1 and SPI-2 serpin mutants, an additional experiment was performed as an initial attempt to resolve the discrepancies in the two independently derived sets of results. This final rabbit experiment examined the disease caused by infecting rabbits with 50 pfu of either wt RPV, RPVΔSPI-1 or RPV SPI-1 (-) in a single dose. However, due to time and budgetary constraints, the effects of RPV SPI-2 mutations were not addressed. Surprisingly, the diseases caused by infection with wt RPV and RPVΔSPI-1 were easily discernable when the viruses were introduced at the lower dose in a single injection. Each of the four rabbits infected with the wild type virus exhibited severe rabbitpox disease characterized by pyrexia, dyspnea, nasal and ocular discharge and large numbers of secondary lesions, and three of the four rabbits died from the infection (Figs. 30 and 31, Table 6). In stark contrast, only one rabbit infected with RPVΔSPI-1 exhibited these same severe symptoms resulting in the death of the animal. Instead, the majority of the

RPVΔSPI-1-infected rabbits suffered viremia accompanied by a moderate number of secondary lesions, but any other symptoms of disease were mild. RPV SPI-1 (-) did not result in death of any rabbit infected with the virus. In fact, although the presence of secondary lesions indicated virus spread throughout the body, few RPV SPI-1(-)-infected animals displayed any symptoms of rabbitpox other than fever, resulting in significantly lower symptom severity scores for the animals infected with this virus than in any other group. Thus, it does appear that there are legitimate differences between RPVΔSPI-1 and RPV SPI-1 (-) that cause them to produce somewhat different disease phenotypes in animals. However, additional experiments using a larger number of rabbits need to be performed to determine if these differences represent a genuine and statistically significant variation. Still, while RPV SPI-1 (-) was mildly more attenuated than RPVΔSPI-1 in rabbits, both SPI-1 mutants were notably less virulent than the wild type virus in this experiment suggesting that SPI-1 does contribute to RPV pathogenesis.

Differences in the primary lesions caused by wt RPV and the serpin mutant viruses were easily appreciated during both rabbit infections performed in this study. In addition to the rabbits infected with wt RPV, RPV ΔSPI-1, RPVΔSPI-2, RPV SPI-1 F322A, RPV SPI-1 (F322A)ΔSPI-2 and RPV ΔSPI-1ΔSPI-2 in order to study the effects of serpin mutations of the ability of RPV to cause gross disease, during the initial rabbit experiment, a second rabbit group was infected in parallel with the same viruses and primary lesions were examined following isolation early after infection in order to observe any differences in the early host response to infection. Remarkably, significant variation was seen in the primary lesions caused by the different viruses at 4 days post-infection even though rabbits in the parallel infection group were only just beginning to

show signs of illness. Primary lesions isolated from rabbits infected with the RPV isolates bearing single serpin mutations consistently exhibited significantly greater inflammation than the corresponding lesion from the wt RPV-infected rabbit, implying that both SPI-1 and SPI-2 each have the capability to inhibit inflammation either directly or indirectly (Fig. 28, Table 5). In addition, although tissue was not processed for histology in the second rabbit experiment, primary lesions caused by infection with both RPVΔSPI-1 and RPV SPI-1 (-) were strikingly different at the gross level than the wt RPV lesion beginning at day 5 post-infection (Fig. 32). While wt RPV caused a progressive necrosis in the infected tissue which ultimately resulted in bleeding and oozing from the injection site by day 12, primary lesions caused by infection by either of the RPV SPI-1 null mutants changed little if at all after day 5 post-infection. Both lesions were notably smaller than the corresponding wt RPV lesion and displayed significantly less necrosis. In fact, lesions formed following RPVΔSPI-1 infection invariably exhibited what appeared to be a massive inflammatory response, as judged by the presence of a yellowish-white infiltrate beneath the skin at the primary inoculation site. Although assays to directly examine the histopathology of primary lesions harvested from the rabbits were not performed in this second experiment, these findings are consistent with the histology results from the initial rabbit infection which demonstrated severe inflammation at the site of injection with 100 pfu of RPVΔSPI-1. Taken together, the preliminary analysis of the primary lesions both at the gross and histological level suggest that SPI-1 expression is necessary for inhibition of the host inflammatory response to RPV infection. These results are in agreement with previous studies demonstrating that inactivation of RPV SPI-1 resulted in the formation of white pocks on

infected CAMs which exhibited increased inflammation relative to the red, hemorrhagic pocks formed by wt RPV (10).

The fact that the primary lesions formed following infection with RPVΔSPI-1 and RPV SPI-1 F322A were nearly identical strongly suggests that SPI-1 serpin activity is necessary for SPI-1 function during animal infection. The same phenylalanine to alanine mutation at residue 322 of the SPI-1 RSL which abolished the ability of SPI-1 to complex with cathepsin G *in vitro* and was additionally shown to cause the same reduced host range as a SPI-1 deletion mutant when expressed during RPV infection of tissue culture cells somehow rendered RPV SPI-1 (F322A) unable to inhibit the massive inflammatory response at the primary site of infection. Extrapolation of these results leads to a model in which the ability of SPI-1 to function as a proteinase inhibitor is necessary for inhibition of inflammation. Taken together with earlier results from this study indicating that SPI-1 preferentially targets proteinases of the chymotrypsin family, these findings further imply that SPI-1 inhibition of a cathepsin G-like proteinase may be necessary for preventing a major inflammatory cell influx at the site of infection. Given that SPI-1 expression is necessary for inhibition of CTL granule-mediated cytolysis of RPV-infected cells (147), perhaps the target proteinase of SPI-1 is an essential component of this cell death pathway. Furthermore, since SPI-1 has been shown to form inhibitory complexes with the major inflammatory mediator cathepsin G, perhaps this enzyme itself is the serpin target in infected animals. SPI-1 expelled following infected cell lysis may be able to inhibit extracellular cathepsin G released from inflammatory cells and thus inhibit the enzyme from acting as a chemoattractant and inducing further inflammation and effector cell activation. In contrast, SPI-1 may act in a manner analogous to PI-6 and form

inhibitory complexes with intracellular cathepsin G in infected cells of the monocyte/macrophage lineage as an alternate tactic for cathepsin G inhibition. Because SPI-1 has been demonstrated to mediate RPV host range in tissue culture through a process dependent on SPI-1 serpin activity, it is possible that inhibition of an intracellular proteinase is necessary for the productive infection of certain cells during infection of animal hosts. Several myxoma virus proteins necessary for virus host range in tissue culture have also been shown to be essential for infection of lymphocytes during animal infections. Mutation of these leporipoxvirus proteins results in virus disease attenuation, accompanied by increased levels of inflammation and apoptosis (see reference (287) for review). During animal infection with RPV mutants lacking serpin activity, infection of lymphocytes or other related cells may be abortive and result in apoptosis or a caspase-independent form of cell death accompanied by cell lysis and the induction of further inflammation.

In addition to the finding that mutation of the single SPI-1 or SPI-2 genes resulted in greater inflammation within the primary lesions caused by infection with RPVΔSPI-1, RPVΔSPI-2 and RPV SPI-1 F322A, infection with RPV ΔSPI-1ΔSPI-2 and RPV SPI-1 (F322A)ΔSPI-2 resulted in considerably more tissue destruction at the primary injection site than was observed following infection with any other virus. These data suggest that not only do SPI-1 and SPI-2 contribute to RPV inhibition of inflammation, but that the two serpin proteins do not have overlapping functions. These data are consistent with a previous study demonstrating the importance of expression of both proteins to completely prevent CTL-mediated lysis of RPV-infected cells (147). While RPV SPI-2 was necessary for the inhibition of Fas-mediated apoptosis directed by CTL in many cell

lines, in alternate target cells, the expression of both SPI-1 and SPI-2 was necessary to prevent cytolysis triggered by engagement of the Fas receptor. In contrast, in addition to SPI-2, SPI-1 was consistently shown to be necessary for inhibition of target cell death mediated by the CTL granule-specific pathway (147).

Possible synergistic function of SPI-1 and SPI-2 during infection *in vivo*. It has been well established that SPI-2/crmA serves to inhibit the inflammatory response during infection of the chorioallontoic membrane of embryonated chicken eggs (209) which at least in part is due to the ability of the serpin to inhibit interleukin-1β converting enzyme (ICE/caspase 1) (217). By inhibiting ICE, SPI-2/crmA has been shown to prevent activation of the pro-inflammatory cytokine IL-1β (217) and likely IL-18 as well(85) and thus helps prevent inflammation to the site of virus infection. However, in addition to this study, a previous report demonstrated no decrease in orthopoxvirus virulence following inactivation of the SPI-2 gene (123). Thus, while SPI-2 clearly has biological activity *in vivo*, its expression is not essential for poxvirus pathogenesis. Undoubtedly this is due to the plethora of poxvirus proteins capable of inhibiting the host inflammatory response to infection even in the absence of SPI-2. Furthermore, a previous study has reported that RPV SPI-1 mutants give rise to white inflammatory pocks following infection of the CAM (10), an observation that is supported by results of this study demonstrating an increased inflammatory response within the primary lesions caused by RPV SPI-1 mutants. As noted above, two independent studies examining the effects of SPI-1 inactivation on RPV, CPV or VV intranasal infection of mice found no difference in disease severity relative to wild type virus (123,281). However, these previous studies were each performed using much higher doses than were used in either

the current study or the one performed by Brooks and co-workers. Here, while no differences in disease severity were appreciated following rabbit infection with 200 pfu of wt RPV, RPVΔSPI-1, RPVΔSPI-2, RPV SPI-1 F322A, RPV SPI-1 (F322A)ΔSPI-2 or RPV ΔSPI-1ΔSPI-2, when rabbits were infected with 50 pfu of either wt RPV, RPV ΔSPI-1 or RPV SPI-1 (-), the SPI-1 mutants were shown to be significantly attenuated relative to wt RPV, consistent with previous observations from our laboratory (M. Brooks, R. Stern and R. Moyer, unpublished results). When the results of each of these studies are considered in sum, together with evidence that both SPI-1 and SPI-2 together function to inhibit CTL-mediated cytolysis of RPV-infected cells (147), a tentative model can be proposed.

When rabbits are infected intradermally using low doses introduced at a single site, the naïve immune system of the infected rabbit is able to mount an early immune response to the RPV serpin mutants that is able to effectively inhibit mutant virus pathogenesis. Mutation of SPI-1 and SPI-2 individually affects the ability of RPV to inhibit inflammation, thus the immune system is able to better recognize and eliminate cells infected with these mutants. However, with its vast array of immunomodulatory proteins, wt RPV introduced at the same infectious dose is able to overcome the early immune response, in large part by inhibiting the activation of pro-inflammatory cytokines, and causes a progressive disease associated with high mortality. Still, when these same viruses are given at higher doses introduced at two different injection sites, the RPV single serpin mutants are able to cause a disease similar to wild type virus. This may occur simply because the host immune response is unable to protect itself against the high levels of alternate immunomodulatory proteins produced during infection with the

increased infectious doses of mutant virus. While the observation that animals infected with 200 pfu of both of the RPV SPI-1/SPI-2 double mutants suffered symptoms at least as severe as those exhibited by wt RPV and the RPV single serpin mutants was initially viewed as an artifact due to the presence of an undiagnosed gastrointestinal disorder in the infected rabbits, it is possible that these results reflect a genuine host response to infection with high doses of these viruses. Studies have shown that intranasal infection of mice with a vaccinia variant unable to produce the B15 R secreted IL-1β receptor was associated with an accelerated disease and more severe symptoms than that caused by wild type infection (7). This phenomenon was proposed to result from the caustic systemic effects of IL-1β expression at the site of infection in the absence of the viral cytokine receptor. Similarly, the absence of SPI-2 inhibition of the ICE-dependent activation of IL-1β during infection with the RPV SPI-2 mutant may have resulted in similar cytokine-mediated tissue damage, which was further exacerbated when SPI-1, an additional inflammation antagonist, was also inactivated. Furthermore, since both SPI-1 and SPI-2 appear to be necessary to relieve both pathways of target cell cytolysis directed by CTL, cell infection with RPV ΔSPI-1ΔSPI-2 or RPV SPI-1 (F322A)ΔSPI-2 which lack expression of both serpins almost certainly resulted in significant CTL-mediated damage. While apoptosis is a form of cell death often associated with causing little damage to surrounding cells, apoptosis of cells of the monocyte/macrophage lineage is uniquely pro-inflammatory (233). If SPI-1 is necessary to allow productive infection of these cell types, infection with any RPV mutant lacking SPI-1 serpin activity may result in an abortive cell death analogous to that seen during infection of restrictive cell lines in this study. Furthermore, while SPI-2 inactivation results in the processing of IL-1β to its

active, pro-inflammatory form and mutation of both SPI-1 and SPI-2 leads to effective CTL-mediated lysis of infected cells, if SPI-1 mutations lead to abortive infection of monocytes/macrophages accompanied by apoptosis, a further stimulus for inflammation would be present. The significant inflammatory response thus targeted to the primary site of infection with RPV SPI-1/SPI-2 double mutants would be expected to cause extensive damage to lesion tissue. Consistent with this model, evidence of massive tissue destruction and hydropic degeneration, a form of cell damage often associated with apoptotic cell death, was observed in the primary lesions formed following infection with both double gene mutants which was judged to be significantly greater than that seen in lesions formed by any other virus tested. Cytokines released during inflammation with these viruses could have the potential to cause an accelerated disease phenotype associated with increased symptom severity, shock-like symptoms, and increased mortality. The high mortality rate seen in animals infected with RPVΔSPI-1ΔSPI-2, diarrhea, and the rapid drop in body temperature experienced by the rabbits just prior to their death are all consistent with cytokine-induced septic shock. While this model is an attractive one, future detailed studies will need to be performed to determine whether it is correct.

Conclusions. Although additional experiments must be performed in order to determine the validity and statistical significance of results reported here, the preliminary data suggests that SPI-1 expression does affect RPV pathogenesis. While at high doses, RPV is able to overcome the host immune response triggered in the absence of SPI-1 to cause virulent disease, when fewer infectious particles are introduced into an infected animal, SPI-1 expression appears to be necessary for productive infection. At both high

and low doses of virus, SPI-1 expression serves to inhibit the host inflammatory response, consistent with previous observations using the CAM animal model of poxvirus pathogenesis (10). Furthermore, this study is the first to show that SPI-1 serpin activity is essential for its role in this regard, indicating that SPI-1 inhibition of a chymotrypsin-like proteinase is likely necessary to inhibit inflammation. While at high doses, rabbit infection with high doses of RPV strains bearing single mutations in either SPI-1 or SPI-2 has no effect on virulence relative to wt RPV, infection with RPV SPI-1/SPI-2 double mutants appears to result in an accelerated disease phenotype, strongly suggesting synergism between the action of both serpins *in vivo*. While much is known regarding the function of SPI-2 in inhibiting inflammation *in vivo*, further analysis should allow determination of the exact role of SPI-1 in preventing the host innate response to poxvirus infection. Parallel studies to determine the function of SPI-1 in mediating RPV host range and productive infection in tissue culture cells and the identification of potential target proteinases through the study of restrictive cell lines and the use of *in vitro* bandshift assays should aid significantly, in this regard.

CHAPTER 9
CONCLUDING REMARKS

Poxviruses represent a large and genetically complex family of viruses which infect animal and insect hosts. Over time, some poxviruses have evolved to exist in symbiosis with their natural hosts, causing persistent infections in the presence of minimal cellular immune recognition. This type of nonpathogenic relationship is best exemplified by myxoma virus infection of North and South American rabbits. However, the vast majority of members of this virus family cause acute, systemic diseases associated with high mortality. Variola virus was responsible for the strictly human disease known as smallpox which during its zenith was associated with mortality rates of 20% to 30%. Detailed analysis of poxvirus replication has provided us with the techniques necessary for the worldwide eradication of smallpox, but has also allowed the realization that poxvirus vectors may someday allow the effective introduction and expression of foreign genes within mammalian cells as a method of gene therapy for human disease. The study of the vast array of immunomodulatory proteins expressed by members of this virus family has further enabled the analysis of the complex interplay between the infecting virus and the host immune system, and has provided effective tools for the examination of complicated intracellular processes such as apoptosis.

This study provides a detailed characterization of the RPV SPI-1 protein. The gene encoding SPI-1 is shared among all members of the orthopoxvirus genus, including variola virus, the causative agent of smallpox. The strict conservation of SPI-1 over time in each of these viruses is a strong indication that expression of the protein provides the viruses with a selective advantage during natural infection. This study is the first to provide evidence that SPI-1 has the properties of an inhibitory serine proteinase inhibitor which appears to preferentially target enzymes of the chymotrypsin family. The serpin activity of SPI-1 was shown to be essential for the complete host range of RPV, as well as for the inhibition of the early inflammatory response during infection of rabbit hosts. Future experiments designed to identify the natural proteinase target of SPI-1 during will help to further define the role of the serpin during infection, and may provide valuable insight into methods used by the virus and the host to promote and prevent disease, respectively.

REFERENCE LIST

1. **Abbas, A.K., A.H. Lichtman, and J.S. Pober**. 1994. The Complement System, pp. 293-316. In Cellular and Molecular Immunology, W.B. Saunders Company, Philadelphia, PA.

2. **Afonso, C.L., E.R. Tulman, Z. Lu, E. Oma, G.F. Kutish, and D.L. Rock**. 1999. The genome of Melanoplus sanguinipes entomopoxvirus. J.Virol. **73**:533-552.

3. **Afonso, C.L., E.R. Tulman, Z. Lu, L. Zsak, G.F. Kutish, and D.L. Rock**. 2000. The genome of fowlpox virus. J Virol **74**:3815-3831.

4. **Ahn, B.Y., P.D. Gershon, E.V. Jones, and B. Moss**. 1990. Identification of rpo30, a vaccinia virus RNA polymerase gene with structural similarity to a eucaryotic transcription elongation factor. Mol.Cell Biol. **10**:5433-5441.

5. **Ahn, B.Y., P.D. Gershon, and B. Moss**. 1994. RNA polymerase-associated protein Rap94 confers promoter specificity for initiating transcription of vaccinia virus early stage genes. J.Biol.Chem. **269**:7552-7557.

6. **Ahn, B.Y., and B. Moss**. 1989. Capped poly(A) leaders of variable lengths at the 5' ends of vaccinia virus late mRNAs. J.Virol. **63**:226-232.

7. **Alcami, A., and G.L. Smith**. 1992. A soluble receptor for interleukin-1β encoded by vaccinia virus: A novel mechanism of virus modulation of the host response to infection. Cell **71**:153-167.

8. **Alcami, A., and G.L. Smith**. 1995. Cytokine receptors encoded by poxviruses: a lesson in cytokine biology. Immunol.Today **16**:474-478.

9. **Alcami, A., and G.L. Smith**. 1996. A mechanism for the inhibition of fever by a virus. Proc.Natl.Acad.Sci.U.S.A. **93**:11029-11034.

10. **Ali, A.N., P.C. Turner, M.A. Brooks, and R.W. Moyer**. 1994. The SPI-1 gene of rabbitpox virus determines host range and is required for hemorrhagic pock formation. Virology **202**:306-314.

11. **Allen, A.M., G.L. Clarke, J.R. Ganaway, A. Lock, and R.M. Werner**. 1981. Pathology and diagnosis of mousepox. Lab.Anim.Sci. **31**:599-608.

12. **Arif, B.M., and E. Kurstak**. 1991. The Entomopoxviruses, pp. 175-195. In E. Kurstak (ed.), Viruses of Invertebrates. Marcel Dekker, Inc., New York.

13. **Atkinson, E.A., M. Barry, A.J. Darmon, I. Shostak, P.C. Turner, R.W. Moyer, and R.C. Bleackley**. 1998. Cytotoxic T lymphocyte-assisted suicide - Caspase 3 activation is primarily the result of the direct action of granzyme B. J.Biol.Chem. **273**:21261-21266.

14. **Baggiolini, M., U. Bretz, B. Dewald, and M.E. Feigenson**. 1978. The polymorphonuclear leukocyte. Agents Actions **8**:3-10.

15. **Baici, A., M. Knopfel, and K. Fehr**. 1982. Cleavage of the four human IgG subclasses with cathepsin G. Scand.J Immunol **16**:487-498.

16. **Baldick, C.J., Jr., and B. Moss** . 1993. Characterization and temporal regulation of mRNAs encoded by vaccinia virus intermediate-stage genes. J.Virol. **67**:3515-3527.

17. **Baroudy, B.M., S. Venkatesan, and B. Moss**. 1982. Incompletely base-paired flip-flop terminal loops link the two DNA strands of the vaccinia virus genome into one uninterrupted polynucleotide chain. Cell **28**:315-324.

18. **Barrett, A.J.** 1981. Cathepsin G. Methods Enzymol. **80 Pt C:561-5**:561-565.

19. **Barry, M., J.A. Heibein, M.J. Pinkoski, S.F. Lee, R.W. Moyer, D.R. Green, and R.C. Bleackley**. 2000. Granzyme B short-circuits the need for caspase 8 activity during granule-mediated cytotoxic T-lymphocyte killing by directly cleaving Bid. Mol.Cell Biol **20**:3781-3794.

20. **Barry, M., S. Hnatiuk, K. Mossman, S.F. Lee, L. Boshkov, and G. McFadden**. 1997. The myxoma virus M-T4 gene encodes a novel RDEL-containing protein that is retained within the endoplasmic reticulum and is important for the productive infection of lymphocytes. Virology **239**:360-377.

21. **Barry, M., and G. McFadden**. 1998. Apoptosis regulators from DNA viruses. Current Opinion In Immunology **10**:422-430.

22. **Bawden, A.L., K.J. Glassberg, J. Diggans, R. Shaw, W. Farmerie, and R.W. Moyer**. 2000. Complete genomic sequence of the Amsacta moorei entomopoxvirus: analysis and comparison with other poxviruses. Virology **274**:120-139.

23. **Beattie, E., K.L. Denzler, J. Tartaglia, M.E. Perkus, E. Paoletti, and B.L. Jacobs**. 1995. Reversal of the interferon-sensitive phenotype of a vaccinia virus lacking E3L by expression of the reovirus S4 gene. J.Virol. **69**:499-505.

24. **Beattie, E., E.B. Kauffman, H. Martinez, M.E. Perkus, B.L. Jacobs, E. Paoletti, and J. Tartaglia**. 1996. Host-range restriction of vaccinia virus E3L-specific deletion mutants. Virus Genes **12**:89-94.

25. **Beattie, E., J. Tartaglia, and E. Paoletti**. 1991. Vaccinia virus-encoded eIF-2 alpha homolog abrogates the antiviral effect of interferon. Virology **183**:419-422.

26. **Bedson, H.S., and M.J. Duckworth**. 1963. Rabbit Pox: An experimental study of the pathways of infection in rabbits. J.Pathol.Bacteriol. **85**:1-20.

27. **Bertholet, C., P. Stocco, E. Van Meir, and R. Wittek**. 1986. Functional analysis of the 5' flanking sequence of a vaccinia virus late gene. EMBO J. **5**:1951-1957.

28. **Bertholet, C., E. Van Meir, ten Heggeler Bordier.B., and R. Wittek**. 1987. Vaccinia virus produces late mRNAs by discontinuous synthesis. Cell **50**:153-162.

29. **Bertin, J., R.C. Armstrong, S. Ottilie, D.A. Martin, Y. Wang, S. Banks, G.H. Wang, T.G. Senkevich, E.S. Alnemri, B. Moss, M.J. Lenardo, K.J. Tomaselli, and J.I. Cohen**. 1997. Death effector domain-containing herpesvirus and poxvirus proteins inhibit both Fas- and TNFR1-induced apoptosis. Proc.Natl.Acad.Sci.U.S.A. **94**:1172-1176.

30. **Best, S.M., and P.J. Kerr**. 2000. Coevolution of host and virus: the pathogenesis of virulent and attenuated strains of myxoma virus in resistant and susceptible European rabbits. Virology **267**:36-48.

31. **Bloom, D.C., R. Stern, M. Duke, D. Smith, and R.W. Moyer**. 1993. A revised HindIII map and sequence analysis of a large 'left- hand' non-essential region of the rabbit poxvirus genome. Virus Res. **28**:125-140.

32. **Bodo, G., P. Palese, I. Horak, J. Hilfenhaus, W. Siegert, and C. Jungwirth**. 1970. Interferon action: effect on the formation of poxvirus specific polysomes and viral RNA. Z.Naturforsch.[B] **25**:1164-1170.

33. **Bottomley, S.P., and S.R. Stone** . 1998. Protein engineering of chimeric Serpins: an investigation into effects of the serpin scaffold and reactive centre loop length. Protein Engineering **11**:1243-1247.

34. **Boudreau, N., C.J. Sympson, Z. Werb, and M.J. Bissell**. 1995. Suppression of ICE and apoptosis in mammary epithelial cells by extracellular matrix. Science **267**:891-893.

35. **Bradford, M.M.** 1976. A rapid and sensitive method for the quantitation of microgram quantities of protein utilizing the principle of protein-dye binding. Anal.Biochem. **72**:248-254.

36. **Brooks, M.A., A.N. Ali, P.C. Turner, and R.W. Moyer**. 1995. A rabbitpox virus serpin gene controls host range by inhibiting apoptosis in restrictive cells. J.Virol. **12**:7688-7698.

37. **Bukowski, J.F., B.A. Woda, S. Habu, K. Okumura, and R.M. Welsh**. 1983. Natural killer cell depletion enhances virus synthesis and virus-induced hepatitis in vivo. J Immunol **131**:1531-1538.

38. **Buller, R.M., and G.J. Palumbo**. 1991. Poxvirus pathogenesis. Microbiol.Rev. **55**:80-122.

39. **Bump, N.J., M. Hackett, M. Hugunin, S. Seshagiri, K. Brady, P. Chen, C. Ferenz, S. Franklin, T. Ghayur, and P. Li**. 1995. Inhibition of ICE family proteases by baculovirus antiapoptotic protein p35. Science **269**:1885-1888.

40. **Bump, N.J., M. Hackett, M. Hugunin, S. Seshagriri, K. Brady, P. Chen, C. Ferenz, S. Franklin, T. Ghayur, L.P.P. Licari, J. Mankovich, L. Shi, A.H. Greenberg, L.K. Miller, and W.W. Wong**. 1995. Inhibition of the ICE family proteases by baculovirus antiapoptotic protein p35. Science **269**:1885-1888.

41. **Cameron, C., S. Hota-Mitchell, L. Chen, J. Barrett, J.X. Cao, C. Macaulay, D. Willer, D. Evans, and G. McFadden**. 1999. The complete DNA sequence of myxoma virus. Virology **264**:298-318.

42. **Cao, J.X., P.D. Gershon, and D.N. Black**. 1995. Sequence analysis of HindIII Q2 fragment of capripoxvirus reveals a putative gene encoding a G-protein-coupled chemokine receptor homologue. Virology **209**:207-212.

43. **Carrell, R.W., and B. Gooptu**. 1998. Conformational changes and disease - serpins, prions and Alzheimer's. Current Opinion In Structural Biology **8**:799-809.

44. **Carrell, R.W., P.A. Pemberton, and D.R. Boswell**. 1987. The serpins: evolution and adaptation in a family of protease inhibitors. Cold Spring Harb.Symp.Quant.Biol. **52**:527-535.

45. **Chang, A., and D.H. Metz**. 1976. Further investigations on the mode of entry of vaccinia virus into cells. J.Gen.Virol. **32**:275-282.

46. **Chang, H.-W., J.C. Watson, and B.L. Jacobs**. 1992. The E3L gene of vaccinia virus encodes an inhibitor of the interferon-induced, double-stranded RNA-dependent protein kinase. Proc.Natl.Acad.Sci.U.S.A. **89**:4825-4829.

47. **Chapes, S.K., and W.A. Tompkins** . 1979. Cytotoxic macrophages induced in hamsters by vaccinia virus: selective cytotoxicity for virus-infected targets by macrophages collected late after immunization. J.Immunol. **123**:303-310.

48. **Chertov, O., H. Ueda, L.L. Xu, K. Tani, W.J. Murphy, J.M. Wang, O.M. Howard, T.J. Sayers, and J.J. Oppenheim**. 1997. Identification of

human neutrophil-derived cathepsin G and azurocidin/CAP37 as chemoattractants for mononuclear cells and neutrophils. J Exp Med **186**:739-747.

49. **Chua, T.P., C.E. Smith, R.W. Reith, and J.D. Williamson**. 1990. Inflammatory responses and the generation of chemoattractant activity in cowpox virus-infected tissues. Immunology **69**:202-208.

50. **Cichy, J., J. Potempa, R.K. Chawla, and J. Travis**. 1995. Regulation of alpha 1-antichymotrypsin synthesis in cells of epithelial origin. FEBS Lett. **359**:262-266.

51. **Clawson, G.A., L.L. Norbeck, C.L. Hatem, C. Rhodes, P. Amiri, J.H. McKerrow, S.R. Patierno, and G. Fiskum**. 1992. Ca(2+)-regulated serine protease associated with the nuclear scaffold. Cell Growth Differ. **3**:827-838.

52. **Colamonici, O.R., P. Domanski, S.M. Sweitzer, A. Larner, and R.M. Buller**. 1995. Vaccinia virus B18R gene encodes a type I interferon-binding protein that blocks interferon alpha transmembrane signaling. J.Biol.Chem. **270**:15974-15978.

53. **Cudmore, S., P. Cossart, G. Griffiths, and M. Way**. 1995. Actin-based motility of vaccinia virus. Nature **378**:636-638.

54. **Cuff, S., and J. Ruby**. 1996. Evasion of apoptosis by DNA viruses. Immunol.Cell Biol. **74**:527-537.

55. **Dales, S., and E.H. Mosbach**. 1968. Vaccinia as a model for membrane biogenesis. Virology **35**:564-583.

56. **Dales, S., and L. Siminovitch**. 1961. The development of vaccinia virus in Earle's L strain cells as examined by electron microscopy. J.Biophys.Biochem.Cytol. **10**:475-503.

57. **Damon, I., P.M. Murphy, and B. Moss**. 1998. Broad spectrum chemokine antagonistic activity of a human poxvirus chemokine homolog. Proc.Natl.Acad.Sci.U.S.A **95**:6403-6407.

58. **Darmon, A.J., D.W. Nicholson, and R.C. Bleackley**. 1996. Activation of the apoptotic protease CPP32 by cytotoxic T-cell derived granzyme B. Nature **377**:446-448.

59. **Davison, A.J., and B. Moss**. 1989a. Structure of vaccinia virus early promoters. J.Mol.Biol. **210**:749-769.

60. **Davison, A.J., and B. Moss**. 1989b. Structure of vaccinia virus late promoters. J.Mol.Biol. **210**:771-784.

61. **Deas, O., C. Dumont, M. MacFarlane, M. Rouleau, C. Hebib, F. Harper, F. Hirsch, B. Charpentier, G.M. Cohen, and A. Senik**. 1998. Caspase-independent cell death induced by anti-CD2 or staurosporine in activated human peripheral T lymphocytes. J Immunol **161**:3375-3383.

62. **Ding, A.H., C.F. Nathan, and D.J. Stuehr**. 1988. Release of reactive nitrogen intermediates and reactive oxygen intermediates from mouse peritoneal macrophages. J.Immunol. **141**:2407-2412.

63. **Dobbelstein, M., and T. Shenk**. 1996. Protection against apoptosis by the vaccinia virus SPI-2 (B13R) gene product. J.Virol. **70**:6479-6485.

64. **Doms, R.W., R. Blumenthal, and B. Moss**. 1990. Fusion of intra- and extracellular forms of vaccinia virus with the cell membrane. J.Virol. **64**:4884-4892.

65. **Douglas, S.R.** 1930. A study of vaccinal immunity in rabbits by means of in vitro methods. Br.J.Exp.Pathol. **11**:96-111.

66. **Dubochet, J., M. Adrian, K. Richter, J. Garces, and R. Wittek**. 1994. Structure of intracellular mature vaccinia virus observed by cryoelectron microscopy. J.Virol. **68**:1935-1941.

67. **Dvorak, H.F., and M.S. Hirsch**. 1971. Role of basophilic leukocytes in cellular immunity to vaccinia virus infection. J.Immunol. **107**:1576-1582.

68. **Epstein, W.L.** 1992. Molluscum contagiosum. Semin.Dermatol. **11**:184-189.

69. **Everett, H., M. Barry, S.F. Lee, X. Sun, K. Graham, J. Stone, R.C. Bleackley, and G. McFadden**. 2000. M11L: a novel mitochondria-localized protein of myxoma virus that blocks apoptosis of infected leukocytes. J Exp Med **191**:1487-1498.

70. **Farrar, M.A., and R.D. Schreiber**. 1993. The molecular cell biology of interferon-gamma and its receptor. Annu.Rev.Immunol. **11**:571-611.

71. **Fenner, F.** 1948. The clinical features of mouse-pox (infectious ectromelia of mice) and the pathogenesis of the disease. J.Pathol.Bacteriol. **60**:529-552.

72. **Fenner, F.** 1977. The eradication of smallpox. Prog.Med.Virol. **23**:1-21.

73. **Fenner, F.** 1990. Wallace P. Rowe lecture. Poxviruses of laboratory animals. Lab.Anim.Sci. **40**:469-480.

74. **Fenner, F.** 1996. Poxviruses, p. 2673-2702. In B.N. Fields, D.M. Knipe, and P.M. Howley (eds.), Fields Virology. Lippincott-Raven, Philadelphia.

75. **Fenner, F., and J.F. Sambrook**. 1966. Conditional lethal mutants of rabbitpox virus. II. Mutants (p) that fail to multiply in PK-2a cells. Virology **28**:600-609.

76. **Fenner, F., R. Wittek, and K.R. Dumbell**. 1989. The Orthopoxviruses. Academic Press, New York.

77. **Fenner, F., and G.M. Woodroffe**. 1953. The pathogenesis of infectious myxomatosis: The mechanism of infection and the immunological response in the European rabbit (ORYCTOLAGUS CUNICULUS). Br.J.Exp.Pathol. **34**:400-411.

78. **Gagliardini, V., P.A. Fernandez, R.K. Lee, H.C. Drexler, R.J. Rotello, M.C. Fishman, and J. Yuan**. 1994. Prevention of vertebrate neuronal death by the crmA gene [see comments] [published erratum appears in Science 1994 Jun 3; 264(5164):1388]. Science **263**:826-828.

79. **Gallin, J.I., B.M. Goldstein, and R. Snyderman**. 1988. Inflammation: basic principles and clinical correlates. Raven Press, New York.

80. **Garon, C.F., E. Barbosa, and B. Moss**. 1978. Visualization of an inverted terminal repetition in vaccinia virus DNA. Proc.Natl.Acad.Sci.U.S.A. **75**:4863-4867.

81. **Gemmell, A., and F. Fenner**. 1960. Genetic studies with mammalian poxviruses. III. White (u) mutants of rabbitpox virus. Virology **11**:219-235.

82. **Gershon, P.D., B.Y. Ahn, M. Garfield, and B. Moss**. 1991. Poly(A) polymerase and a dissociable polyadenylation stimulatory factor encoded by vaccinia virus. Cell **66** :1269-1278.

83. **Geshelin, P., and K.I. Berns**. 1974. Characterization and localization of the naturally occurring cross-links in vaccinia virus DNA. J.Mol.Biol. **88**:785-796.

84. **Gettins, P., P.A. Patston, and M. Schapira**. 1993. The role of conformational change in serpin structure and function. Bioessays **15**:461-467.

85. **Ghayur, T., S. Banerjee, M. Hugunin, D. Butler, L. Herzog, A. Carter, L. Quintal, L. Sekut, R. Talanian, M. Paskind, W. Wong, R. Kamen, D. Tracey, and H. Allen**. 1997. Caspase-1 processes IFN-gamma-inducing factor and regulates LPS- induced IFN-gamma production. Nature **386**:619-623.

86. **Glasgow, L.A.** 1965. Leukocytes and interferon in the host response to viral infections. J Exp Med **121**:1001-1007.

87. **Glasgow, L.A., and K. Habel**. 1962. The role of interferon in vaccinia virus infection of mouse embryo tissue culture. J Exp Med **115**:503-512.

88. **Glasgow, L.A., and K. Habel**. 1963. Interferon production by mouse leukocytes in vitro and in vivo. J Exp Med **117**:149-161.

89. **Goebel, S.J., G.P. Johnson, M.E. Perkus, S.W. Davis, J.P. Winslow, and E. Paoletti**. 1990. The complete DNA sequence of vaccinia virus. Virology **179**:247-66, 517-63.

90. **Gordon, M.H.** 1925. Studies of the viruses of vaccinia and variola. Med.Res.Counc.Spec.Rep.Ser. **98**:1-135.

91. **Gottlieb, S.L., and P.L. Myskowski**. 1994. Molluscum contagiosum. [Review]. Int J Dermatol. **33**:453-461.

92. **Graham, K.A., A.S. Lalani, J.L. Macen, T.L. Ness, M. Barry, L.Y. Liu, A. Lucas, I. Clark-Lewis, R.W. Moyer, and G. McFadden**. 1997. The T1/35kDa family of poxvirus secreted proteins bind chemokines and modulate leukocyte influx into virus infected tissues. Virology **229**:12-24.

93. **Graham, K.A., A. Opgenorth, C. Upton, and G. McFadden**. 1992. Myxoma virus M11L ORF encodes a protein for which cell surface localization is critical in manifestation of viral virulence. Virology **191**:112-124.

94. **Green, D.R., and J.C. Reed**. 1998. Mitochondria and apoptosis. Science **281**:1309-1312.

95. **Greene, H.** 1933. A pandemic of rabbit-pox. Proc.Soc.Exp.Biol.Med. **30**:892-894.

96. **Greene, H.** 1934a. Rabbit pox I. Clinical manifestations and course of disease. J Exp Med **60**:427-439.

97. **Greene, H.** 1934b. Rabbit pox II. Pathology of the epidemic disease. J Exp Med **60**:441-458.

98. **Greene, H.** 1935. Rabbit pox III. Report of an epidemic with especial reference to epidemiological factors. J.Exp.Med. **61**:807-831.

99. **Handa, K., H. Suzuki, H. Matsui, Y. Shimizu, and K. Kumagai**. 1983. Natural killer (NK) cells as a responder to interleukin 2 (IL 2). II. IL 2-induced interferon γ production. J.Immunol. **130**:988-992.

100. **Hazuda, D.J., J. Strickler, F. Kueppers, P.L. Simon, and P.R. Young**. 1990. Processing of precursor interleukin 1 beta and inflammatory disease. J Biol Chem **265**:6318-6322.

101. **Heibein, J.A., M. Barry, B. Motyka, and R.C. Bleackley**. 1999. Granzyme B-induced loss of mitochondrial inner membrane potential (Delta Psi m) and cytochrome c release are caspase independent. J Immunol **163**:4683-4693.

102. **Herberman, R.B., C.W. Reynolds, and J.R. Ortaldo**. 1986. Mechanism of cytotoxicity by natural killer (NK) cells. Annu.Rev.Immunol. **4**:651-680.

103. **Hiemstra, P.S., W.S. van, and J. Stolk**. 1998. Neutrophil serine proteinases and defensins in chronic obstructive pulmonary disease: effects on pulmonary epithelium [see comments]. Eur.Respir.J **12**:1200-1208.

104. **Hirsch, R.** 1982. The complement system: its importance in the host response to viral infection. Microbiol.Rev. **46**:71-85.

105. **Hollinshead, M., A. Vanderplasschen, G.L. Smith, and D.J. Vaux**. 1999. Vaccinia virus intracellular mature virions contain only one lipid membrane. J.Virol. **73**:1503-1517.

106. **Howard, S.T., Y.S. Chan, and G.L. Smith**. 1991. Vaccinia virus homologues of the Shope fibroma virus inverted terminal repeat proteins and a discontinuous ORF related to the tumor necrosis factor receptor family. Virology **180**:633-647.

107. **Hu, F.Q., C.A. Smith, and D.J. Pickup**. 1994. Cowpox virus contains two copies of an early gene encoding a soluble secreted form of the type II TNF receptor. Virology **204**:343-356.

108. **Hu, S., C. Vincenz, M. Buller, and V.M. Dixit**. 1997. A novel family of viral death effector domain-containing molecules that inhibit both CD-95- and tumor necrosis factor receptor-1-induced apoptosis. J.Biol.Chem. **272**:9621-9624.

109. **Huber, R., and R.W. Carrell**. 1989. Implications of the three-dimensional structure of alpha 1- antitrypsin for structure and function of serpins. Biochemistry **28**:8951-8966.

110. **Hyde, J.M., L.G. Gafford, and C.C. Randall**. 1967. Molecular weight determination of fowlpox virus DNA by electron microscopy. Virology **33**:112-120.

111. **Ichihashi, Y.** 1996. Extracellular enveloped vaccinia virus escapes neutralization. Virology **217**:478-485.

112. **Ink, B.S., C.S. Gilbert, and G.I. Evan**. 1995. Delay of vaccinia virus-induced apoptosis in nonpermissive Chinese hamster ovary cells by the cowpox virus CHOhr and adenovirus E1B 19K genes. J.Virol. **69**:661-668.

113. **Isaacs, S.N., G.J. Kotwal, and B. Moss**. 1992. Vaccinia virus complement-control protein prevents antibody- dependent complement-enhanced neutralization of infectivity and contributes to virulence. Proc.Natl.Acad.Sci.U.S.A. **89**:628-632.

114. **Jacoby, R.O., P.N. Bhatt, and D.G. Brownstein**. 1989. Evidence that NK cells and interferon are required for genetic resistance to lethal infection with ectromelia virus. Arch.Virol. **108**:49-58.

115. **Janusz, M.J., and N.S. Doherty** . 1991. Degradation of cartilage matrix proteoglycan by human neutrophils involves both elastase and cathepsin G. J Immunol **146**:3922-3928.

116. **Jochum, M., J. White, K.H. Duswald, D. Inthorn, H. Welter, and H. Fritz**. 1986. Pathobiochemistry of sepsis: role of proteinases, proteinase inhibitors and oxidizing agents. Behring.Inst.Mitt. 121-130.

117. **Joklik, W.** 1990. Interferons, pp. 383-411. In B. Fields and D.E. Knipe (eds.), Virology. Raven Press, New York.

118. **Joklik, W.K.** 1968. Vaccinia virus deoxyribonucleic acid: a genome replicating in the cytoplasm. Res.Publ.Assoc.Res.Nerv.Ment.Dis. **44**:87-101.

119. **Joklik, W.K., and T.C. Merigan** . 1966. Concerning the mechanism of action of interferon. Proc.Natl.Acad.Sci.U.S.A. **56**:558-565.

120. **Karupiah, G., R.V. Blanden, and I.A. Ramshaw**. 1990. Interferon gamma is involved in the recovery of athymic nude mice from recombinant vaccinia virus/interleukin 2 infection. J.Exp.Med. **172**:1495-1503.

121. **Karupiah, G., Q.W. Xie, R.M. Buller, C. Nathan, C. Duarte, and J.D. MacMicking**. 1993. Inhibition of viral replication by interferon-gamma-induced nitric oxide synthase. Science **261**:1445-1448.

122. **Keck, J.G., C.J. Baldick, Jr., and B. Moss**. 1990. Role of DNA replication in vaccinia virus gene expression: a naked template is required for transcription of three late trans-activator genes. Cell **61**:801-809.

123. **Kettle, S., N.W. Blake, K.M. Law, and G.L. Smith**. 1995. Vaccinia virus serpins B13R (SPI-2) and B22R (SPI-1) encode M(r) 38.5 and 40K, intracellular polypeptides that do not affect virus virulence in a murine intranasal model. Virology **206**:136-147.

124. **Kibler, K.V., T. Shors, K.B. Perkins, C.C. Zeman, M.P. Banaszak, J. Biesterfeldt, J.O. Langland, and B.L. Jacobs**. 1997. Double-stranded RNA is a trigger for apoptosis in vaccinia virus- infected cells. J.Virol. **71**:1992-2003.

125. **Kidd, V.J.** 1998. Proteolytic activities that mediate apoptosis. Annual Review Of Physiology **60**:533-573.

126. **Kohonen-Corish, M.R., N.J. King, C.E. Woodhams, and I.A. Ramshaw**. 1990. Immunodeficient mice recover from infection with vaccinia virus expressing interferon-gamma. Eur.J.Immunol. **20**:157-161.

127. **Koopman, R.J., M.F. van, S.G. Vreden, and W.M. Dolmans**. 1992. Molluscum contagiosum; a marker for advanced HIV infection [letter]. Br.J.Dermatol. **126**:528-529.

128. **Kotwal, G.J., and B. Moss**. 1988. Vaccinia virus encodes a secretory polypeptide structurally related to complement control proteins. Nature **335**:176-178.

129. **Kroemer, G., B. Dallaporta, and M. Resche-Rigon**. 1998. The mitochondrial death/life regulator in apoptosis and necrosis. Annual Review Of Physiology **60**:619-642.

130. **Lalani, A.S., J. Masters, W. Zeng, J. Barrett, R. Pannu, H. Everett, C.W. Arendt, and G. McFadden**. 1999. Use of chemokine receptors by poxviruses. Science **286**:1968-1971.

131. **Lalani, A.S., T.L. Ness, R. Singh, J.K. Harrison, B.T. Seet, D.J. Kelvin, G. McFadden, and R.W. Moyer**. 1998. Functional comparisons among members of the poxvirus T1/35kDa family of soluble CC-chemokine inhibitor glycoproteins. Virology **250**:173-184.

132. **Langland, J.O., S. Pettiford, B. Jiang, and B.L. Jacobs**. 1994. Products of the porcine group C rotavirus NSP3 gene bind specifically to double-stranded RNA and inhibit activation of the interferon-induced protein kinase PKR. J.Virol. **68**:3821-3829.

133. **Law, K.M., and G.L. Smith**. 1992. A vaccinia serine protease inhibitor which prevents virus- induced cell fusion. J.Gen.Virol. **73**:549-557.

134. **Lawrence, D.A., D. Ginsburg, D.E. Day, M.B. Berkenpas, I.M. Verhamme, J. Kvassman, and J.D. Shore**. 1995. Serpin-protease complexes are trapped as stable acyl-enzyme intermediates. J.Biol.Chem. **270**:25309-25312.

135. **Lawrence, D.A., S.T. Olson, S. Palaniappan, and D. Ginsburg**. 1994. Serpin reactive center loop mobility is required for inhibitor function but not for enzyme recognition. J.Biol.Chem. **269**:27657-27662.

136. **Lawrence, D.A., L. Strandberg, J. Ericson, and T. Ny**. 1990. Structure-function studies of the SERPIN plasminogen activator inhibitor type 1. Analysis of chimeric strained loop mutants. J Biol Chem **265**:20293-20301.

137. **Lee, S.B., and M. Esteban**. 1994. The interferon-induced double-stranded RNA-activated protein kinase induces apoptosis. Virology **199**:491-496.

138. **Lemasters, J.J., A.L. Nieminen, T. Qian, L.C. Trost, S.P. Elmore, Y. Nishimura, R.A. Crowe, W.E. Cascio, C.A. Bradham, D.A. Brenner, and B. Herman**. 1998. The mitochondrial permeability transition in cell death: a common mechanism in necrosis, apoptosis and autophagy. Biochim.Biophys.Acta **1366**:177-196.

139. **Li, M., and A.A. Beg**. 2000. Induction of necrotic-like cell death by tumor necrosis factor alpha and caspase inhibitors: novel mechanism for killing virus-infected cells. J Virol **74**:7470-7477.

140. **Li, X., J.W. Barrett, L. Yuen, and B.M. Arif**. 1997. Cloning, sequencing and transcriptional analysis of the Choristoneura fumiferana entomopoxvirus spheroidin gene. Virus Res. **47**:143-154.

141. **Lindmark, B.E., M.J. Arborelius, and S.G. Eriksson**. 1990. Pulmonary function in middle-aged women with heterozygous deficiency of the serine protease inhibitor alpha 1-antichymotrypsin. Am.Rev.Respir.Dis. **141**:884-888.

142. **Liptakova, H., E. Kontsekova, A. Alcami, G.L. Smith, and P. Kontsek**. 1997. Analysis of an interaction between the soluble vaccinia virus- coded type I interferon (IFN)-receptor and human IFN- alpha 1 and IFN-alpha 2. Virology **232**:86-90.

143. **Lomas, D.A., D.L. Evans, C. Upton, G. McFadden, and R.W. Carrell**. 1993. Inhibition of plasmin, urokinase, tissue plasminogen activator, and C1S by a myxoma virus serine proteinase inhibitor. J.Biol.Chem. **268**:516-521.

144. **Los, M., S. Wesselborg, and K. Schulze-Osthoff'**. 1999. The role of caspases in development, immunity, and apoptotic signal transduction: lessons from knockout mice. Immunity **10**:629-639.

145. **Lucas, A., L.Y. Liu, J. Macen, P. Nash, E. Dai, M. Stewart, K. Graham, W. Etches, L. Boshkov, P.N. Nation, D. Humen, M.L. Hobman, and G. McFadden**. 1996. Virus-encoded serine proteinase inhibitor SERP-1 inhibits atherosclerotic plaque development after balloon angioplasty. Circulation **94**:2890-2900.

146. **Macen, J., A. Takahashi, K.B. Moon, R. Nathaniel, P.C. Turner, and R.W. Moyer**. 1998. Activation of caspases in pig kidney cells infected with wild-type and CrmA/SPI-2 mutants of cowpox and rabbitpox viruses. J.Virol. **72**:3524-3533.

147. **Macen, J.L., R.S. Garner, P.Y. Musy, M.A. Brooks, P.C. Turner, R.W. Moyer, G. McFadden, and R.C. Bleackley**. 1996. Differential inhibition

of the Fas- and granule-mediated cytolysis pathways by the orthopoxvirus cytokine response modifier A/SpI-2 and SPI-1 protein. Proc.Natl.Acad.Sci.U.S.A. **93**:9108-9113.

148. **Macen, J.L., K.A. Graham, S.F. Lee, M. Schreiber, L.K. Boshkov, and G. McFadden**. 1996. Expression of the myxoma virus tumor necrosis factor receptor homologue and M11L genes is required to prevent virus-induced apoptosis in infected rabbit T lymphocytes. Virology **218**:232-237.

149. **Macen, J.L., C. Upton, N. Nation, and G. McFadden**. 1993. SERP1, a serine proteinase inhibitor encoded by myxoma virus, is a secreted glycoprotein that interferes with inflammation. Virology **195**:348-363.

150. **Maison, C.M., C.L. Villiers, and M.G. Colomb**. 1991. Proteolysis of C3 on U937 cell plasma membranes. Purification of cathepsin G. J Immunol **147**:921-926.

151. **Maksymowych, W.P., N. Nation, P. Nash, J. Macen, A. Lucas, G. McFadden, and A.S. Russell**. 1996. Amelioration of antigen induced arthritis in rabbits treated with a secreted viral serine proteinase inhibitor. J.Rheumatol. **23**:878-882.

152. **Maniatis, T., E.F. Fritsch, and J. Sambrook**. 1982. Molecular Cloning: A Laboratory Manual. Cold Spring Harbor Laboratory, Cold Spring Harbor, N.Y.

153. **Martin, S.A., E. Paoletti, and B. Moss**. 1975. Purification of mRNA guanylyltransferase and mRNA (guanine- 7-) methyltransferase from vaccinia virions. J.Biol.Chem. **250**:9322-9329.

154. **Martin, S.J., G.P. Amarante Mendes, L. Shi, T.H. Chuang, C.A. Casiano, G.A. O'Brien, P. Fitzgerald, E.M. Tan, G.M. Bokoch, A.H. Greenberg, and D.R. Green**. 1996. The cytotoxic cell protease granzyme B initiates apoptosis in a cell-free system by proteolytic processing and activation of the ICE/CED-3 family protease, CPP32, via a novel two-step mechanism. EMBO J. **15**:2407-2416.

155. **Massung, R.F., J.J. Esposito, L.I. Liu, J. Qi, T.R. Utterback, J.C. Knight, L. Aubin, T.E. Yuran, J.M. Parsons, V.N. Loparev, N.A. Selivanov, K.F. Cavallaro, A.R. Kerlavage, B.W.J. Mahy, and J.C. Venter**. 1993. Potential virulence determinants in terminal regions of variola smallpox virus genome [see comments]. Nature **366** :748-751.

156. **Massung, R.F., V. Jayarama, and R.W. Moyer**. 1993. DNA sequence analysis of conserved and unique regions of swinepox virus: Identification of genetic elements supporting phenotypic observations including a novel G protein-coupled receptor homologue. Virology **197**:511-528.

157. **Matis, W.L., A. Triana, R. Shapiro, L. Eldred, B.F. Polk, and A.F. Hood.** 1987. Dermatologic findings associated with human immunodeficiency virus infection. J.Am.Acad.Dermatol. **17**:746-751.

158. **McCarthy, N.J., M.K. Whyte, C.S. Gilbert, and G.I. Evan.** 1997. Inhibition of Ced-3/ICE-related proteases does not prevent cell death induced by oncogenes, DNA damage, or the Bcl-2 homologue Bak. J.Cell Biol. **136**:215-227.

159. **McConkey, D.J.** 1996. Calcium-dependent, interleukin 1-converting enzyme inhibitor- insensitive degradation of lamin B1 and DNA fragmentation in isolated thymocyte nuclei. J.Biol.Chem. **271**:22398-22406.

160. **McFadden, G., A. Lalani, H. Everett, P. Nash, and X. Xu.** 1998. Virus-encoded receptors for cytokines and chemokines. Seminars In Cell & Developmental Biology **9**:359-368.

161. **McFadden, G., M. Schreiber, and L. Sedger.** 1997. Myxoma T2 protein as a model for poxvirus TNF receptor homologs. J.Neuroimmunol. **72**:119-126.

162. **McKenzie, R., G.J. Kotwal, B. Moss, C.H. Hammer, and M.M. Frank.** 1992. Regulation of complement activity by vaccinia virus complement- control protein. J.Infect.Dis. **166**:1245-1250.

163. **Medema, J.P., R.E.M. Toes, C. Scaffidi, T.S. Zheng, R.A. Flavell, C.J.M. Melief, M.E. Peter, R. Offringa, and P.H. Krammer.** 1997. Cleavage of FLICE (caspase-8) by granzyme B during cytotoxic T lymphocyte-induced apoptosis. Eur.J.Immunol. **27**:3492-3498.

164. **Mellet, P., and J.G. Bieth.** 2000. Evidence that translocation of the proteinase precedes its acylation in the serpin inhibition pathway. J Biol Chem **275**:10788-10795.

165. **Menna, A., R. Wittek, P.A. Bachmann, A. Mayr, and R. Wyler.** 1979. Physical characterization of a stomatitis papulosa virus genome: a cleavage map for the restriction endonucleases HindIII and EcoRI. Arch.Virol. **59**:145-156.

166. **Messud-Petit, F., J. Gelfi, M. Delverdier, M.F. Amardeilh, R. Py, G. Sutter, and S. Bertagnoli.** 1998a. Serp2, an inhibitor of the interleukin-1 beta-converting enzyme, is critical in the pathobiology of myxoma virus. J.Virol. **72**:7830-7839.

167. **Messud-Petit, F., J. Gelfi, M. Delverdier, M.F. Amardeilh, R. Py, G. Sutter, and S. Bertagnoli.** 1998b. Serp2, an inhibitor of the interleukin-1beta-converting enzyme, is critical in the pathobiology of myxoma virus. J Virol. **72**:7830-7839.

168. **Metz, D.H., and M. Esteban**. 1972. Interferon inhibits viral protein synthesis in L cells infected with vaccinia virus. Nature **238**:385-388.

169. **Miller, C.G., D.E. Justus, S. Jayaraman, and G.J. Kotwal**. 1995. Severe and prolonged inflammatory response to localized cowpox virus infection in footpads of C5-deficient mice: investigation of the role of host complement in poxvirus pathogenesis. Cell Immunol. **162**:326-332.

170. **Miller, C.G., S.N. Shchelkunov, and G.J. Kotwal**. 1997. The cowpox virus-encoded homolog of the vaccinia virus complement control protein is an inflammation modulatory protein. Virology **229**:126-133.

171. **Mims, C.A.** 1964. Aspects of the pathogenesis of virus diseases. Bacteriol.Rev. **28**:30-71.

172. **Monney, L., I. Otter, R. Olivier, H.L. Ozer, A.L. Haas, S. Omura, and C. Borner**. 1998. Defects in the ubiquitin pathway induce caspase-independent apoptosis blocked by Bcl-2. J.Biol.Chem. **273**:6121-6131.

173. **Morgan, C.** 1976. Vaccinia virus reexamined: development and release. Virology **73**:43-58.

174. **Morishima, T., and K. Hayashi**. 1978. Meningeal exudate cells in vaccinia meningitis of mice: role of local T cells. Infect.Immun. **20**:752-759.

175. **Moss, B.** 1996. *Poxviridae*: The viruses and their replication, p. 2637-2672. In B.N. Fields, D.M. Knipe, and P.M. Howley (eds.), Fields Virology. Lippincott-Reven, Philadelphia.

176. **Moss, B., B.Y. Ahn, B. Amegadzie, P.D. Gershon, and J.G. Keck**. 1991. Cytoplasmic transcription system encoded by vaccinia virus. J.Biol.Chem. **266**:1355-1358.

177. **Mossman, K., M. Barry, and G. McFadden**. 1994. Interferon-γ receptors encoded by poxviruses, pp. 41-54. In G. McFadden (ed.), Viroceptors, virokines and related immune modulators. RG Landes Company, Austin, TX.

178. **Mossman, K., S.F. Lee, M. Barry, L. Boshkov, and G. McFadden**. 1996. Disruption of M-T5, a novel myxoma virus gene member of poxvirus host range superfamily, results in dramatic attenuation of myxomatosis in infected European rabbits. J.Virol. **70**:4394-4410.

179. **Mossman, K., P. Nation, J. Macen, M. Garbutt, A. Lucas, and G. McFadden**. 1996. Myxoma virus M-T7, a secreted homolog of the interferon-gamma receptor, is a critical virulence factor for the development of myxomatosis in European rabbits. Virology **215**:17-30.

180. **Mossman, K., C. Upton, and G. McFadden**. 1995. The myxoma virus-soluble interferon-gamma receptor homolog, M-T7, inhibits interferon-gamma in a species-specific manner. J.Biol.Chem. **270**:3031-3038.

181. **Moyer, R.W., and R.L. Graves**. 1981. The mechanism of cytoplasmic orthopoxvirus DNA replication. Cell **27**:391-401.

182. **Moyer, R.W., and C.T. Rothe**. 1980. The white pock mutants of rabbit poxvirus. I. Spontaneous host range mutants contain deletions. Virology **102**:119-132.

183. **Muchmore, S.W., M. Sattler, H. Liang, R.P. Meadows, J.E. Harlan, H.S. Yoon, D. Nettesheim, B.S. Chang, C.B. Thompson, S.-L. Wong, S.-C. Ng, and S.W. Fesik**. 1996. X-ray and NMR structure of human Bcl-X_L, an inhibitor of programmed cell death. Nature **381**:335-341.

184. **Mukinda, V.B., G. Mwema, M. Kilundu, D.L. Heymann, A.S. Khan, and J.J. Esposito**. 1997. Re-emergence of human monkeypox in Zaire in 1996. Monkeypox Epidemiologic Working Group [letter]. Lancet **349**:1449-1450.

185. **Musy, P. Y.** 1998. Molecular and Biological Characterization of a serpin-like protein encoded by swinepox virus. University of Florida.

186. **Nagata, S.** 1997. Apoptosis by death factor. Cell **88**:355-365.

187. **Nash, P., A. Whitty, J. Handwerker, J. Macen, and G. McFadden**. 1998. Inhibitory specificity of the anti-inflammatory myxoma virus serpin, SERP-1. J.Biol.Chem. **273** :20982-20991.

188. **Nicholson, D.W., and N.A. Thornberry**. 1997. Caspases: killer proteases. Trends.Biochem.Sci. **22**:299-306.

189. **O'Brien, V.** 1998. Viruses and apoptosis. J.Gen.Virol. **79**:1833-1845.

190. **Oda, K.I., and W.K. Joklik**. 1967. Hybridization and sedimentation studies on "early" and "late" vaccinia messenger RNA. J.Mol.Biol. **27**:395-419.

191. **Ohta, H., C. Kai, Y. Yoshikawa, and K. Yamanouchi**. 1983. Activation of chicken alternative complement pathway by fowlpox virus-infected cells. Infect.Immun. **42**:721-727.

192. **Ohta, H., Y. Yoshikawa, C. Kai, K. Yamanouchi, H. Taniguchi, K. Komine, Y. Ishijima, and H. Okada**. 1986. Effect of complement depletion by cobra venom factor on fowlpox virus infection in chickens and chicken embryos. J.Virol. **57**:670-673.

193. **Okada, H., N. Wakamiya, N. Okada, and S. Kato**. 1987. Sensitization of human tumor cells to homologous complement by vaccinia virus treatment. Cancer Immunol.Immunother. **25**:7-9.

194. **Okuno, S., S. Shimizu, T. Ito, M. Nomura, E. Hamada, Y. Tsujimoto, and H. Matsuda**. 1998. Bcl-2 prevents caspase-independent cell death. J.Biol.Chem. **273**:34272-34277.

195. **Opgenorth, A., K. Graham, N. Nation, D. Strayer, and G. McFadden**. 1992. Deletion analysis of two tandemly arranged virulence genes in myxoma virus, M11L and myxoma growth factor. J.Virol. **66**:4720-4731.

196. **Padrines, M., M. Wolf, A. Walz, and M. Baggiolini**. 1994. Interleukin-8 processing by neutrophil elastase, cathepsin G and proteinase-3. FEBS Lett. **352**:231-235.

197. **Palumbo, G.J., R.M. Buller, and W.C. Glasgow**. 1994. Multigenic evasion of inflammation by poxviruses. J.Virol. **68**:1737-1749.

198. **Palumbo, G.J., D.J. Pickup, T.N. Fredrickson, L.J. McIntyre, and R.M. Buller**. 1989. Inhibition of an inflammatory response is mediated by a 38-kDa protein of cowpox virus. Virology **172**:262-273.

199. **Park, H., M.V. Davies, J.O. Langland, H.W. Chang, Y.S. Nam, J. Tartaglia, E. Paoletti, B.L. Jacobs, R.J. Kaufman, and S. Venkatesan**. 1994. TAR RNA-binding protein is an inhibitor of the interferon- induced protein kinase PKR. Proc.Natl.Acad.Sci.U.S.A. **91**:4713-4717.

200. **Patel, D.D., and D.J. Pickup**. 1987. Messenger RNAs of a strongly-expressed late gene of cowpox virus contain 5'-terminal poly(A) sequences. EMBO J. **6**:3787-3794.

201. **Patston, P.A.** 1995. Studies on inhibition of neutrophil cathepsin G by alpha 1-antichymotrypsin. Inflammation **19**:75-81.

202. **Payne, L.** 1978. Polypeptide composition of extracellular enveloped vaccinia virus. J.Virol. **27**:28-37.

203. **Payne, L.G.** 1980. Significance of extracellular enveloped virus in the in vitro and in vivo dissemination of vaccinia. J.Gen.Virol. **50**:89-100.

204. **Pemberton, P.A.** 1997. The role of serpin superfamily members in cancer. Canc.J. **10** :24-30.

205. **Pennington, T.H., and E.A. Follett**. 1974. Vaccinia virus replication in enucleate BSC-1 cells: particle production and synthesis of viral DNA and proteins. J.Virol. **13**:488-493.

206. **Perkus, M.E., S.J. Goebel, S.W. Davis, G.P. Johnson, E.K. Norton, and E. Paoletti**. 1991. Deletion of 55 open reading frames from the termini of vaccinia virus. Virology **180**:406-410.

207. **Petit, F., S. Bergagnoli, J. Gelfi, F. Fassy, C. Boucraut-Baralon, and A. Milon**. 1996. Characterization of a myxoma virus-encoded serpin-like protein with activity against interleukin-1β converting enzyme. J.Virol. **70** :5860-5866.

208. **Pewarchuk, W.J., F. Fernandez Rachubinski, R.A. Rachubinski, and M.A. Blajchman**. 1990. Antithrombin III Sudbury: an Ala384----Pro mutation with abnormal thrombin-binding activity and thrombotic diathesis. Thromb.Res. **59**:793-797.

209. **Pickup, D.J., B.S. Ink, W. Hu, C.A. Ray, and W.K. Joklik**. 1986. Hemorrhage in lesions caused by cowpox virus is induced by a viral protein that is related to plasma protein inhibitors of serine proteases. Proc.Natl.Acad.Sci.U.S.A. **83**:7698-7702.

210. **Plotnick, M.I., N.M. Schechter, Z.M. Wang, X.Z. Liu, and H. Rubin**. 1997. Role of the P6-P3' region of the serpin reactive loop in the formation and breakdown of the inhibitory complex. Biochemistry **36**:14601-14608.

211. **Potempa, J., E. Korzus, and J. Travis**. 1994. The serpin superfamily of proteinase inhibitors: structure, function, and regulation. J.Biol.Chem. **269**:15957-15960.

212. **Quan, L.T., A. Caputo, R.C. Bleackley, D.J. Pickup, and G.S. Salvesen**. 1995. granzyme B is inhibited by the cowpox virus serpin cytokine response modifier A. J.Biol.Chem. **270**:10377-10379.

213. **Ramsey-Ewing, A., and B. Moss**. 1995. Restriction of vaccinia virus replication in CHO cells occurs at the stage of viral intermediate protein synthesis. Virology **206**:984-993.

214. **Ramsey-Ewing, A.L., and B. Moss**. 1996. Complementation of a vaccinia virus host-range K1L gene deletion by the nonhomologous CP77 gene. Virology **222**:75-86.

215. **Ramshaw, I., J. Ruby, A. Ramsay, G. Ada, and G. Karupiah**. 1992. Expression of cytokines by recombinant vaccinia viruses: a model for studying cytokines in virus infections in vivo. Immunol.Rev. **127**:157-182.

216. **Rathmell, J.C., and C.B. Thompson**. 1999. The central effectors of cell death in the immune system. Annual Review Of Immunology **17**:781-828.

217. **Ray, C.A., R.A. Black, S.R. Kronheim, T.A. Greenstreet, P.R. Sleath, G.S. Salvesen, and D.J. Pickup**. 1992. Viral inhibition of inflammation: cowpox virus encodes an inhibitor of the interleukin-1 beta converting enzyme. Cell **69**:597-604.

218. **Ray, C.A., and D.J. Pickup**. 1996. The mode of death of pig kidney cells infected with cowpox virus is governed by the expression of the crmA gene. Virology **217**:384-391.

219. **Rice, A.P., and I.M. Kerr**. 1984. Interferon-mediated, double-stranded RNA-dependent protein kinase is inhibited in extracts from vaccinia virus-infected cells. J.Virol. **50**:229-236.

220. **Riewald, M., and R.R. Schleef**. 1996. Human cytoplasmic antiproteinase neutralizes rapidly and efficiently chymotrypsin and trypsin-like proteases utilizing distinct reactive site residues. J Biol Chem **271**:14526-14532.

221. **Robinson, A.J., G. Barns, K. Fraser, E. Carpenter, and A.A. Mercer**. 1987. Conservation and variation in orf virus genomes. Virology **157**:13-23.

222. **Rohrmann, G., L. Yuen, and B. Moss**. 1986. Transcription of vaccinia virus early genes by enzymes isolated from vaccinia virions terminates downstream of a regulatory sequence. Cell **46**:1029-1035.

223. **Rosales, R., N. Harris, B.Y. Ahn, and B. Moss**. 1994. Purification and identification of a vaccinia virus-encoded intermediate stage promoter-specific transcription factor that has homology to eukaryotic transcription factor SII (TFIIS) and an additional role as a viral RNA polymerase subunit. J.Biol.Chem. **269**:14260-14267.

224. **Rosales, R., G. Sutter, and B. Moss**. 1994. A cellular factor is required for transcription of vaccinia viral intermediate-stage genes. Proc.Natl.Acad.Sci.U.S.A. **91**:3794-3798.

225. **Rosel, J.L., P.L. Earl, J.P. Weir, and B. Moss**. 1986. Conserved TAAATG sequence at the transcriptional and translational initiation sites of vaccinia virus late genes deduced by structural and functional analysis of the HindIII H genome fragment. J.Virol. **60**:436-449.

226. **Rosengard, A.M., and J.M. Ahearn**. 1999. Viral complement regulatory proteins. Immunopharmacology **42**:99-106.

227. **Rubin, H.** 1992. The biology and biochemistry of antichymotrypsin and its potential role as a therapeutic agent. Biol Chem Hoppe Seyler **373**:497-502.

228. **Rubin, H.** 1996. Serine protease inhibitors (SERPINS): where mechanism meets medicine. Nat.Med. **2**:632-633.

229. **Rubin, H., M. Plotnick, Z.M. Wang, X. Liu, Q. Zhong, N.M. Schechter, and B.S. Cooperman**. 1994. Conversion of alpha 1-antichymotrypsin into a human neutrophil elastase inhibitor: demonstration of variants with different association rate constants, stoichiometries of inhibition, and complex stabilities. Biochemistry **33**:7627-7633.

230. **Ruby, J., and I. Ramshaw**. 1991. The antiviral activity of immune CD8+ T cells is dependent on interferon-gamma. Lymphokine Cytokine.Res. **10**:353-358.

231. **Samuel, C.E., R. Duncan, G.S. Knutson, and J.W. Hershey**. 1984. Mechanism of interferon action. Increased phosphorylation of protein synthesis initiation factor eIF-2 alpha in interferon-treated, reovirus- infected mouse L929 fibroblasts in vitro and in vivo. J Biol.Chem. **259**:13451-13457.

232. **Sarin, A., E.K. Haddad, and P.A. Henkart**. 1998. Caspase dependence of target cell damage induced by cytotoxic lymphocytes. Journal Of Immunology **161**:2810-2816.

233. **Savill, J.** 1997. Apoptosis in resolution of inflammation. J Leukoc.Biol **61**:375-380.

234. **Schechter, N.M., L.M. Jordan, A.M. James, B.S. Cooperman, Z.M. Wang, and H. Rubin**. 1993. Reaction of human chymase with reactive site variants of alpha 1- antichymotrypsin. Modulation of inhibitor versus substrate properties. J.Biol.Chem. **268** :23626-23633.

235. **Schick, C., Y. Kamachi, A.J. Bartuski, S. Cataltepe, N.M. Schechter, P.A. Pemberton, and G.A. Silverman**. 1997. Squamous cell carcinoma antigen 2 is a novel serpin that inhibits the chymotrypsin-like proteinases cathepsin G and mast cell chymase. J.Biol.Chem. **272**:1849-1855.

236. **Schick, C., P.A. Pemberton, G.P. Shi, Y. Kamachi, S. Cataltepe, A.J. Bartuski, E.R. Gornstein, D. Bromme, H.A. Chapman, and G.A. Silverman**. 1998. Cross-class inhibition of the cysteine proteinases cathepsins K, L, and S by the serpin squamous cell carcinoma antigen 1: A kinetic analysis. Biochemistry **37**:5258-5266.

237. **Schlesinger, P.H., A. Gross, X.M. Yin, K. Yamamoto, M. Saito, and et al.** 1997. Comparison of the ion channel characteristics of proapoptotic BAX and antiapoptotic BCL-2. Proc.Natl.Acad.Sci.USA **94**:11357-11362.

238. **Schmid, W., U. Strahle, G. Schutz, J. Schmitt, and H. Stunnenberg.** 1989. Glucocorticoid receptor binds cooperatively to adjacent recognition sites. EMBO J. **8**:2257-2263.

239. **Schreiber, M., and G. McFadden** . 1994. The myxoma virus TNF-receptor homologue (T2) inhibits tumor necrosis factor-alpha in a species-specific fashion. Virology **204** :692-705.

240. **Schreiber, M., and G. McFadden** . 1996. Mutational analysis of the ligand-binding domain of M-T2 protein, the tumor necrosis factor receptor homologue of myxoma virus. J.Immunol. **157**:4486-4495.

241. **Schreiber, M., L. Sedger, and G. McFadden**. 1997. Distinct domains of M-T2, the myxoma virus tumor necrosis factor (TNF) receptor homolog, mediate extracellular TNF binding and intracellular apoptosis inhibition. J.Virol. **71**:2171-2181.

242. **Schulze, A.J., R. Huber, E. Degryse, D. Speck, and R. Bischoff**. 1991. Inhibitory activity and conformational transition of alpha 1-proteinase inhibitor variants. Eur.J.Biochem. **202**:1147-1155.

243. **Scott, F.L., C.E. Hirst, J. Sun, C.H. Bird, S.P. Bottomley, and P.I. Bird**. 1999. The intracellular serpin proteinase inhibitor 6 is expressed in monocytes and granulocytes and is a potent inhibitor of the azurophilic granule protease, cathepsin G. Blood **93**:2089-2097.

244. **Sedger, L., and G. McFadden**. 1996. M-T2: a poxvirus TNF receptor homologue with dual activities. Immunol.Cell Biol. **74**:538-545.

245. **Senkevich, T.G., J.J. Bugert, J.R. Sisler, E.V. Koonin, G. Darai, and B. Moss**. 1996. Genome sequence of a human tumorigenic poxvirus: Prediction of specific host response-evasion genes. Science **273**:813-816.

246. **Senkevich, T.G., E.V. Koonin, J.J. Bugert, G. Darai, and B. Moss**. 1997. The genome of molluscum contagiosum virus: Analysis and comparison with other poxviruses. Virology **233**:19-42.

247. **Shafer, W.M., M.E. Shepherd, B. Boltin, L. Wells, and J. Pohl**. 1993. Synthetic peptides of human lysosomal cathepsin G with potent antipseudomonal activity. Infect.Immun. **61**:1900-1908.

248. **Shand, J.H., P. Gibson, D.W. Gregory, R.J. Cooper, H.M. Keir, and R. Postlethwaite**. 1976. Molluscum contagiosum -- a defective poxvirus. J.Gen.Virol. **33**:281-295.

249. **Shchelkunov, S.N.** 1995. Functional organization of variola major and vaccinia virus genomes. [Review]. Virus Genes **10**:53-71.

250. **Shchelkunov, S.N., V.M. Blinov, and L.S. Sandakhchiev**. 1993. Genes of variola and vaccinia viruses necessary to overcome the host protective mechanisms. FEBS Lett. **319**:80-83.

251. **Shisler, J.L., S.N. Isaacs, and B. Moss**. 1999. Vaccinia virus serpin-1 deletion mutant exhibits a host range defect characterized by low levels of intermediate and late mRNAs. Virology **262**:298-311.

252. **Shisler, J.L., T.G. Senkevich, M.J. Berry, and B. Moss**. 1998. Ultraviolet-induced cell death blocked by a selenoprotein from a human dermatotropic poxvirus. Science **279**:102-105.

253. **Shuman, S., D.G. Bear, and J. Sekiguchi**. 1997. Intramolecular synapsis of duplex DNA by vaccinia topoisomerase. EMBO J. **16**:6584-6589.

254. **Shuman, S., and B. Moss**. 1989. Bromouridine triphosphate inhibits transcription termination and mRNA release by vaccinia virions. J.Biol.Chem. **264**:21356-21360.

255. **Shuman, S., M. Surks, H. Furneaux, and J. Hurwitz**. 1980. Purification and characterization of a GTP-pyrophosphate exchange activity from vaccinia virions. Association of the GTP-pyrophosphate exchange activity with vaccinia mRNA guanylyltransferase. RNA (guanine-7-)methyltransferase complex (capping enzyme). J.Biol.Chem. **255**:11588-11598.

256. **Skriver, K., W.R. Wikoff, P.A. Patston, F. Tausk, M. Schapira, A.P. Kaplan, and S.C. Bock**. 1991. Substrate properties of C1 inhibitor Ma (alanine 434--glutamic acid). Genetic and structural evidence suggesting that the P12-region contains critical determinants of serine protease inhibitor/substrate status. J Biol Chem **266**:9216-9221.

257. **Smith, C.A., T. Davis, J.M. Wignall, W.S. Din, T. Farrah, C. Upton, G. McFadden, and R.G. Goodwin**. 1991. T2 open reading frame from the Shope fibroma virus encodes a soluble form of the TNF receptor. Biochem.Biophys.Res.Commun. **176**:335-342.

258. **Smith, C.A., T.D. Smith, P.J. Smolak, D. Friend, H. Hagen, M. Gerhart, L. Park, D.J. Pickup, D. Torrance, K. Mohler, K. Schooley, and R.G. Goodwin**. 1997. Poxvirus genomes encode a secreted, soluble protein that preferentially inhibits beta chemokine activity yet lacks sequence homology to known chemokine receptors. Virology **236**:316-327.

259. **Smith, G.L.** 1996. Virus proteins that bind cytokines, chemokines or interferons. Curr.Opin.Immunol. **8**:467-471.

260. **Smith, G.L., S.T. Howard, and Y.S. Chan**. 1989. Vaccinia virus encodes a family of genes with homology to serine proteinase inhibitors. J.Gen.Virol. **70**:2333-2343.

261. **Sodeik, B., R.W. Doms, M. Ericsson, G. Hiller, C.E. Machamer, W. van 't Hof, G. van Meer, B. Moss, and G. Griffiths**. 1993. Assembly of

vaccinia virus: role of the intermediate compartment between the endoplasmic reticulum and the Golgi stacks. J.Cell Biol. **121**:521-541.

262. **Spehner, D., S. Gillard, R. Drillien, and A. Kirn**. 1988. A cowpox virus gene required for multiplication in Chinese hamster ovary cells. J.Virol. **62**:1297-1304.

263. **Spitznagel, J.K.** 1990. Antibiotic proteins of human neutrophils. J Clin.Invest. **86** :1381-1386.

264. **Spriggs, M.K., D.E. Hruby, C.R. Maliszeswki, D.J. Pickup, J.E. Sims, R.M.L. Buller, and J. VanSlyke**. 1992. Vaccinia and Cowpox viruses encode a novel secreted interleukin-1 binding protein. Cell **71**:145-152.

265. **Srinivasula, S.M., M. Ahmad, T. Fernandes Alnemri, G. Litwack, and E.S. Alnemri**. 1996. Molecular ordering of the Fas-apoptotic pathway: the Fas/APO-1 protease Mch5 is a CrmA-inhibitable protease that activates multiple Ced-3/ICE-like cysteine proteases. Proc.Natl.Acad.Sci.U.S.A. **93**:14486-14491.

266. **Stefanis, L., C.M. Troy, H. Qi, M.L. Shelanski, and L.A. Greene**. 1998. Caspase-2 (Nedd-2) processing and death of trophic factor-deprived PC12 cells and sympathetic neurons occur independently of caspase-3 (CPP32)-like activity. J Neurosci. **18**:9204-9215.

267. **Stitz, L., A. Althage, H. Hengartner, and R. Zinkernagel**. 1985. Natural killer cells vs cytotoxic T cells in the peripheral blood of virus-infected mice. J.Immunol. **134**:598-602.

268. **Stratikos, E., and P.G. Gettins**. 1999. Formation of the covalent serpin-proteinase complex involves translocation of the proteinase by more than 70 A and full insertion of the reactive center loop into beta-sheet A. Proc.Natl.Acad.Sci.U.S.A. **96**:4808-4813.

269. **Stuart, D., K. Ellison, K. Graham, and G. McFadden**. 1992. In vitro resolution of poxvirus replicative intermediates into linear minichromosomes with hairpin termini by a virally induced Holliday junction endonuclease. J.Virol. **66**:1551-1563.

270. **Subrahmanyan, T.P., and C.A. Mims**. 1966. Fate of intravenously administered interferon and the distribution of interferon during virus infections in mice. Br.J.Exp.Pathol. **47**:168-176.

271. **Susin, S.A., H.K. Lorenzo, N. Zamzami, I. Marzo, B.E. Snow, G.M. Brothers, J. Mangion, E. Jacotot, P. Costantini, M. Loeffler, N. Larochette, D.R. Goodlett, R. Aebersold, D.P. Siderovski, J.M. Penninger, and G. Kroemer**. 1999. Molecular characterization of mitochondrial apoptosis-inducing factor. Nature **397**:441-446.

272. **Sutter, G., and B. Moss**. 1992. Nonreplicating vaccinia vector efficiently expresses recombinant genes. Proc.Natl.Acad.Sci.U.S.A. **89**:10847-10851.

273. **Symons, J.A., A. Alcami, and G.L. Smith**. 1995. Vaccinia virus encodes a soluble type I interferon receptor of novel structure and broad species specificity. Cell **81**:551-560.

274. **Takahashi, A., H. Hirata, S. Yonehara, Y. Imai, K.K. Lee, R.W. Moyer, P.C. Turner, P.W. Mesner, T. Okazaki, H. Sawai, S. Kishi, K. Yamamoto, M. Okuma, and M. Sasada**. 1997. Affinity labeling displays the stepwise activation of ICE- related proteases by Fas, staurosporine, and CrmA-sensitive caspase-8. Oncogene **14**:2741-2752.

275. **Takeda, A., T. Yamamoto, Y. Nakamura, T. Takahashi, and T. Hibino**. 1995. Squamous cell carcinoma antigen is a potent inhibitor of cysteine proteinase cathepsin L. FEBS Lett. **359**:78-80.

276. **Tartaglia, J., S. Pincus, and E. Paoletti**. 1990. Poxvirus-based vectors as vaccine candidates. Crit.Rev.Immunol. **10**:13-30.

277. **Teodoro, J.G., and P.E. Branton**. 1997. Regulation of apoptosis by viral gene products. J.Virol. **71**:1739-1746.

278. **Tewari, M., and V.M. Dixit**. 1995. Fas- and tumor necrosis factor-induced apoptosis is inhibited by the poxvirus crmA gene product. J.Biol.Chem. **270**:3255-3260.

279. **Tewari, M., W.G. Telford, R.A. Miller, and V.M. Dixit**. 1995. CrmA, a poxvirus-encoded serpin, inhibits cytotoxic T-lymphocyte- mediated apoptosis. J.Biol.Chem. **270**:22705-22708.

280. **Thompson, C.B.** 1995. Apoptosis in the pathogenesis and treatment of disease. Science **267**:1456-1462.

281. **Thompson, J.P., P.C. Turner, A.N. Ali, B.C. Crenshaw, and R.W. Moyer**. 1993. The effects of serpin gene mutations on the distinctive pathobiology of cowpox and rabbitpox virus following intranasal inoculation of Balb/c mice. Virology **197**:328-338.

282. **Traktman, P.** 1990. The enzymology of poxvirus DNA replication. Curr.Top.Microbiol.Immunol. **163**:93-124.

283. **Traktman, P., M. Kelvin, and S. Pacheco**. 1989. Molecular genetic analysis of vaccinia virus DNA polymerase mutants. J.Virol. **63**:841-846.

284. **Tschopp, J., M. Thome, K. Hofmann, and E. Meinl**. 1998. The fight of viruses against apoptosis. Current Opinion In Genetics & Development **8**:82-87.

285. **Turner, P.C., M.T. Baquero, S. Yuan, S.R. Thoennes, and R.W. Moyer**. 2000. The cowpox virus serpin SPI-3 complexes with and inhibits urokinase-type and tissue-type plasminogen activators and plasmin. Virology **272**:267-280.

286. **Turner, P.C., and R.W. Moyer**. 1992. An orthopoxvirus serpinlike gene controls the ability of infected cells to fuse. J.Virol. **66**:2076-2085.

287. **Turner, P.C., and R.W. Moyer**. 1998. control of apoptosis by poxviruses. Seminars in Virology **8**:453-469.

288. **Turner, P.C., M.C. Sancho, S.R. Thoennes, A. Caputo, R.C. Bleackley, and R.W. Moyer**. 1999. Myxoma virus Serp2 is a weak inhibitor of granzyme B and interleukin- 1beta-converting enzyme in vitro and unlike CrmA cannot block apoptosis in cowpox virus-infected cells. J Virol. **73**:6394-6404.

289. **Ueda, Y., S. Morikawa, and Y. Matsuura**. 1990. Identification and nucleotide sequence of the gene encoding a surface antigen induced by vaccinia virus. Virology **177**:588-594.

290. **Upton, C., A.M. Delange, and G. McFadden**. 1987. Tumorigenic poxviruses: genomic organization and DNA sequence of the telomeric region of the Shope fibroma virus genome. Virology **160**:20-30.

291. **Upton, C., J.L. Macen, M. Schreiber, and G. McFadden**. 1991. Myxoma virus expresses a secreted protein with homology to the tumor necrosis factor receptor gene family that contributes to viral virulence. Virology **184**:370-382.

292. **Upton, C., J.L. Macen, D.S. Wishart, and G. McFadden**. 1990. Myxoma virus and malignant rabbit fibroma virus encode a serpin-like protein important for virus virulence. Virology **179**:618-631.

293. **Upton, C., and G. McFadden**. 1986. Tumorigenic poxviruses: analysis of viral DNA sequences implicated in the tumorigenicity of Shope fibroma virus and malignant rabbit virus. Virology **152**:308-321.

294. **Upton, C., K. Mossman, and G. McFadden**. 1992. Encoding of a homolog of the IFN-gamma receptor by myxoma virus. Science **258**:1369-1372.

295. **Vanderplasschen, A., M. Hollinshead, and G.L. Smith**. 1997. Antibodies against vaccinia virus do not neutralize extracellular enveloped virus but prevent virus release from infected cells and comet formation. J.Gen.Virol. **78**:2041-2048.

296. **Vanderplasschen, A., M. Hollinshead, and G.L. Smith**. 1998. Intracellular and extracellular vaccinia virions enter cells by different mechanisms. J.Gen.Virol. **79**:877-887.

297. **Vanderplasschen, A., E. Mathew, M. Hollinshead, R.B. Sim, and G.L. Smith**. 1998. Extracellular enveloped vaccinia virus is resistant to complement because of incorporation of host complement control proteins into its envelope. Proc.Natl.Acad.Sci.U.S.A. **95**:7544-7549.

298. **Vanderplasschen, A., and G.L. Smith**. 1997. A novel virus binding assay using confocal microscopy: Demonstration that the intracellular and extracellular vaccinia virions bind to different cellular receptors. J.Virol. **71**:4032-4041.

299. **Vaux, D.L., G. Haecker, and A. Strasser**. 1994. An evolutionary perspective on Apoptosis. Cell **76**:777-779.

300. **Virgin, H.W., P. Latreille, P. Wamsley, K. Hallsworth, K.E. Weck, A.J. Dalcanto, S.H. Speck, H.W.4. Virgin, and A.J. Dal Canto**. 1997. Complete sequence and genomic analysis of murine gammaherpesvirus 68 Complete sequence and genomic analysis of murine gammaherpesvirus 68. J.Virol. **71**:5894-5904.

301. **von Magnus, P., Andresen EK, K. Petersen, and A. Birch-Andersen**. 1959. A pox-like disease in cynomolgus monkeys. Acta Pathol.Microbiol.Scand. **46**:156-176.

302. **Vos, J.C., M. Sasker, and H.G. Stunnenberg**. 1991a. Promoter melting by a stage-specific vaccinia virus transcription factor is independent of the presence of RNA polymerase. Cell **65**:105-113.

303. **Vos, J.C., M. Sasker, and H.G. Stunnenberg**. 1991b. Vaccinia virus capping enzyme is a transcription initiation factor. EMBO J. **10**:2553-2558.

304. **Vos, J.C., and H.G. Stunnenberg**. 1988. Derepression of a novel class of vaccinia virus genes upon DNA replication. EMBO J. **7**:3487-3492.

305. **Wakamiya, N., N. Okada, Y.L. Wang, T. Ito, S. Ueda, S. Kato, and H. Okada**. 1989. Tumor cells treated with vaccinia virus can activate the alternative pathway of mouse complement. Jpn.J.Cancer Res. **80**:765-770.

306. **Wang, S., M. Miura, Jung Yk, H. Zhu, V. Gagliardini, L. Shi, A.H. Greenberg, and J. Yuan**. 1996. Identification and characterization of Ich-3, a member of the interleukin-1beta converting enzyme (ICE)/Ced-3 family and an upstream regulator of ICE. J.Biol.Chem. **271**:20580-20587.

307. **Wang, Y.X., P.C. Turner, T.L. Ness, K.B. Moon, T.R. Schoeb, and R.W. Moyer**. 2000. The cowpox virus SPI-3 and myxoma virus SERP1 serpins

are not functionally interchangeable despite their similar proteinase inhibition profiles in vitro. Virology **272**:281-292.

308. **Waring, P., and A. Mullbacher**. 1999. Cell death induced by the Fas/Fas ligand pathway and its role in pathology. Immun.Cell Biol. **77**:312-317.

309. **Watorek, W., D. Farley, G. Salvesen, and J. Travis**. 1988. Neutrophil elastase and cathepsin G: structure, function, and biological control. Adv.Exp Med Biol **240:23-31**:23-31.

310. **Watson, J.C., H.W. Chang, and B.L. Jacobs**. 1991. Characterization of a vaccinia virus-encoded double-stranded RNA- binding protein that may be involved in inhibition of the double- stranded RNA-dependent protein kinase. Virology **185**:206-216.

311. **Welsh, R.M.** 1986. Regulation of virus infections by natural killer cells. A review. Nat.Immun.Cell Growth Regul. **5**:169-199.

312. **Welsh, R.M., R.M. Zinkernagel, and L.A. Hallenbeck**. 1979. Cytotoxic cells induced during lymphocytic choriomeningitis virus infection of mice. II. "Specificities" of the natural killer cells. J.Immunol. **122**:475-481.

313. **Westwood, J.C., E.A. Boulter, E.T. Bowen, and H.B. Maber**. 1966. Experimental respiratory infection with poxviruses. I. Clinical virological and epidemiological studies. Br.J.Exp.Pathol. **47**:453-465.

314. **Whitaker Dowling, P., and J.S. Youngner**. 1984. Characterization of a specific kinase inhibitory factor produced by vaccinia virus which inhibits the interferon- induced protein kinase. Virology **137**:171-181.

315. **Willer, D.O., G. McFadden, and D.H. Evans**. 1999. The complete genome sequence of shope (rabbit) fibroma virus. Virology **264**:319-343.

316. **Wittek, R., A. Menna, H.K. Muller, D. Schumperli, P.G. Boseley, and R. Wyler**. 1978. Inverted terminal repeats in rabbit poxvirus and vaccinia virus DNA. J.Virol. **28**:171-181.

317. **Xiang, J., D.T. Chao, and S.J. Korsmeyer**. 1996. BAX-induced cell death may not require interleukin 1 beta-converting enzyme-like proteases. Proc.Natl.Acad.Sci.U.S.A. **93**:14559-14563.

318. **Xue, D., and H.R. Horvitz**. 1995. Inhibition of the *Caenorhabditis elegans* cell-death protease CED-3 by a CED-3 cleavage site in baculovirus p35 protein. Nature **377**:248-251.

319. **Yamazaki, T., and Y. Aoki**. 1998. Cathepsin G enhances human natural killer cytotoxicity. Immunology **93**:115-121.

320. **Yang, X.H., H.R. Stennicke, B.K. Wang, D.R. Green, R.U. Janicke, A. Srinivasan, P. Seth, G.S. Salvesen, and C.J. Froelich**. 1998. Granzyme B mimics apical caspases - Description of a unified pathway for trans-activation of executioner caspase-3 and -7. J.Biol.Chem. **273**:34278-34283.

321. **Zhivotovsky, B., A. Gahm, M. Ankarcrona, P. Nicotera, and S. Orrenius**. 1995. Multiple proteases are involved in thymocyte apoptosis. Exp.Cell Res. **221**:404-412.

322. **Zhivotovsky, B., A. Gahm, and S. Orrenius**. 1997. Two different proteases are involved in the proteolysis of lamin during apoptosis. Biochem.Biophys.Res.Commun. **233**:96-101.

323. **Zhou, J., X.Y. Sun, G.J. Fernando, and I.H. Frazer**. 1992. The vaccinia virus K2L gene encodes a serine protease inhibitor which inhibits cell-cell fusion. Virology **189**:678-686.

324. **Zhou, Q., S. Snipas, K. Orth, M. Muzio, V.M. Dixit, and G.S. Salvesen**. 1997. Target protease specificity of the viral serpin CrmA - Analysis of five caspases. J.Biol.Chem. **272**:7797-7800.

BIOGRAPHICAL SKETCH

Kristin Moon was born in St. Petersburg, Florida, in 1972. With her brother Matthew, she was raised by her parents David Bruce and Patricia Black in Lecanto, Florida. She graduated with honors from Lecanto High School in 1990. She attended the University of Florida as an undergraduate from 1990 until 1994 where she majored in microbiology and cell science. She graduated with honors in 1994 with a Bachelor of Science degree and immediately began the graduate program in the Department of Molecular Genetics and Microbiology in the fall of 1994 under the supervision of Dr. Richard Moyer. She lives in Ocala, Florida with her husband Joel and her son Joel Davis, "J.D."

I certify that I have read this study and that in my opinion it conforms to acceptable standards of scholarly presentation and is fully adequate, in scope and quality, as a dissertation for the degree of Doctor of Philosophy.

Richard W. Moyer, Chair
Professor of Molecular Genetics
and Microbiology

I certify that I have read this study and that in my opinion it conforms to acceptable standards of scholarly presentation and is fully adequate, in scope and quality, as a dissertation for the degree of Doctor of Philosophy.

John Aris
Associate Professor of Anatomy and
Cell Biology

I certify that I have read this study and that in my opinion it conforms to acceptable standards of scholarly presentation and is fully adequate, in scope and quality, as a dissertation for the degree of Doctor of Philosophy.

William Dunn
Associate Professor of Anatomy and
Cell Biology

I certify that I have read this study and that in my opinion it conforms to acceptable standards of scholarly presentation and is fully adequate, in scope and quality, as a dissertation for the degree of Doctor of Philosophy.

Alfred Lewin
Professor of Molecular Genetics and
Microbiology

I certify that I have read this study and that in my opinion it conforms to acceptable standards of scholarly presentation and is fully adequate, in scope and quality, as a dissertation for the degree of Doctor of Philosophy.

Thomas Rowe
Associate Professor of
Pharmacology and Therapeutics

This dissertation was submitted to the Graduate Faculty of the College of Medicine and to the Graduate School and was accepted as partial fulfillment of the requirements for the degree of Doctor of Philosophy.

December, 2000

Dean, College of Medicine

Dean, Graduate School